# DEVELOPMENT OF PROCEDURES AND TECHNOLOGIES FOR CHIP SEAL CONSTRUCTION QUALITY CONTROL IN OREGON

**Final Report** 

PROJECT SPR 858



Oregon Department of Transportation

# DEVELOPMENT OF PROCEDURES AND TECHNOLOGIES FOR CHIP SEAL CONSTRUCTION QUALITY CONTROL IN OREGON

## **SPR 858**

by

Servan Baran - Graduate Research Assistant Mayank Sukhija, Ph.D. – Postdoctoral Scholar Erdem Coleri, Ph.D. - Associate Professor (PI)

OSU-Asphalt Materials and Pavements (AMaP) Laboratory School of Civil and Construction Engineering Oregon State University 101 Kearney Hall Corvallis, OR 97331 Phone: 541-737-0944

for

Oregon Department of Transportation Research Section 555 13<sup>th</sup> Street NE, Suite 1 Salem OR 97301

and

Federal Highway Administration 1200 New Jersey Avenue SE Washington, DC 20590

February 2025

Technical Report Documentation Page

1 8		
1. Report No.	2. Government Accession No.	3. Recipient's Catalog No.
FHWA-OR-RD-25-01		
4. Title and Subtitle	5. Report Date	
DEVELOPMENT OF PROCE	February 2025	
OREGON	TION QUALITY CONTROL IN	6. Performing Organization
ORLGON		Code
7. Author(s)		8. Performing Organization
Servan Baran; 0000-0003-2136-14	9X	Report No. TBD
Mayank Sukhija, PhD; 0000-0002-	-7062-1406	
Erdem Coleri, PhD; 0000-0002-19		
9. Performing Organization Name	10. Work Unit No. (TRAIS)	
School of Civil and Construction	2 2	TBD
Oregon State University, 101 K	11. Contract or Grant No.	
12. Sponsoring Agency Name and	Address	13. Type of Report and Period
Oregon Dept. of Transportation	Covered	
Research Section and	Draft Report	
555 13 <sup>th</sup> Street NE, Suite 1	14. Sponsoring Agency Code	
Salem, OR 97301		

15. Supplementary Notes

16. Abstract: Given budget constraints and increasing traffic in Oregon, chip seals have emerged as a cost-effective and practical approach for maintaining and preserving the existing highway network. This study focused on establishing efficient Quality Assurance (QA) procedures for chip seals, aligning with SPR777's design method to increase the performance and longevity of chip seals in Oregon. Modified sweep and pull-off tests were developed and complemented by Vialit tests to assess the adhesion properties between the aggregate and the binder. Subsequently, laboratory tests were conducted using aggregates and emulsions sampled from two construction projects. The results were compared to identify the most effective and practical test method, utilizing the correlation of the obtained results. Using the recommended test methods, the effect of dust and surface moisture on aggregate retention performance was evaluated. Moreover, the study reports the aggregate retention performance of four different aggregates from various Oregon regions using the two most commonly used emulsions. A laboratory bleeding test using the Hamburg Wheel Tracking Test device was also developed. The aggregate retention and bleeding performance of RAP were examined. The OreTackRate, developed in SPR 818, was tested in chip seal construction for in-situ emulsion application rate measurement. To assess the bleeding susceptibility of chip seals in situ, macro texture measurements were taken using the developed laser texture scanner, sand patch test, and high-speed profiler, both before and immediately after the completion of chip seal construction. The obtained results were correlated, and an MPD-MTD correlation was established. The test methods and the QA processes developed and proposed for implementation in this study are expected to enhance the performance of chip-seal surfaced roadways in Oregon.

1 1			3	
17. Key Words		18. Distr	ribution Statement	
Chip seal, emulsions, adhesion, RA	Copies available from NTIS, and online at			
retention, bleeding, embedment, qua	http://www.oregon.gov/ODOT/TD/TP_RES/			
assurance, asphalt.			<del></del>	
19. Security Classification	20. Security Cla	ssification	21. No. of Pages	22. Price
(of this report)	(of this page	<b>:</b> )	193	
Unclassified Unclassifie		d		

	SI* (MODERN METRIC) CONVERSION FACTORS								
A	APPROXIMATE (	CONVERSI	ONS TO SI UNI	TS	AP	PROXIMATE C	ONVERSIO	ONS FROM SI UN	ITS
Symbol	l When You Know	Multiply By	To Find	Symbol	Symbol	When You Know	Multiply By	To Find S	Symbol
		<b>LENGTH</b>					LENGTH	<u>[</u>	
in	inches	25.4	millimeters	mm	mm	millimeters	0.039	inches	in
ft	feet	0.305	meters	m	m	meters	3.28	feet	ft
yd	yards	0.914	meters	m	m	meters	1.09	yards	yd
mi	miles	1.61	kilometers	km	km	kilometers	0.621	miles	mi
		<b>AREA</b>					<b>AREA</b>		
$in^2$	square inches	645.2	millimeters squared	$mm^2$	mm <sup>2</sup>	millimeters squared	0.0016	square inches	$in^2$
$\mathrm{ft}^2$	square feet	0.093	meters squared	$m^2$	$m^2$	meters squared	10.764	square feet	$ft^2$
$yd^2$	square yards	0.836	meters squared	$m^2$	$m^2$	meters squared	1.196	square yards	$yd^2$
ac	acres	0.405	hectares	ha	ha	hectares	2.47	acres	ac
$mi^2$	square miles	2.59	kilometers squared	$km^2$	km <sup>2</sup>	kilometers squared	0.386	square miles	$mi^2$
		<b>VOLUME</b>					<b>VOLUMI</b>	<u>E</u>	
fl oz	fluid ounces	29.57	milliliters	ml	ml	milliliters	0.034	fluid ounces	fl oz
gal	gallons	3.785	liters	L	L	liters	0.264	gallons	gal
$\mathrm{ft}^3$	cubic feet	0.028	meters cubed	$m^3$	$m^3$	meters cubed	35.315	cubic feet	gal ft³
$yd^3$	cubic yards	0.765	meters cubed	$m^3$	$m^3$	meters cubed	1.308	cubic yards	$yd^3$
NO	OTE: Volumes grea	ter than 100	L shall be shown	n in m <sup>3</sup> .					
		<b>MASS</b>					<b>MASS</b>		
oz	ounces	28.35	grams	g	g	grams	0.035	ounces	oz
lb	pounds	0.454	kilograms	kg	kg	kilograms	2.205	pounds	lb
T	short tons (2000 lb)	0.907	megagrams	Mg	Mg	megagrams	1.102	short tons (2000 lb	) T
	<b>TEMP</b>	ERATURE	(exact)			<u>TEM</u>	PERATURI	E (exact)	
°F	Fahrenheit	(F- 32)/1.8	Celsius	°C	°C	Celsius	1.8C+3 2	Fahrenheit	°F
*SI is th	SI is the symbol for the International System of Measurement								

## **ACKNOWLEDGEMENTS**

The authors would like to thank the Oregon Department of Transportation (ODOT) for providing funding for this research study. The authors thank the members of the ODOT Project Technical Advisory Committee and ODOT Research for their advice and assistance in the preparation of this report. In particular, Jon Lazarus, Cristhian Galvez, Cole Mullis, Bert Perisho, Tim Earnest, Chris Duman, Mike Stennett, Larry Ilg, Stephen Van De Bogert, Ashley Buss, Troy Hooker, David Anderson, Jason Lampley, David Zimmerly, and Justin Moderie participated on the TAC. The authors would like to thank Dave Zhai, Alejandro Rosales, and Doug Olsen for their help in collecting macrotexture data with the high-speed profiler. The authors also thank the graduate and undergraduate students of the OSU-Asphalt Materials and Pavements (AMaP) Research Group for their help with the experiments. Keven Heitschmidt of Albina Asphalt provided the emulsions used for laboratory testing. His continuous support for many research projects is gratefully acknowledged. We would also like to thank David Zimmerly (Sierra Santa Fe Corporation) and David W Anderson (ODOT) for their help with field trials. The authors would also like to thank Tim Earnest of ODOT for his help with organizing field trials and for all the valuable feedback and support throughout the research project.

#### **DISCLAIMER**

This document is disseminated under the sponsorship of the Oregon Department of Transportation and the United States Department of Transportation in the interest of information exchange. The State of Oregon and the United States Government assume no liability of its contents or use thereof.

The contents of this report reflect the view of the authors who are solely responsible for the facts and accuracy of the material presented. The contents do not necessarily reflect the official views of the Oregon Department of Transportation or the United States Department of Transportation.

The State of Oregon and the United States Government do not endorse products of manufacturers. Trademarks or manufacturers' names appear herein only because they are considered essential to the object of this document.

This report does not constitute a standard, specification, or regulation.

# TABLE OF CONTENTS

1.0	INTRODUCTION	. 1
1.1	KEY OBJECTIVES OF THE STUDY	. 5
1.2		
2.0	LITERATURE REVIEW	. 7
2.1	CHIP SEAL DESIGN METHODS	. 7
2	2.1.1 Chip Seal Design Method of Oregon DOT	
	2.1.2 Other Chip Seal Design Methods	.13
2.2		
2.3	· · · · · · · · · · · · · · · · · · ·	19
_	2.3.1 Adhesion Tests	.19
	2.3.2 Chip Seal Aggregate and Binder Application Rate Measurement	
2.4	2.3.3 Macrotexture Measurement MethodsLABORATORY TEST METHODS TO PREDICT AND EVALUATE IN-SITU CHI	
	AL PERFORMANCE	
	2.4.1 Intra Scale Model Mobile Lodding Simulator (MMLSS)	
	2.4.3 Hamburg Wheel Tracking (HWT) Test	
2.5	8 7	
2.6		
3.0	AGGREGATE-BINDER ADHESION	
3.1	INTRODUCTION	
3.2		
-	3.2.1 Objectives	
	3.2.3 Results & Discussion of Preliminary Laboratory Tests	
3.3		
	3.3.1 Objectives	
3	3.3.2 Materials and Methods	
3	3.3.3 Results & Discussions	. 74
3.4	ADHESION TESTS ON LABORATORY-PREPARED SAMPLES USING	
MA	ATERIALS SAMPLED FROM CONSTRUCTION	
	3.4.1 Objectives	
	3.4.2 Materials and Methods	
_	3.4.3 Results & Discussions	
3.5		
	3.5.1 Objectives	
	3.5.2 Materials and Methods	
3.6		
4.0	A FIELD WIRELESS SCALE SYSTEM TO MEASURE EMULSION	01
	LICATION RATES 1	07
4.1	INTRODUCTION1	07
	1.1.1 Objectives	
4.2	J .	

4.3	RESULTS & DISCUSSIONS	110
4.4	CONCLUSIONS	112
5.0	IN-SITU MACROTEXTURE MEASUREMENTS USING DIFFERENT	
TECH	INOLOGIES	113
5.1	INTRODUCTION	
	.1.1 Objectives	113
5.2	MATERIALS & METHODS	
	.2.1 Sand Patch Test	
	.2.2 Mean Profile Depth Measurements with Laser Texture Scanner	
	.2.3 Mean Profile Depth Measurements with High-Speed Profiler	
5.3	RESULTS & DISCUSSIONS	
5.4	CONCLUSIONS	
6.0	BLEEDING TESTS	
6.1	INTRODUCTION	
_	.1.1 Objectives	
6.2	MATERIALS & METHODS	
6.3	RESULTS & DISCUSSIONS	
6.4	CONCLUSIONS	
7.0	AGGREGATE RETENTION & BLEEDING PERFORMANCE OF RAP	IN CHIP
SEAL		
7.1	INTRODUCTION	1/10
,	.1.1 Objectives	
7.2	MATERIALS & METHODS	
7.3	RESULTS & DISCUSSIONS	
	3.1 Adhesion Performance of RAP Chip Seal	
7.	.3.2 Bleeding Performance of RAP Chip Seal	
7.4	CONCLUSIONS	156
8.0	SUMMARY AND CONCLUSIONS	158
8.1	MAJOR CONCLUSIONS	159
8.2	FUTURE WORK	
9.0	REFERENCES	164
APPF	ENDIX A: ONE-YEAR POST-CONSTRUCTION MACROTEXTURE	
	SUREMENTS	A-123
	LIST OF TABLES	
	2.1: Emulsion and aggregate application rates (ODOT 2021)	
	2.2: Traffic wastage factor and percent waste allowed (McLeod 1969)	
	2.3: Traffic Factor (T) and AADT (McLeod 1969)	
Table 2	2.4: Surface texture correction (S) for different pavement conditions (McLeod 1969)	10

Table 2.5: Aggregate absorption correction factor (McLeod, 1969)	11
Table 3.1: Physical properties of aggregates	52
Table 3.2: Experimental plan for preliminary tests (HFRS-2P: anionic polymer-modified high-float rapid set, C	RS-
2P: cationic polymer-modified rapid set emulsion)	56
Table 3.3: Chip Seal Construction Details	
Table 3.4: Physical properties of the aggregates sampled from the field	
Table 3.5: Weather Station Data (Average of all data points)	
Table 3.6: Chip seal design rates for each aggregate	
Table 3.7: Assumptions made during chip seal design	
Table 4.1:Tack Lifter trial/sensitivity test results	
Table 4.2: In-situ EAR measurements	
Table 4.3: Tack lifter measurements	
Table 5.1: MTD measurements of sections along US-730 and OR-11 (STD is the standard deviation)	
Table 5.2: MPD measurements from laser texture scanner along US-730 and OR-11 (STD is the standard device)	
TILL SACO CONTROL OF THE CONTROL OF	
Table 5.4: Comparison of MTD measurements conducted by the ODOT crew and the OSU-AMaP research tea	m
along US-730 before chip seal construction (STD is the standard deviation)	
Table 5.5: Cluster analysis of laser texture scanner data	
Table 5.6: Cluster analysis of high-speed profiler data	129
Table A.1: One-year post-construction (22 July 2024) sand patch (MTD) and laser texture scanner (MPD)	A 1
measurements of sections along US-730 and OR-11 (STD is the standard deviation)	A-1
LICT OF FIGURES	
LIST OF FIGURES	
Figure 1.1: Pavement condition-cost per lane mile relationship (Coplantz 2021)	
Figure 1.2: Chip seal and paving lane miles in Oregon between 1999-2022 and projection through 2027 (Copla	
2023)	
Figure 2.1: Average Least Dimension (ALD) concept (McLeod 1969)	9
Figure 2.2: Conditions of chip seal embedment in the binder(NRB 1968)	
Figure 2.3: Asphalt application rate nomogram suggested by Kearby (1953)	
Figure 2.4: Flowchart for determining aggregate and binder application rates (Alderson 2006)	
Figure 2.5: The chip seal construction phases; (a) spraying emulsion (b) aggregate spread on emulsion (c) chip	
were compacted by a pneumatic-tired roller (Buss et al. 2016)	
Figure 2.6: Vialit test described in EN 12272-3 (a) emulsion-asphalt cement application; (b) spreading chips; (c)	
compaction; (d) curing of chip seal samples; (e) free fall of the ball over the plate; (f) counting fallen chip	-
(Gurer 2010)	
Figure 2.7: Sweet test (ASTM D7000 2010) conducted on ahin seel sample (a) proportion of exploit falt disco	(h a)
Figure 2.7: Sweep test (ASTM D7000 2019) conducted on chip seal sample (a) preparation of asphalt felt disc;	(b-c)
applying emulsion on asphalt felt disc; (d) flatting the emulsion surface; (e-f) chip spread process; (g)	(b-c)
applying emulsion on asphalt felt disc; (d) flatting the emulsion surface; (e-f) chip spread process; (g) compaction of chip seal sample; (h) curing the specimens in the oven; (i) performing sweep test using minutes of the control	(b-c)
applying emulsion on asphalt felt disc; (d) flatting the emulsion surface; (e-f) chip spread process; (g) compaction of chip seal sample; (h) curing the specimens in the oven; (i) performing sweep test using mand nylon brush (Wasiuddin et al. 2013)	(b-c) ixer 22
applying emulsion on asphalt felt disc; (d) flatting the emulsion surface; (e-f) chip spread process; (g) compaction of chip seal sample; (h) curing the specimens in the oven; (i) performing sweep test using mi and nylon brush (Wasiuddin et al. 2013)	ixer 22 era et
applying emulsion on asphalt felt disc; (d) flatting the emulsion surface; (e-f) chip spread process; (g) compaction of chip seal sample; (h) curing the specimens in the oven; (i) performing sweep test using mi and nylon brush (Wasiuddin et al. 2013)	ixer 22 era et
applying emulsion on asphalt felt disc; (d) flatting the emulsion surface; (e-f) chip spread process; (g) compaction of chip seal sample; (h) curing the specimens in the oven; (i) performing sweep test using mi and nylon brush (Wasiuddin et al. 2013)	ixer 22 era et 25
applying emulsion on asphalt felt disc; (d) flatting the emulsion surface; (e-f) chip spread process; (g) compaction of chip seal sample; (h) curing the specimens in the oven; (i) performing sweep test using mi and nylon brush (Wasiuddin et al. 2013)	ixer22 era et25
applying emulsion on asphalt felt disc; (d) flatting the emulsion surface; (e-f) chip spread process; (g) compaction of chip seal sample; (h) curing the specimens in the oven; (i) performing sweep test using mi and nylon brush (Wasiuddin et al. 2013)	ixer22 era et252626
applying emulsion on asphalt felt disc; (d) flatting the emulsion surface; (e-f) chip spread process; (g) compaction of chip seal sample; (h) curing the specimens in the oven; (i) performing sweep test using mand nylon brush (Wasiuddin et al. 2013)	ixer 22 era et 25 26 over
applying emulsion on asphalt felt disc; (d) flatting the emulsion surface; (e-f) chip spread process; (g) compaction of chip seal sample; (h) curing the specimens in the oven; (i) performing sweep test using mi and nylon brush (Wasiuddin et al. 2013)	ixer 22 era et 25 27 over 28
applying emulsion on asphalt felt disc; (d) flatting the emulsion surface; (e-f) chip spread process; (g) compaction of chip seal sample; (h) curing the specimens in the oven; (i) performing sweep test using mi and nylon brush (Wasiuddin et al. 2013)	ixer22 era et25 26 over28 29
applying emulsion on asphalt felt disc; (d) flatting the emulsion surface; (e-f) chip spread process; (g) compaction of chip seal sample; (h) curing the specimens in the oven; (i) performing sweep test using mi and nylon brush (Wasiuddin et al. 2013)	ixer22 era et2527 over282930
applying emulsion on asphalt felt disc; (d) flatting the emulsion surface; (e-f) chip spread process; (g) compaction of chip seal sample; (h) curing the specimens in the oven; (i) performing sweep test using mi and nylon brush (Wasiuddin et al. 2013)	ixer22 era et252627 over28293031

Figure 2.17: OreTackRate method to determine the asphalt binder application rate (a) The calibration of wi-fi so	cales
and tablet computer (b) scales covered asphalt shingles next to textile pads used for ASTM D2995 (c)	
performing application rate and variability measurements in the field (Coleri et al. 2020b)	34
Figure 2.18: The correlation between application rate measurements obtained from OreTackRate and ASTM D2	2995
(2014)(Coleri et al. 2020b)	
Figure 2.19: The illustration of microtexture and macrotexture terms (TNZ 2005)	36
Figure 2.20: Sand patch test on (a)Laboratory samples (Gheni et al. 2017) and (b) Field pavement surface (Buss	et
al. 2016)	38
Figure 2.21: Outflow test meter application in the field (Aktas et al. 2011)	39
Figure 2.22: Mean segment (profile) depth introduced by ASTM E1845 (2015)	40
Figure 2.23: Stages of determination of percent embedment (Kutay et al. 2016)	42
Figure 2.24: MMLS3 test setup: (a) mounting of samples on steel platform (b) MMLS3 device (c) placing the d	evice
in a climate chamber (d) MMLS3 test ready to perform a test (Adams and Kim 2014)	44
Figure 2.25: HSKSC test setup (Aktas and Karasahin 2013)	45
Figure 2.26: (a) Conventional HWT device (b) modified HWT device (Boz et al. 2018)	46
Figure 3.1: Aggregates acquired from different regions in Oregon	
Figure 3.2: The gradations of aggregates from different regions of Oregon	53
Figure 3.3: Experimental process stages of the sweep and Vialit tests: (a) emulsion application on the plates, (b-	-c)
spread of chips on the emulsion using the apparatus developed by Weaver et al. (2023), (d) sample	
compaction using a rubber wheel, (e) sample curing at 25 °C for 24 hours, (f) conducting the modified sw	eep
test on the plates (25 °C), (g) execution of the Vialit test after conditioning the samples at 5 °C and 40 °C	55
Figure 3.4: Trial tests with the OFTCT on chip seal samples	57
Figure 3.5: Trial tests with PosiTest on chip seal samples	58
Figure 3.6: Adhesive failure between the dolly and epoxy	58
Figure 3.7: Introducing threads in dollies to increase the contact area with epoxy	
Figure 3.8: Performing pull-off test via PosiTest in the environmental chamber (5°C)	59
Figure 3.9: Performing pull-off test with the UTM-30 test system	60
Figure 3.10: Pull-off test dolly after the test. The red circle shows the area for the circular method, while the gre	en
lines show the Pline method	61
Figure 3.11: Steps for calibration of effective binder area measurement	
Figure 3.12: The correlation between sand weight and binder area	62
Figure 3.13: The experimental process stages for pull-off tests: (a) chip seal samples on Vialit test (cured), (b)	
sweeping excessive aggregate, (c) spread of standard sand to cover binder, (d) adhering dollies on the chip	ρs
using epoxy, (e) conducting the pull-off test	
Figure 3.14: Sweep test results (average) at 25 °C testing temperature (a) HFRS-2P (b) CRS-2P (Error bars are	one
standard deviation height)	
Figure 3.15: Vialit test results (average) at 40°C and 5°C testing temperatures (a) HFRS-2P (anionic binder) (b)	)
CRS- 2P (cationic binder) (Error bars are one standard deviation height)	67
Figure 3.16: Samples after the pull-off tests (5°C) (brown color showed insufficient curing)	68
Figure 3.17: The gradation of field aggregates	70
Figure 3.18: Pendleton chip seal sampling section	71
Figure 3.19: Woodburn chip seal sampling section	71
Figure 3.20: Compacting samples after emulsion and aggregate application	
Figure 3.21: Temperature, Relative humidity, and wind speed measured in Pendleton and Woodburn	73
Figure 3.22: The change in moisture loss in emulsions over time (Field evaporation measurements)	
Figure 3.23: Sweep and Vialit test results of field samples (Error bars are one standard deviation height)	75
Figure 3.24: Pull-off test results (Field samples) (Error bars are one standard deviation height)	76
Figure 3.25: Sweep test results (25 °C) (Error bars are one standard deviation height)	
Figure 3.26: Results of the Vialit test conducted at 25°C (Error bars are one standard deviation height)	
Figure 3.27: Results of the Vialit test conducted at 5°C (Error bars are one standard deviation height)	
Figure 3.28: Pull-off test results at 25°C (Error bars are one standard deviation height)	
Figure 3.29: Pull-off test results at 5°C (Error bars are one standard deviation height)	
Figure 3.30: The correlation between the sweep test (25°C) and Pull-off test results (25°C) (a) with the outlier, (	
without the outlier	
Figure 3.31: The correlation between the Vialit test (25°C) and Pull-off test results (25°C)	
Figure 3.32: The correlation between the Vialit test (5°C) and Pull-off test results (5°C)	86

Figure 3.33: The threshold values determined (a) sweep & pull-off test (25°C), (b) Vialit & pull-off (5°C).				
Figure 3.34: Sweep test results of damp and dry aggregates (Error bars are one standard deviation height)				
Figure 3.35: Flip-over test results of damp and dry aggregates (Error bars are one standard deviation height				
Figure 3.36: Vialit test (5°C) results of damp and dry aggregates (Error bars are one standard deviation height				
Figure 3.37: Pull-off test results of damp and dry aggregates (a) at 25°C (b) at 5°C (Error bars are one stand				
deviation height)				
Figure 3.38: Cleaned aggregate tests (a) Flip-over (b) Sweep test at 25°C (c) Vialit test at 5°C (Error bars are				
standard deviation height)				
Figure 3.39: Comparison of damp-dusty aggregates with dry-clean aggregates - flip-over test at 25°C (Error				
one standard deviation height)				
Figure 3.40: Comparison of damp-dusty aggregates with dry-clean aggregates - sweep test at 25°C (Error b one standard deviation height)				
Figure 3.41: Comparison of damp-dusty aggregates with dry-clean aggregates - Vialit test at 5°C (Error bar				
standard deviation height)				
Figure 3.42: The test results of Pendleton and Woodburn aggregates with CRS-3P (cationic) and HFRS-2P				
binders (a) Flip-over (b) Sweep test at 25°C (c) Vialit test at 5°C (Error bars are one standard deviation				
of the standard deviation of the standard de				
Figure 3.43: Pull-off test results of chip seal samples on metal plates and AC discs (a) 25°C (b) at 5°C (Erro				
are one standard deviation height)	100			
Figure 3.44: Sweep test results (25°C) of aggregates with anionic HFRS-2P and cationic CRS-2P emulsion	s (Error			
bars are one standard deviation height)				
Figure 3.45: Vialit test results (5°C) of aggregates with HFRS-2P and CRS-2P emulsions (Error bars are or	ne			
standard deviation height)	103			
Figure 4.1: The preparation steps for the OreTackRate system: (a) cutting 1 ft x 1 ft (30.48 cm x 30.48 cm)	plastic			
plate, (b) attaching shingle plates (32.5 cm x 32.5 cm) on the plastic plate, (c) folding the corners of s	hingles			
and securing with clips, (d-e) attaching shingle tray to the wireless scale using Velcro, (f) side view o				
OreTackRate system				
Figure 4.2: OreTackRate system for measuring EAR of chip seal				
Figure 4.3: Tack Lifter device and trial tests	110			
Figure 4.4: In-situ EAR measurements (a) Pendleton (b) Woodburn				
Figure 5.1: Sand patch test performed after chip seal construction (Pendleton-OR 11)				
Figure 5.2: Laser texture scanner developed at OSU-AMaP				
Figure 5.3: Mean segment depth calculation (ASTM E1845 2015)				
Figure 5.5: High-speed profiler system used in this study (Photo credit: Alejandro Rosales of Idaho Asphal				
Figure 5.6: Macrotexture measurement sections on US-730 and OR-11 highways (Google Maps 2024; Map				
2023)				
Figure 5.7: Chip seal locations and schedule (ODOT 2023)				
Figure 5.8: Macrotexture measurement test plan for each section				
Figure 5.9: Macrotexture measurements from the field (a) before construction (b) after construction (Pendle				
11)				
bars represent one standard deviation in height)				
Figure 5.11: Correlation of MTD results between ODOT crew and OSU-AMaP research team				
Figure 5.12: MTD (sand patch-MPD (laser texture scanner) correlation				
Figure 5.13: MTD (sand patch)-MPD (high-speed profiler) correlation				
Figure 5.14: MPD (laser texture scanner)-MPD (high-speed profiler) correlation	130			
Figure 5.15: Comparison of MPD-MTD data with other studies	131			
Figure 6.1: Sample preparation stages of chip seal samples for bleeding test: (a) compacted and trimmed H				
samples, (b) emulsion application, (c) aggregate spread over emulsion (d) chip seal samples compact				
rubber wheel, (e) samples after cured at 45 °C for 24 hours and excess aggregates were removed, (f)				
sample placed in HWT mold				
Figure 6.2: Bleeding testing of chip seal samples: (a) macrotexture measurement (MPD) with laser texture				
before trafficking, (b) HWT test with rubber wheels, (c) macrotexture measurement after trafficking				
Figure 6.3: MPD-HWT Passes of laboratory-prepared Pendleton samples (Error bars are one standard devia	ation			
height)	137			

# 1.0 INTRODUCTION

Chip sealing is one of the most effective and inexpensive preventive maintenance techniques used for pavements in the United States. The chip seal is made up of an asphalt binder layer covered with embedded aggregates. The primary goal of chip sealing is to seal minor cracks on the pavement's surface, prevent water penetration into the unbound subgrade and base layers, and provide a high enough macrotexture that creates a skid-resistant surface for vehicles (Gransberg and James 2005). Several chip seal types are available, i.e., single chip seal, multiple chip seal, racked-in seal, cape seal, etc. However, the single-chip seal is the most commonly used method in the United States and Oregon (Buss et al. 2016).

A successful chip seal application is possible only if there is no structural damage to the underlying pavement layers (Gransberg & James, 2005). Since the chip seal consists of a single-layer asphalt binder and aggregate coating, it does not contribute to the pavement's structural resistance. Hence, the chip seal should be implemented when pavement distress is relatively low. Therefore, the selection of pavements for chip seal application is of critical importance (Mahoney et al. 2014). Chip sealing protects the pavement against harmful impacts such as moisture, aging, and traffic and can extend the resurfacing interval of underlying asphalt layers up to 30 years for low to moderate-traffic asphalt-surfaced roads (Coplantz 2021).

As long as the foundation and base layers of the pavement are unharmed, the surface layer of the pavement can be constantly repaired in cases where the deterioration is limited to the surface. In this scenario, only periodic preservation is conducted on the surface instead of repaving the entire roadway. However, if the resurfacing technique is postponed for an extended period, the pavement structure and underlying components might deteriorate severely, necessitating the replacement of the entire roadway. Consequently, the required reconstruction or major rehabilitation of the pavement structure can be considerably more expensive than resurfacing (Figure 1.1). Therefore, consistent pavement repair and preservation is considered to be the most effective technique for protecting infrastructure investments (Coplantz 2021; Gransberg and James 2005).

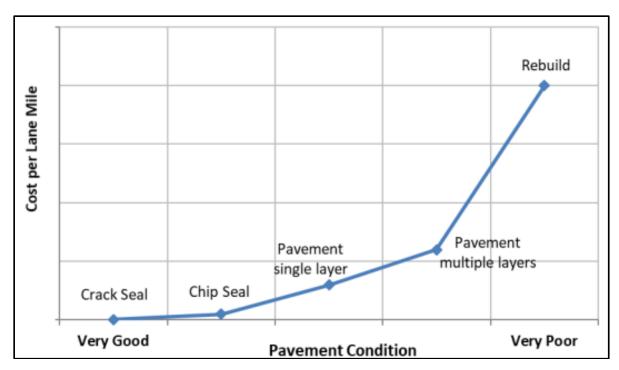


Figure 1.1: Pavement condition-cost per lane mile relationship (Coplantz 2021)

The current Oregon Department of Transportation (ODOT) pavement program is underfunded (Coplantz 2021). This insufficient funding level, combined with the increasing cost of paving and increasing traffic levels, has necessitated the development of low-cost but effective alternative solutions for preserving and maintaining Oregon's roadway network. Chip seals are low-cost pavement preservation solutions that enable transportation authorities to pave more lane miles while improving the state's overall pavement quality and user comfort despite budgetary constraints. Figure 1.2 summarizes Oregon's average annual treatments by lane miles. Coplantz (2023) reported that the increase in paving costs due to inflation and the reduction in funding led to a decrease in the length of annually treated lane miles. This reduction in treated lane miles is expected to worsen (increased reduction) in 2025 and 2027. However, as seen in Figure 1.2, even though a significant reduction in paving lane miles is anticipated through 2027, chip seal lane miles are expected to remain constant. This prediction again shows the chip seal's necessity and significance for Oregon's roadway network. To preserve the network-level pavement condition, the percentage of lower-cost paving alternatives, such as chip seals and thin asphalt overlays, may need to increase in the long run.

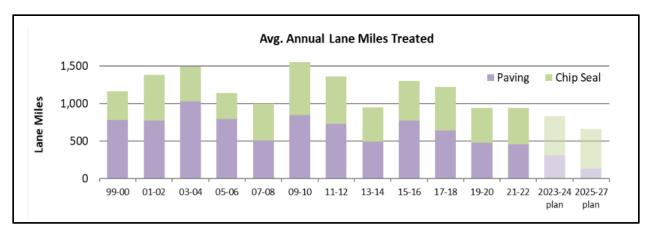


Figure 1.2: Chip seal and paving lane miles in Oregon between 1999-2022 and projection through 2027 (Coplantz 2023)

The efficacy of chip sealing is strongly dependent on the material quality, design, construction technique, equipment, workmanship, traffic, substrate condition, and environmental factors such as temperature, humidity, wind, etc. (Buss et al. 2016). In addition, an efficient quality assurance methodology for chip seals plays a significant role in achieving the intended service life of chip seal applications (Gransberg and James 2005; Kumbargeri et al. 2018; Malladi and Castorena 2019; Rawls et al. 2016). Chip seal quality assurance parameters can be listed as follows: aggregate-binder adhesion, aggregate and binder application rate and uniformity, aggregate embedment depth, aggregate retention, asphalt binder quality and temperature, the performance of the binder and aggregate, and pavement substrate condition (Gransberg and James 2005; Ozdemir et al. 2018; Praticò et al. 2015).

In the ODOT research report SPR 777 (Buss et al. 2016), a chip seal design method was adapted for ODOT. ODOT is currently in the process of implementing this new design method. It is expected that this new design method is going to improve the long-term performance of chip seal roadway sections in Oregon. However, it is critical to ensure that the construction applications follow the guidelines in the design method developed for ODOT. It is essential to design, develop, and implement technologies for field and laboratory test procedures for chip seal quality control. Without a comprehensive, periodic, and effective quality assurance (QA) / quality control (QC) strategy, it may not be possible to observe the benefits of new design methods or any other improvement in chip sealing technologies. It is even possible that the constructed chip seal roads may fail before the intended service life, although they were designed by following comprehensive methods and procedures.

Considering budgetary challenges and growing traffic demands in Oregon, chip seals offer a practical and affordable method for preserving and maintaining existing pavements. To maximize the benefits of chip seals, implementing robust QA/QC measures is crucial for long-term success and reliability on highway network. In this research study, QA/QC procedures were developed to increase the performance and longevity of chip seals in Oregon. The primary distresses in chip sealing; aggregate loss, and bleeding were quantitatively evaluated. Modified sweep and pull-off tests were developed to address aggregate loss in chip seals, with their effectiveness compared to the Vialit test. Samples from chip seal constructions located in two distinct regions of Oregon (Pendleton and Woodburn) were collected and tested in the laboratory

to assess adhesion performance. Aggregates and binders from these projects were also used to prepare specimens in the laboratory, which were then subjected to various curing times to assess their aggregate retention performance. The outcomes obtained from all three experimental methods were compared and correlated to recommend the most effective and practical testing approaches. Based on the results obtained, threshold limits were established to differentiate between "good" and "poor" adhesion characteristics. The recommended methods were utilized to investigate the impact of dustiness and surface moisture on the aggregate retention performance of the chip seal samples. It has been observed that the developed adhesion test methods effectively reported aggregate retention performance. While dustiness was seen to have a negative effect on aggregate retention, it was found that wet surface aggregates provided higher aggregate retention compared to dry surface aggregates. Using developed adhesion tests, the aggregate retention performance of chip seal samples prepared with four different aggregates from various regions of Oregon and the two most commonly used emulsions—one anionic and one cationic—was also reported.

Monitoring the Emulsion Application Rate (EAR) before construction is crucial for the success of chip seal projects. Ensuring the quantity of applied emulsion aligns with the target EAR is critical for achieving a high-performance chip seal. The wireless OreTackRate system, developed in project SPR818 (Coleri et al. 2020b), for measuring tack coat application rate was utilized to measure the in-situ EAR of chip seals in two construction projects. The tack lifter recommended by Rawls et al. (2016) was developed at Oregon State University Asphalt Materials and Pavements (OSU-AMaP) for this research project and was used to determine the amount of emulsion absorbed by the pavement. To assess the bleeding susceptibility of chip seals, pre- and post-construction macrotexture measurements were performed using a costeffective laser texture scanner developed by the OSU-AMaP research group and a commercial high-speed profiler system. In Oregon, the sand patch method, which can be influenced by the operator and necessitates traffic closures, is currently employed for measuring macrotexture (Buss et al. 2016). To overcome those problems and to increase the practicality of macrotexture measurements, sand patch test outcomes were correlated with a laser texture scanner and highspeed profiler readings. It was found that the laser texture scanner demonstrated higher accuracy in classifying near-failing sections and susceptibility to bleeding in chip seal compared to the high-speed profiler, achieving classification rates of 98% and 95%, respectively. The high accuracy in classification ability and the strong correlation obtained between these measurements offer a practical, reliable, and safer method for macrotexture assessment in chip seal sections. The high-speed profiler system can be used to identify sections with potential issues, which can be further assessed by conducting laser texture scanner measurements. Due to their practicality (no traffic closure and conducting measurements at highway speeds), high-speed profilers are important systems for finding locations with issues (low texture), but they were determined to lack the accuracy and precision the laser texture scanner would have.

A laboratory bleeding test was also developed using the Hamburg Wheel Tracker (HWT) device and the laser texture scanner. Rubber wheels replaced steel wheels in the HWT tests to prevent aggregate crushing. Both field samples and laboratory-prepared samples, using aggregates and binders sampled from the construction sites, were tested. Based on the results obtained, the bleeding failure thresholds were determined. Lastly, to reduce the environmental impact of future chip seal construction, Reclaimed Asphalt Pavement (RAP) was substituted with natural aggregates in chip seal samples at a 100% replacement rate. The aggregate retention and

bleeding susceptibility of these samples were then reported using the test methods developed in this report. It has been observed that RAP aggregates provide nearly the same level of aggregate retention as Natural Aggregates (NA), and it has been concluded that RAP is more compatible with cationic binders. It has also been found that the binder surrounding RAP aggregates makes chip seals more susceptible to bleeding. However, these bleeding issues can be mitigated by reducing the emulsion application rates, ultimately reducing the paving cost and their environmental impact. Implementing these developed methods and technologies is expected to enhance Oregon's chip seals' longevity, performance, and sustainability.

## 1.1 KEY OBJECTIVES OF THE STUDY

The study's main goals are to:

- Identify the primary factors influencing chip seal performance.
- Develop laboratory and in-situ test methods to assess chip seal performance in Oregon.
- Assess the performance of RAP in chip seal applications.
- Evaluate different emulsions and aggregate sources commonly utilized by ODOT and document their performance outcomes.
- Test the OreTackRate system's ability to measure emulsion application rate in chip seal construction.
- Investigate the effectiveness of high-speed profiler and laser texture scanner systems in measuring macrotexture instead of sand patch tests to increase reliability, practicality, and safety.

## 1.2 ORGANIZATION OF THE REPORT

This research study focused on the development of reliable, cost-effective, and practical testing methods and technologies for enhancing quality control in chip seal construction within Oregon. The layout of this report is organized as follows:

- Chapter 1.0 emphasizes the necessity for this research, presents the general methodology adopted, and lists the core objectives pursued.
- Chapter 0 presents a comprehensive literature review, examines chip seal design methods currently in use, and details existing chip seal quality control procedures.
- Chapter 3.0 of this report is titled "Aggregate Binder Adhesion". The primary objective of this section is to develop an effective, practical, and reliable test method that can be utilized both in the laboratory and in the field to assess the aggregate retention performance of chip seals. Modified sweep and pull-off tests were developed, and their results were compared with those of the Vialit tests. These tests were conducted on both field samples and laboratory samples prepared using aggregates and binders sampled from the construction site. The results obtained were correlated, and thresholds were established to distinguish between poor and good adhesion levels. Using the developed method, the effects of dustiness and surface moisture on aggregate retention were investigated. This chapter also reports on the

- aggregate retention performance of four distinct aggregates, sourced from various locations in Oregon, using the two most widely used emulsions.
- Chapter 4.0 is titled "A Field Wireless Scale System to Measure Emulsion Application Rates" and focuses on in-situ measurements of the emulsion application rate (EAR) in chip seal projects, employing the OreTackRate system, a wireless scale technology developed in SPR818 (2020). It also highlights the use of the Tack Lifter to determine effective EAR.
- Chapter 5.0 is titled "In-Situ Macrotexture Measurements Using Different Technologies". It addresses the evaluation of bleeding and embedment susceptibility in chip seals using macrotexture measurements. These measurements were performed with a low-cost laser texture scanner developed by OSU-AMaP, a high-speed profiler system, and the sand patch test. The data obtained from these tests were correlated, and their performance was reported.
- Chapter 6.0 is titled "Bleeding Tests". The main objective of this section is to introduce a laboratory bleeding test utilizing the Hamburg Wheel Tracker (HWT) device with rubber wheels and the developed laser texture scanner.
- Chapter 7.0 is titled "Aggregate Retention & Bleeding Performance of RAP in Chip Seal". The main objective of this chapter is to assess bleeding susceptibility and aggregate retention performance of RAP aggregates in chip seals.
- Chapter 8.0 provides a summary of the key findings and conclusions derived from the research conducted in this study.
- Chapter 9.0 offers a detailed list of all the references cited throughout this report.

# 2.0 LITERATURE REVIEW

## 2.1 CHIP SEAL DESIGN METHODS

In many countries, the success of chip seal application is expected to be highly controlled by the experience and judgment of the construction crew, while the engineering component is often overlooked (Gransberg and James 2005). However, various engineering approaches to chip seal design have been developed and implemented over time. Chip seal design methods used in Oregon and other states are summarized in this section, along with other methods followed in other countries.

# 2.1.1 Chip Seal Design Method of Oregon DOT

The chip seal design criteria in Oregon are outlined in the Oregon Standard Specifications for Construction (OSSC) under subsections 00710-Single Chip Seals and 00711-Pre-Coated Chip Seals, and 00712-Multi-layer Chip Seals(ODOT 2021). The single chip seal application was referred to as 'Single Application Emulsified Asphalt Surface Treatment' in subsection 00710. In the ODOT research project SPR777, Buss et al. (2016) conducted laboratory and field tests to assess the performance of Oregon's chip seals. Following that research study, the "Implementation Phase of SPR 777 Study and Guidance for a Chip Seal Performance Specification (Buss et al. 2021)" report was published by Oregon DOT with two workshops conducted with chip seal stakeholders (contractors, binder suppliers, and ODOT personnel). This report re-assessed the chip seal performance specifications in SPR 777 (2016), and suggested potential modifications for Oregon Standard Specifications for Construction (ODOT 2021). Buss et al. (2021) stated that having a performance-based criterion for the contractors would increase the performance of the chip seal treatments. In the following paragraphs, some essential requirements and specifications given in OSSC together with the research studies conducted by Iowa State University (Buss et al. 2016 and 2021) are summarized.

In the OSSC section 00710, the application rate for emulsion and aggregate was given in Table 2.1. When the values given in Table 2.1 were examined, it can be observed that the provided application range is quite broad. The specification also mentions that the engineer would determine the exact emulsion and aggregate application rates. OSSC (2021) also highlights that grading, unit weight, soundness, durability, and harmful substance tests should be conducted on the aggregates used in chip seal projects. In OSSC, only emulsified asphalt was mentioned since hot asphalt binders are not commonly used in the chip seals of Oregon anymore.

Table 2.1: Emulsion and aggregate application rates (ODOT 2021)

Chip Seal Design	Emulsified Asphalt Application Rate (gal/yd²)	Aggregate Spread Rate (yd³/yd²)	
Fine	0.25-0.40	0.004-0.009	
Single Size Medium	0.40-0.65	0.005-0.015	
Graded Medium	0.40-0.65	0.005-0.015	
Coarse	0.33-0.70	0.009-0.018	

In the reports published by Buss et al. (2016) and Buss et al. (2021), the McLeod and New Zealand chip seal design methodologies were investigated and compared with the application rates given in OSSC (ODOT 2021). In addition, a spreadsheet was prepared by Buss et al. (2021) so that the contractors can use it to determine emulsion and aggregate rates in chip seal construction. The following sections summarize the McLeod and New Zealand chip seal designs, which Buss et al. (2021) suggested utilizing for the Oregon chip seal design.

## 2.1.1.1 McLeod design method

McLeod improved empirical formulas for determining asphalt binder and aggregate rates for chip sealing by using construction and performance data (McLeod 1969). The provided formula considers traffic, climate, aggregate embedment depth, and several other parameters to determine application rates. The aggregate application rate provided by McLeod is presented in Equation (2-1).

$$C = 46.8(1 - 0.4V)HGE$$
(2-1)

Where:

C=Aggregate application rate (lb/yd²)

V=Voids in Loose Aggregate (%)

H=Average least dimension of aggregate (in)

G=Bulk specific gravity of aggregate

E=Traffic wastage factor

The wastage allowed, and traffic wastage factor used in the McLeod design method are given in Table 2.2. Buss et al. (2016) stated that percent wastage can be selected as 5% for rural & residential pavements, 10% for higher volume roads, and 15% for state highways.

Table 2.2: Traffic wastage factor and percent waste allowed (McLeod 1969)

Wastage allowed	Traffic wastage factor
1%	1.01
2%	1.02
3%	1.03
4%	1.04
5%	1.05
6%	1.06
7%	1.07
8%	1.08
9%	1.09
10%	1.10
11%	1.11
12%	1.12
13%	1.13
14%	1.14
15%	1.15
· ·	·

In McLeod's design, the average least dimension (ALD) parameter given in Equation (2-1) is illustrated in Figure 2.1. The aggregate least dimension, often known as the ALD, is the average of the aggregate particles with the most diminutive dimensions. This concept was developed by Hanson (1935) and is considered one of the essential parameters in the McLeod Design procedure. Cover aggregate particles on the asphalt binder tend to settle on their flattest surfaces after sufficient traffic (Hanson 1935). The wastage factor is the anticipated aggregate loss due to whip-off by traffic and uneven application.

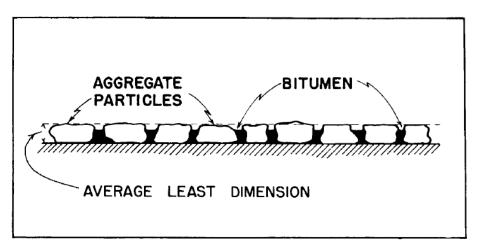


Figure 2.1: Average Least Dimension (ALD) concept (McLeod 1969)

This ALD method proposed by Hanson (1935) showed the significance of the 'aggregate embedment' phenomenon. If the aggregates do not embed sufficiently into the binder, then the aggregate retention performance of the chip seal may be poor. On the other hand, having a high aggregate embedment value may increase the possibility of bleeding. Considering that bleeding and aggregate loss are the two most significant failure mechanisms for chip seals (Gransberg & James 2005), the relevance of the aggregate embedment value may become more evident. In this regard, a more detailed discussion related to aggregate embedment will be provided in the following sections.

McLeod (1969) stated that the proper application of asphalt binder should embed each particle of cover aggregate to a depth of 70 percent; particles embedded to less than 50 percent are susceptible to being ripped out by vehicles. Also, factors such as traffic, existing pavement surface conditions, and the binder that the aggregate may absorb should be considered in the determination of asphalt binder content. The asphalt binder quantity to be applied can be calculated using Equation (2-2).

$$B = \frac{2.244HTV + S + A}{R}$$

(2-2)

Where:

B=Asphalt binder application rate (gal/yd<sup>2</sup>)

H=Average least dimension of aggregate (in)

T=Traffic factor

V=Voids in Loose Aggregate (%)

S=Surface texture correction (gal/yd<sup>2</sup>)

A=Aggregate absorption correction (gal/yd<sup>2</sup>)

R=Fraction residual asphalt in the emulsion (%)

The traffic correction factor (T) is crucial in determining the binder application rate for the specified number of vehicles per day to achieve the desired 70%–80% aggregate embedment. Average Annual Daily Traffic (AADT) and traffic correction factor values are given in Table 2.3.

Table 2.3: Traffic Factor (T) and AADT (McLeod 1969)

AADT	Traffic factor (T)
Under 100	0.85
100-500	0.75
500-1,000	0.70
1,000-2,000	0.65
Over 2,000	0.60

A surface texture correction (S) in gallons per square yard must be added to the amount of asphalt binder used for chip sealing due to the texture of the existing surface. Based on pavement conditions, suggested surface condition factors are given in Table 2.4. If there is bleeding or flushed asphalt on the existing surface, up to 0.06 gal/yd<sup>2</sup> emulsion can be subtracted from the emulsion required for a "smooth" surface. On the contrary, if the existing surface is porous or has a high macrotexture value, up to 0.09 gal/yd<sup>2</sup> emulsion can be added to the normal emulsion requirement.

Table 2.4: Surface texture correction (S) for different pavement conditions (McLeod 1969)

Texture condition of the surface	Surface texture correction (S) (gal/yd²)
Black, flushed asphalt	Up to -0.06
Smooth, non-porous	0
Slightly porous and oxidized	0.03
Slightly pocked, porous	0.06
Badly pocked, porous	0.09

McLeod (1969) also developed a correction factor (A) for the asphalt binder that may be absorbed by chip seal aggregates. Aggregate absorption correction factor values are given in Table 2.5.

Table 2.5: Aggregate absorption correction factor (McLeod, 1969)

Aggregate	Aggregate absorption
absorption (%)	correction factor (gal/yd²)
<1	0
1-1.25	0.01
1.25-1.8	0.02
>1.8	0.023

Although McLeod did not include any parameter regarding climate in formulations given for aggregate and emulsion application rates, it was suggested that chip seal must be constructed in warm and dry weather in the early summer to embed aggregates into asphalt binder with the help of hot weather and traffic. In addition, it was emphasized that the chip seal should not be constructed after August 31. This is to ensure that the cover aggregate particles are adequately embedded before the start of winter by allowing at least one month of traffic during warm weather.

#### 2.1.1.2 New Zealand design method

It has been reported that chip seal treatments in New Zealand last for a long time (9.6 years) (Gransberg and James 2005). New Zealand owes this achievement to a successful design method, construction and contract processes, and quality control strategies (TNZ 2005). However, it should also be noted that the traffic levels and vehicle types in New Zealand are not identical to the U.S. New Zealand's design process is an advanced variation of Hanson's (1935) approach. Following a lengthy period of trial and error and field performance observations, they developed a chip seal design method that also considers elements such as the existing features of the substrate and the traffic conditions. The binder application rate formulation is provided in Equations (2-3) and (2-4).

$$V_b = [(ALD+0.7Td)(0.42-0.0485 \times log_{10}(elv \times v/l/d))] \times 0.221$$
 (2-3) 
$$R = V_b + A_s + S_S + G_S + C_s + U_s$$
 (2-4)

Where:

 $V_b$  =Binder application rate (gal/yd<sup>2</sup>)

ALD=Average least dimension (mm)

Td = Texture depth of existing road (mm)

elv =Equivalent light vehicles

v/l/d=Vehicles per lane per day

R=Final residual asphalt binder application rate (gal/yd<sup>2</sup>)

As=Absorptive surface tolerance (gal/yd $^2$ )

Ss=Soft substrate tolerance (gal/yd<sup>2</sup>)

Gs=Steep grade tolerance (gal/yd<sup>2</sup>)

Cs=Chip seal tolerance (%)
Us=Allowance for urban and/or low-traffic volumes (gal/yd²)

The equivalent light vehicles (*elv*) value given in the formula is provided to equate heavy trucks to light vehicles (cars). Based on this approach, one heavy truck is equated to ten cars. For instance, if the truck population is around 10-11%, the *elv* value would be equal to 2. On the other hand, "Ss, Gs, Cs, Us" parameters given in Equation (2-4) are defined as "site-specific adjustments" in New Zealand chip seal design specification (TNZ 2005).

"As" given in Equation (2-3) provided for the absorptive surfaces (e.g. open-graded porous asphalt (OGPA), an open-graded emulsion mix (OGEM), or a grader-laid asphalt), causing the binder to essentially "fade away" into the surface. This may result in a lower binder application rate, and the residual binder may not be sufficient to hold the aggregates together. In this situation, the rate of binder application can be raised by 0.022 to 0.044 gal/yd<sup>2</sup>.

The "Ss" parameter is given for soft substrates. First, the hardness of the surface is measured using the ball penetration test. If the ball penetration value is;

- Less than 1 mm, the ALD value should be increased by 1 mm.
- 2-3 mm, no change is needed.
- 3-4 mm, the ALD value should be decreased by 1 mm.
- Higher than 5 mm, chip seal should not be implemented; pavement should be repaired.

"Gs" is given for steep grades. Heavy trucks that move slowly and are traveling uphill can hasten the process of flushing the surface. The New Zealand technique suggests a reduction of 0.022 to 0.033 gal/yd² to prevent this early indication of failure. The "Cs" value given in Equation (2-3) is provided as a control on the aggregate shape. The maximum cubical aggregate is controlled by a ratio of ALD: AGD of 1:2.25. For instance, the binder should be increased by 10% if the ALD: AGD ratio is 1:20 and the gradation contains more cubical aggregate.

"Us" is given for lower traffic roads. Road control authorities and contractors in New Zealand were concerned about loose aggregate on the center line and street parking places; thus, they suggested raising application rates for lower-traffic roads. It was reported that the problem of chip loss might be handled by increasing the amount of binder applied from 10% to 20%.

The aggregate application rate for chip seal design can be calculated using Equation (2-5).

Aggregate application rate = 
$$\frac{750}{4LD}$$
 (m<sup>2</sup>/m<sup>3</sup>)

(2-5)

In New Zealand, aggregate application rates are often defined in terms of area per volume (m²/m³). The reason for that is that the team responsible for sealing can readily estimate the area (in m²) that will be covered with one load of chips (of a known volume in m³). In a compacted chip seal, the voids between the aggregates are assumed to be around 20%. Taking this into account, the aggregate application rate should be 625/ALD (m²/m³). However, with a 10% whip-off allowance, the aggregate application rate forms as Equation (2-5).

The expression given in Equation (2-5) was converted into gal/yd<sup>2</sup> and given in Equation (2-6).

$$\frac{1 \times ALD \times 25.4}{750} \times (LUW \times 16.02) \times 1.84 \text{ (lb/yd}^2)$$
(2-6)

Where:

ALD=Average least dimension (in) LUW=Loose Unit Weight (lb/yd²)

# 2.1.2 Other Chip Seal Design Methods

Chip seal design methods are based on experience or formulas obtained using various engineering approaches. Typically, contractors have evolved chip seal designs based on their field experiences in response to often changing materials and equipment, higher pavement performance expectations resulting from technology advances in vehicles, and changing road surface conditions (Gransberg and James 2005). Some other design approaches developed over the years were provided in this section.

#### 2.1.2.1 Hanson method

F.M. Hanson was the first to offer a scientific approach to the design of chip seals in 1935 (Hanson 1935). Hanson mentioned that the voids between the aggregates after the spreading process are about 50% of the total volume. However, compaction and traffic reduce this ratio to approximately 20%. Hanson also stated that if an appropriate amount of chips were placed on bitumen, the aggregates would bed into a single layer at their flattest surface, in shoulder-to-shoulder contact after the compaction. The average compacted depth of the seal coat after compaction due to traffic was almost equivalent to the average least dimension (ALD) of the sealing chips in any chip seal and with any size of the sealing chip. Figure 2.2 shows the chip embedment before and after the compaction.

Hanson (1935) highlights that for an efficient chip seal surface, the 20% air void content between the aggregates should be achieved by filling 65 to 70% of the void space with asphalt binder (Hanson 1935). Hence, the binder application rate can be calculated by using Equation (2-7).

$$R = ALD \times 0.20 \times 0.70 \ or \ R = 0.14 \ ALD$$

Where:

R=Residual binder application rate (1/m<sup>2</sup>)

ALD=Average least dimension (mm)

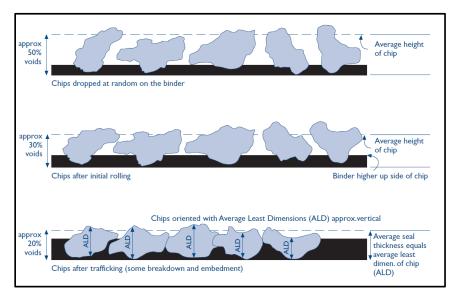


Figure 2.2: Conditions of chip seal embedment in the binder(NRB 1968)

#### 2.1.2.2 Kearby and modified Kearby method

Kearby (1953), considered a pioneer in chip seal design for many, developed approaches related to chip seal application rates for asphalt binder and aggregate (Kearby 1953). In this method, the unit weight, specific gravity, percentage of voids, and gradation of aggregates should be determined to calculate the application rates. The aggregate application rate can be found by performing the Board test method. In the Board test, an aggregate layer (one stone thick) was applied on a board that was half a square yard in size. This area and aggregate weight are measured and transformed into pounds per square yard.

The asphalt application rate can also be determined using a nomogram provided by Kearby (1953). The illustration of the nomogram is given in Figure 2.3. In this nomogram, average aggregate size, percent embedment of aggregates, and void percentage of aggregates were given as inputs, and asphalt binder rate in terms of gal/yd² was provided as output. Percent embedment is a crucial parameter often used to evaluate the chip seal performance (Boz et al. 2019; Kumbargeri et al. 2018; Ozdemir et al. 2018). As mentioned earlier, bleeding may arise if the aggregate embedment exceeds a particular threshold. On the contrary, the debonding of aggregate and binder may occur if the embedment percent is low.

Epps et al. (1981) updated the Kearby design technique to make the design consistent with field results. Texas Transportation Institute suggested the modified Kearby design to

TxDOT in 1981, which is still utilized in chip seal design by TxDOT today (TxDOT 2010). In the modified Kearby design, correction parameters for binder application rates under changing situations such as traffic and surface conditions were established. Aggregate application rates can be determined using a board test or Equation (2-8) given below (TxDOT 2010).

$$S = 27W/Q \tag{2-8}$$

Where:

S=Application rate of chips (yd<sup>2</sup>./yd<sup>3</sup>)

W=Loose unit weight (lb/ft<sup>3</sup>)

Q=The aggregate amount determined using the board test (lb/yd<sup>2</sup>.)

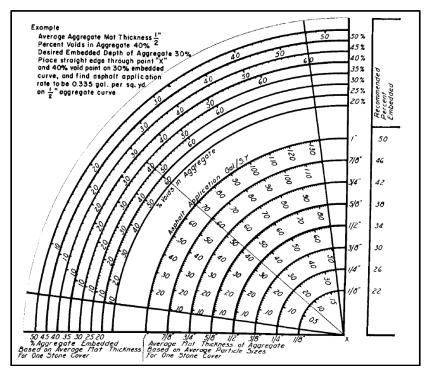


Figure 2.3: Asphalt application rate nomogram suggested by Kearby (1953)

Once the aggregate characteristics and current highway conditions are determined, Equation (2-9) can be used to calculate the asphalt cement application rate.

$$A = 5.61E \left(1 - \frac{W}{62.4G}\right)T + V \tag{2-9}$$

Where:

A=Binder application rate (gal/yd<sup>2</sup>.)

E=Aggregate embedment depth desired (in)
W=The aggregate amount determined using the board test (lb/yd²)
G=Dry bulk specific gravity of aggregate
T=Traffic adjustment factor
V=Surface condition adjustment factor

# 2.1.2.3 Austroads sprayed seal design method

Austroads (Alderson 2006) uses a modified version of the approach developed by Hanson (1935) for chip seal design. In addition to Hanson's approach, the formulas presented in the design also consider conditions such as traffic, underlying surface condition, embedment of the seal into the underlying substrate, and asphalt material that can potentially be absorbed by the chip seal aggregate or base layer aggregate. For the chip seal application to be successful, Alderson (2006) stated that it is essential to choose an appropriate treatment method suitable for the pavement surface's current condition. Details on the process for selecting the proper treatment are presented in the 'Selection and Design of Initial Treatments for Sprayed Seal Surfacing' report (Patrick 2016).

According to Alderson (2006), similar to Hanson's (1935) design method, ALD is one of the essential design data used to determine aggregate and binder application rates. A sprayed seal's volumetric design is based on the idea that aggregate particles tend to lay with their smallest vertical dimension (also called the lowest energy position). The ALD definition is the particle's minimum thickness when positioned on a horizontal surface. ALD can be determined by direct measurement or calculation using grading, median size, and flakiness index data. The application rate of aggregate and asphalt binder was provided separately for aggregate sizes 10 mm and larger, size 7mm and larger, and sizes smaller than 7 mm, separately. The design flow chart for single-coat surface coatings, according to Alderson (2006), is shown in Figure 2.4

The flowchart in Figure 2.4 starts with an assessment of traffic volume, which determines the basic void factor. This factor is then adjusted based on traffic conditions and aggregate shape (flakiness) to establish the design void factor. Once established, the design void factor is used to calculate the basic binder application rate using the average least dimension (ALD) principle. Lastly, the basic binder application rate is adjusted for embedment allowance, existing surface condition allowance, and aggregate adsorption allowance to determine the final design binder application rate.

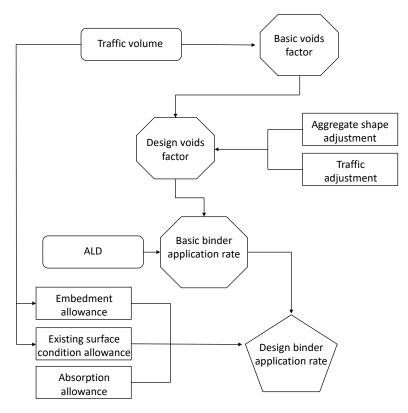


Figure 2.4: Flowchart for determining aggregate and binder application rates (Alderson 2006)

# 2.2 CHIP SEAL CONSTRUCTION METHODS

The construction phase is as critical as the design phase for chip seal roads to function well for their intended service life. For an effective chip seal construction, the existing condition of the infrastructure and environmental factors must be considered. Furthermore, chip seal construction equipment should be calibrated and validated regularly. Road construction personnel should also be trained. Lastly, an effective construction quality control procedure must be developed and implemented. Oregon Standard Specifications for Construction provided Oregon's chip seal construction details (ODOT 2021). This section summarizes the construction methodology and requirements set by ODOT (2021).

The company/contractor should have the equipment listed to perform chip seal construction.

- Asphalt Distributor
- Chip Spreaders
- Compactors (Pneumatic-tired or steel-wheeled rollers)
- Power Brooms

It was also noted that in order to ensure coordinated and consistent development of the job, the provided equipment should be at a sufficient number and capacity.

The construction phases of chip seal application are illustrated in Figure 2.5.

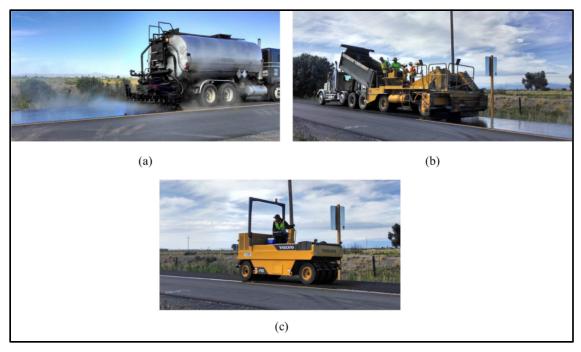


Figure 2.5: The chip seal construction phases; (a) spraying emulsion (b) aggregate spread on emulsion (c) chips were compacted by a pneumatic-tired roller (Buss et al. 2016)

The asphalt distributor truck must spray emulsified asphalt uniformly over the road. Emulsified asphalt may not be applied if the pavement temperature is below 70 °F or when humidity exceeds 75%. The application of the asphalt and chips should be finished at least 3 hours before sunset to ensure a good curing condition for the chip seal treatment. Due to climate conditions in Oregon, the chip seal construction can only be performed in July and August (ODOT 2021).

The surface condition of the existing pavement highly affects the chip seal performance. For instance, chips can penetrate through a relatively soft substrate, or the substrate may absorb some emulsion, negatively affecting the bond between the chips and the binder. In addition, chip seal treatment does not retrofit the pavement structurally. Therefore, all the pavement distresses (Potholes, rutting, large cracks, etc.) should be repaired/sealed before chip seal construction. Gransberg and James (2005) recommended that this sealing/patching should be completed 3-6 months before the chip seal construction in order to provide patches enough time to cure and avoid any bleeding issues.

Before applying the asphalt, the pavement's surface should be dry and clean to achieve proper bonding between the asphalt binder and the pavement surface. The temperature of applied emulsified asphalt should be between 140 °F- 185 °F. The aggregates should "immediately" cover the emulsified asphalt layer sprayed, and the operation speed should not exceed 15 mph. After the aggregates are applied, the surface should be compacted by at least two coverages with a pneumatic-tired roller and one coverage with a steel-wheeled roller. The rolling speed of compactors may not be more than 5 mph. After the compaction process and emulsified asphalt curing, the surface should be broomed to eliminate loose aggregates.

Important decisions, such as when the road can be opened to traffic and the quality control of the constructed chip seal layer, were left to the judgment of the project engineers. Visual inspections may produce erroneous results due to the subjectivity of the process, and premature chip seal failures may occur in the absence of adequate inspection. Achieving higher-quality chip seals in Oregon necessitates the development of test methodologies and quality assurance procedures with quantitative thresholds for acceptance or rejection.

# 2.3 CHIP SEAL QUALITY CONTROL TECHNOLOGIES

Monitoring the quality of chip seals has become extremely important, particularly in recent years, as funding for paving has decreased significantly while the number of heavy vehicles on the roads is continuously increasing. Developing adequate and effective quality assurance systems and procedures can lead to longer service life, higher-quality chip seal roads, and, consequently, more comfortable and safer roads. This section summarized current quality assurance methods and technologies available in the literature for chip seals.

#### 2.3.1 Adhesion Tests

In chip seal treatments, the adhesion between the asphalt emulsion and aggregates plays a key role in achieving high-quality final products. A strong bond between aggregate and binder would decrease the possibility of chip loss, which is one of the main failure mechanisms for chip seal roads (Gransberg and James 2005; Miller et al. 1991). The adhesion of aggregate and asphalt binder often depends on binder quality, aggregate shape, specific gravity, the level of clay content in the aggregates, temperature, the moisture of aggregate, binder and aggregate application rates, electrical properties of aggregates and binder and their agreement, etc. (Gransberg and James 2005). Most commonly used adhesion tests on chip seals are summarized in this section.

#### 2.3.1.1 Vialit test

The Vialit test is a widely used test method to determine the bond characteristics between asphalt binder/emulsion and aggregates for chip sealing. (BS EN 12272-3 2003). The Vialit test steps are illustrated in Figure 2.6. First, a certain amount (depending on the aggregate size used) of asphalt binder/emulsion (at the required temperature) is applied to the 20 cm by 20 cm metal plate. Afterward, depending on the aggregate size, 50 or 100 chips are dropped onto the binder/emulsion-covered plate using a suitable apparatus (to simulate the actual operation of the aggregate spreader in the field). Then, the chip seal layer on the plate is compacted in three passes of a 25 kg rubber wheel roller in both directions. The sample is then cured at room temperature for 24 hours. Before the test, the plate should be maintained in an environmental chamber at 5 °C for 20 minutes. The sample, which is taken out of the environmental chamber close to the test time, is then placed on the 3-pointed supports in an upside-down position, and the 510±10-gram steel ball is dropped three times within 10 seconds from a 50 cm height. After this process, the aggregates remaining on the plate are counted. The resulting 'adhesivity value' is calculated as shown in Equation (2-10).

Adhesivity value = b + c (for 100 chippings) or 2(b + c) (for 50 chippings)

#### Where:

b= the number of chippings that have fallen and been discolored by the binder c= the number of chippings adhered (retained) to the plate



Figure 2.6: Vialit test described in EN 12272-3 (a) emulsion-asphalt cement application; (b) spreading chips; (c) compaction; (d) curing of chip seal samples; (e) free fall of the ball over the plate; (f) counting fallen chips (Gurer 2010)

Although BS EN 12272-3 (2003) stated that the above-mentioned method should be followed for the determination of the adhesion properties of the asphalt binder/emulsion, some researchers preferred to make some modifications for the implementation of the Vialit test (Gurer 2010; Lee and Kim 2014, 2010; ODOT 2022). For example, Gurer (2010) used aggregate and asphalt cement/emulsion amounts used in the field rather than the aggregate and asphalt cement/emulsion amounts specified in the standard. Additionally, it was noted that rather than counting aggregates, percent aggregate loss (by weight) was computed and utilized as a performance criterion for binder adhesion; the lower the aggregate loss, the stronger the bond between the aggregate and the asphalt cement/emulsion was reported.

Lee and Kim (2014) used the Vialit test to assess the bond quality difference for two different asphalt emulsions (CRS-2-unmodified and CRS-2L-polymer modified) and two different aggregates (lightweight and granite) at different curing temperatures (25°C, 35°C, and 45°C) and different curing durations (1, 2, 3, 6, 12 and 24 hours). It was found that polymer-modified emulsion required a shorter curing time, reducing the time needed to open the road to traffic. In addition, lightweight aggregate provided lower aggregate loss values in early curing time than granite. For the higher curing durations (after 6 hours), no significant difference was observed between granite and lightweight aggregate

in terms of aggregate retention for both emulsion types. When the adhesion behavior at various curing temperatures was examined, the authors concluded that aggregate loss reduced as the curing temperature or curing time increased.

Lee and Kim (2014) also examined the adhesion behavior of asphalt emulsions at low temperatures (5°C and -20 °C). The samples were cured at 35 °C for 24 hours. Then, specimens were put in an environmental chamber at 5 °C and -20 °C for 24 hours and then tested. To prevent brittle detachment of emulsion as a result of shock impact, a 3-minute delay was planned before performing the Vialit test at low temperatures. The authors reported that the CRS-2L emulsion outperforms the CRS-2 emulsion in enhancing aggregate retention performance at low temperatures (below 5°C). Further, the aggregate loss ratio increased as the temperature reduced from 25 °C to below 5 °C (testing temperature); however, the aggregate loss values obtained at 5 °C and -20 °C were close to each other. The authors concluded that the polymer-modified emulsion performed well and satisfied the maximum aggregate loss value declared by the state (10% for North Carolina). In contrast, the non-modified emulsion failed that requirement.

ODOT (2022) – "Laboratory Manual of Test Procedures-TM426" also recommended using the Vialit test to determine adhesion characteristics between asphalt binder and aggregate. "Laboratory Manual of Test Procedures" (ODOT 2022) described the Vialit test procedure as follows;

- One hundred 6.3 9.5 mm reference aggregates should be washed and let dry for 24 hours at 50 °C
- 20 ×20 cm stainless steel plates are coated with asphalt emulsion or hot asphalt cement.
- Aggregates embedded in the binder as 10 rows and 10 columns
- For 48 hours, the plate was allowed to cure at 60 °C.
- After the plate is taken out of the oven, it is left to cool for 30 minutes at 25 °C.
- The plates were then conditioned for 30 minutes at -22° C after this cure.
- Then, a 500 g ball is dropped three times onto the upside-down plate from a 50 cm height. Results are expressed as a percentage of average retention.

The main advantages of the Vialit test are that it is a practical, affordable, and relatively less time-consuming test. On the other hand, the major drawback of the Vialit test method is that the test methodology uses impact and gravitational force to separate the chips from the binder, which can barely simulate the actual field chip loss mechanism. In addition, despite the fact that the Vialit test is recognized globally, several research studies have indicated that it is insufficient as a performance measure for chip seals (Louw et al. 2004; Walter S. Jordan III and Isaac L. Howard 2011). In contrast, some research reported that Vialit test is effective and reliable for determining aggregate-binder adhesion (Adams et al. 2018; Ignatavicius et al. 2021). Therefore, it is necessary to conduct the Vialit test alongside other adhesion tests to verify its accuracy.

## 2.3.1.2 Sweep test

The sweep test (ASTM D7000 2019) is one of the laboratory tests for evaluating the aggregate loss performance of chip seals. This test technique assessed the curing performance parameters of emulsified asphalt and aggregates by replicating the brooming of surface treatment in the laboratory.

In the sweep test (ASTM D7000 2019), a particular amount of emulsion (the standard recommends 1.42 kg/m² (0.32 gal/yd²)) is first applied onto an asphalt felt disc. Later, the aggregates are laid on this emulsion layer and compacted in both directions using a standard sweep test compactor. Finally, the test phase is initiated once the samples have been cured at the prescribed temperatures and times. During testing, a standard mixer abrades the sample's surface for 60 seconds using a nylon brush to simulate the sweeping action caused by the broom in the field. At the end of testing, % aggregate loss (by weight) is calculated. A schematic illustration of the sweep test is given in Figure 2.7.



Figure 2.7: Sweep test (ASTM D7000 2019) conducted on chip seal sample (a) preparation of asphalt felt disc; (b-c) applying emulsion on asphalt felt disc; (d) flatting the emulsion surface; (e-f) chip spread process; (g) compaction of chip seal sample; (h) curing the specimens in the oven; (i) performing sweep test using mixer and nylon brush (Wasiuddin et al. 2013)

Johannes et al. (2011) performed the sweep test as a performance indicator of chip seal. The researchers tested three different emulsion types (CRS-2, HFRS-2L, and HFRS-2) at three different application rates (Low (fills 35% of voids)-Medium (fills 50% of voids)-High (fills 70% of voids)), two different aggregate types (limestone and granite), aggregate gradations (fine and coarse) and curing times (2h and 6h). Aggregate loss

calculated from the sweep test was used as assessment criteria, i.e., the lesser the aggregate loss, the higher the bond between the aggregate and emulsion. Based on the results obtained, the authors stated that the sweep test is a useful tool for assessing the evolution of the emulsion-aggregate bond during the early stages of application. However, it cannot be used as a design tool for chip seals because the aggregate loss value obtained was not correlated with the binder rates used. In addition, aggregate gradation was found to be an important parameter that affected aggregate loss as a result of the sweep test. Fine-graded chip seal samples outperformed the coarse-graded chip seal specimens. Hence, the authors suggested a revision in the ASTM D7000 (2019); instead of using aggregate gradation and aggregate application rate provided in ASTM D7000, the actual field application rates and gradation should be used in the test. The authors also stated that emulsion type significantly affected aggregate loss percentage. CRS-2P provided better results than HFRS-2P and HFRS-2L, regardless of aggregate type, gradation, and binder application rate used.

Wasiuddin et al. (2013) conducted the sweep test and visual inspections on both emulsion (CRS-2P) and hot asphalt (PAC-15 and AC20-5TR) chip seals. Five different aggregate types (coated and uncoated expanded shale lightweight, limestone, granite, and expanded lightweight clay aggregate) were tested. Based on their trial tests, the authors declared that the optimum curing temperature and time were 28 °C and 48h. Also, it was found that as the aggregate size increased, the percentage of aggregate loss increased. The measured performance of expanded shale aggregate was better than expanded clay aggregates for both field and laboratory tests.

Contrary to the conclusion drawn by Johannes et al. (2011), Wasiuddin et al. (2013) reported that increasing the emulsion/hot asphalt rate reduced the aggregate loss rate. Overall, aggregate and emulsion types significantly affected the aggregate loss percentage obtained from the sweep test. One of the most important conclusions drawn by Wasiuddin et al. (2013) was that sweep test results were well correlated with the field performance rankings (based on visual inspection), i.e., the chip seal design with lower aggregate loss maintained its good condition longer in the field.

Shuler (2011) suggested a modification to the sweep test; that is, a 40% percent aggregate embedment requirement is necessary to eliminate the difference between aggregate gradation. Moreover, curing time should be based on the percentage of moisture loss in the emulsion. Shuler (2011) indicated that chip loss could be reduced below 1% if the moisture loss in chip seal emulsion is above 80% (meaning a significant percentage of the water in the emulsion evaporated). Howard et al. (2011) also recommended monitoring the moisture of the chip seal surface to decide when to open the road brooming process and traffic based on the modified sweep test.

The sweep test was designed as a laboratory test attempted to simulate the brooming effect in the field. Nonetheless, several research studies employed it as a performance indicator. A limitation of this test method is that it cannot be used in the field, and the sample preparation phase is relatively long.

#### 2.3.1.3 Flip over test

The flip-over test examines the quantity of extra aggregate on the specimen as part of the sweep test process ASTM D7000 (2019). In this test, the samples prepared for the sweep test should be rotated vertically (90 degrees). The sample is gently brushed to separate the loose aggregates from the bitumen-based material. Then, samples are weighed before and after the test to determine the aggregate loss (% by weight). In some research projects, a flip-over test was performed to assess the chip seal performance (J. Lee & Kim, 2014, 2010).

#### 2.3.1.4 Pull-out test

The pull-out test determines the maximum load value obtained by pulling the aggregates embedded in a certain amount of asphalt binder or the area covered with bitumen material after being pulled out from the binder. This pull-out force or the contact area data provides information about the adhesion level between aggregate and bituminous binder. This section summarizes some of the pull-out test methods available in the literature.

The Road and Traffic Authority (RTA 2012) of New South Wales, Australia, has been employing the pull-out test technique (T238-Initial adhesion of cover aggregates and binders) to assess the compatibility of the aggregate and bituminous binder (under both wet and dry circumstances) in chip seals. In the T-238 (also known as the Australian pullout test) test, cutback asphalt binders (viscosity should be around 15000 stokes) are used to conduct the test at room temperature. In addition, the method has defined the necessary conditions for five types of aggregate moisture conditions (i.e., as received, clean and dry, dusty, saturated surface dry, and saturated surface wet). During the test phase, the bitumen-based material is heated and homogeneously applied to the tray in approximately a 3 mm film layer. Afterward, 20 aggregates are manually embedded in the binder. After cured as soaked or unsoaked, the aggregates embedded in the binder are pulled-out from the bitumen at a constant vertical pressure using a long-nose plier while the aggregates are still in the water at room temperature. Aggregates are divided into three classes based on how much of the asphalt they have taken off: entirely stripped, slightly stripped, and not stripped. After each aggregate particle has been visually inspected, the percentage of aggregate particles (measured by number) that have been stripped from the binder should be computed as follows;

- Fully stripped count one unit
- Partly stripped count one-half unit
- Not stripped count nil

The percentage stripping of aggregate can be determined with the abovementioned percentages.

A modified Australian pull-out test (T-238) test was recommended by Senadheera et al. (2006). In this modified test, amendments were made to both the sample preparation and testing stages. Instead of using the cutback approach in the T-238 test, the authors preferred to heat the asphalt binder up to 320 °F and emulsions up to 170 °F to eliminate

the water requirement and better simulate the field conditions in Texas (Senadheera et al. 2006). Samples were prepared using 72g of asphalt on a 6" by 6" square metal tray heated to a contact temperature of 100 °F, representing surface temperatures during chip seal construction season in Texas. The target binder thickness was kept at around 3 mm, as in the original T-238 test technique. For an efficient pull-out process, aggregates were attached to the metal nails using glue, as shown in Figure 2.8.

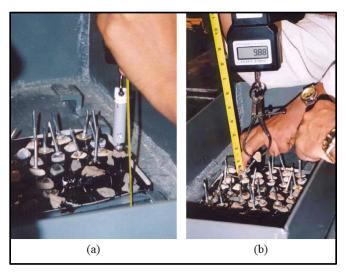


Figure 2.8: Modified Australian pull-out test; (a) sample preparation (b) performing the pull-out test (Senadheera et al. 2006)

Senadheera et al. (2006) used thirty clean and dry aggregates with the nail adhered to the top placed into the asphalt binder at the same temperature, and the metal tray with aggregates was cured for 24 hours at room temperature. Unlike the T-238 test, except for the bitumen-coated area, the parameters of ultimate tensile stress, elongation length, and pseudo energy were also determined in the modified Australian test. Peak force and projected contact surface area were used for tensile strength calculation. A picture of aggregates after the pull-out test is illustrated in Figure 2.9a. The coated area can be found using the following assessment criteria;

- 100% rating Asphalt covers nearly 75% of the area.
- 50% rating After pulling out, 25 to 75 percent of the contact area remains asphalt.
- 0% rating Asphalt covers less than 25% of the area.

An aggregate with a rating of 100 percent is considered as one, a rating of 50 percent is counted as half, and a rating of 0 percent is counted as zero.

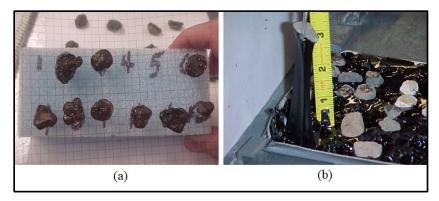


Figure 2.9: (a) Detached aggregate samples after modified Australian pull-out test (b) Elongation length measurement during the pull-out test (Senadheera et al. 2006)

The longest asphalt string created was also measured during the pull-out test, as shown in Figure 2.9b). This metric is intended to assess the aggregate's ability to revert to its former position following a period of distress. Pseudo energy, on the other hand, can be calculated by multiplying tensile strength and elongation measurement data.

Queensland Department of Transport and Main Roads (2022) and Southern African Bitumen Association (SABITA 2020) also recommended the pull-out test for the chip seal treatments. First, temperature measurements are taken from a few aggregates on the road surface to the nearest 0.5°C and recorded. The start time and temperature values of the test should be recorded. Next, the alligator clips are attached by selecting a stone from the road surface. With the help of a spring scale, the upper part is lifted slowly (20 g/s) until the aggregate separates from the bituminous material and the maximum load value is recorded. The test should be repeated nine times, and if the stone twists during the test and results in a significantly reduced pulling force, the result should be disregarded. A temperature correction factor can be applied to the pull-out force obtained to modify the pull-out force to 40 °C as follows:

$$A = log f_2 = log f_1 - 0.05(40 - T)$$
(2-11)

Where:

f<sub>2</sub>=Pull-out force corresponding to 40°C (g)

 $f_1$ =Pull-out force (g)

T=Surface temperature (°C)

The advantage of the pull-out test is that it is practical and low-cost. Also, it provides valuable information about the aggregate and binder adhesion both in the laboratory and the field. The major limitation of this test is that it provides bond properties of a specific point rather than a large area.

The pull-off test (also known as 'PATTI- Pneumatic Adhesion Tension Test' or 'BBS-bitumen bond strength') is a test method developed for testing the adhesion of coating systems from metal substrates (ASTM D4541 2022). In the pull-off test (Figure 2.10), the

coating was fixed on a dolly or stud with an adhesive. After the glue has cured, a test apparatus is attached to the loading fixture, and a direct tensile load is applied. The test is then performed until a specific load value is reached or the material has fully detached from the surface. Numerous studies used the pull-off test to evaluate the adhesion properties between different asphalt binders/emulsions (Miller et al. 2010; Pasquini et al. 2014; Rahman et al. 2020; Zhou et al. 2014).

ASTM D4541 (2022) specified that the pull-off test might be conducted on any flat metallic/plastic substrate. In some investigations, researchers chose to use a metal surface for the pull-off test (Zhou et al. 2014). On the other hand, in some of the investigations, the researchers found that it was more appropriate to conduct this test on a big piece of aggregate since they believed that it would more accurately represent the aggregate-binder bond strength (Miller et al. 2010; Pasquini et al. 2014; Rahman et al. 2020). The primary shortcoming of the PATTI test is that it does not take aggregate and macrotexture factors into account. Consequently, it may be used to evaluate the performance of various types of binders by neglecting the aggregate effect.



Figure 2.10: Pull-off test setup (Zhou et al. 2014)

#### 2.3.1.5 Frosted marble test

The frosted marble test (FMT) is a method that is being used to examine the adhesion between the aggregate and asphalt binder/emulsion. A schematic illustration of FMT is given in Figure 2.11. Benedict (1990) created the first test procedure. The FMT apparatus is a modified cohesiveness tester with a hooked foot and a torque wrench for removing an acid-etched glass bead (Jordan 2010). Howard and Baumgardner (2009) described the test technique utilized to assess aggregate retention performance for the US Highway 84 project. The test procedure is explained as follows;

- A. Change the regular 28.6 mm diameter cohesiveness tester foot to a 50 mm hooked foot, then set it to make contact with the frosted marbles immediately below the center of the stone. The jamb nut secures in position.
- B. The air pressure should be set to 70 kPa (10 psi) to reduce friction. (It is optional but recommended).
- C. 9.0 + 0.2 g of chip seal emulsion should be added to three standard-size plates. The plate should be placed on a level surface, allowing the emulsion to set a level position. When the emulsion is level, the acrylic template should be placed directly over the trough plate, and 15 frosted marbles (5 per trough) should be attached. The template may be removed in a few minutes or when the initial set occurs. The template could be discarded after a short while or after the initial set. Then, specimens should be cured.
- D. After the prescribed curing period, the trough plate was positioned on the cohesion testing base with the hooked foot for 2-point static contact. The torque needed to displace the marble was measured and reported by the follow-up pointer. The chip retention strength was calculated using the average torque values of five subsequent tests.
- E. The leftover bitumen in the trough may be removed after the test and analyzed for moisture or solvent content.

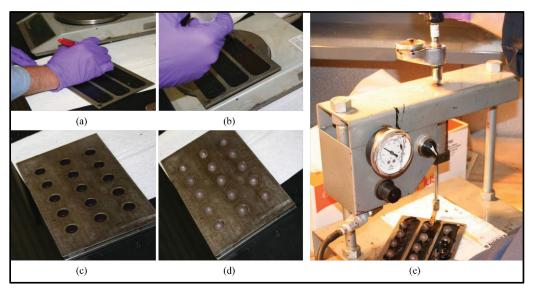


Figure 2.11: Frosted marble test setup (a) marking procedure (b) emulsion application (c) positioning template over the tray (d) placing marbles (e) performing frosted marble test (Jordan, 2010)

Suppliers frequently utilize the conventional FMT to get information on cure rates to determine when to open the road to traffic; however, Howard et al. (2011) stated that the moisture loss parameter is more effective than cure time in deciding traffic opening based on FMT test conducted on several types of emulsions. A dramatic strength gain was reported when the emulsion's moisture loss exceeded 75-80%.

The primary advantage of the frosted marble test is that it is one of the few procedures for evaluating binder performance that uses torque (which can approximate wheel movement

to some extent). However, it does not provide direct information on the aggregate (chip)-binder adhesion.

## 2.3.1.6 Pennsylvania aggregate retention test

Kandhal and Motter (1991) developed the Pennsylvania Aggregate Retention Test (PART) to model the effect of traffic on chip seal treatments. The test apparatus consists of a balance, a sieve, a pan, a sieve shaker, rubber pads, and a compression machine. First, chip seal samples are prepared in the pan and subjected to the necessary compaction and curing processes. Then, the first aggregate loss is calculated by flipping the pan upside down. The pan is then positioned upside-down and at a 45° angle in the sieve shaker. After shaking for five minutes, the total loss is determined and expressed as a percentage. The test setup used by Kandhal and Motter (1991) is illustrated in Figure 2.12. Although PART is seen to be an acceptable test for comparing various aggregates and binders, it is not considered to represent the field circumstances.



Figure 2.12: Pennsylvania aggregate retention test (Rahman et al. 2020)

#### 2.3.1.7 Skid resistance tests

The skid resistance test does not directly assess the bond properties between the aggregate and the asphalt binder. However, it can offer useful information about these properties in an indirect fashion. Chip seal owes its widespread use in pavements as a preservation treatment, among other features, to the skid resistance provided by the aggregate coating. The measurement of skid resistance is routinely performed as part of the pavement management system in most organizations on a predetermined schedule. The data from these tests are crucial for determining whether roads need to be chip-sealed

(Gransberg and James 2005). It was known that the skid resistance of the surface depends on the surface's micro and macro texture properties. Aggregate loss and bleeding reduce the skid resistance of the chip seal and may require a replacement. Hence, some studies used skid resistance to assess the chip seal quality (Buss et al. 2016; Gheni et al. 2017; Lee et al. 2012; Roque et al. 1991). There are several test methods to determine the skid resistance of pavement surfaces. These include, but are not limited to, the British pendulum test (ASTM E303 2022), the Locked-wheel test (ASTM E274 2015), and the Dynamic friction test (ASTM E1911 2019).

The British pendulum test (BPT) (Figure 2.13) quantifies the amount of energy dissipated when a rubber slider edge is driven across a wet test surface. The British Pendulum Testing (BPT) apparatus is made up of a pendulum with a weight at one end, a rubber shoe that is rubbed against the sample, and a gauge that yields a British pendulum (tester) number (BPN) (ASTM E303 2022). The most significant benefits of the BPT are its worldwide recognition in the assessment of skid resistance, the test's practicality and the equipment's lightweight, and the test's versatility in both the laboratory and the field. On the other hand, the drawbacks include the fact that the test can only be conducted at low speeds, the operator's influence on the results, the wind's impact on the observations, and the need to close traffic lanes when the test is conducted in the field (Mataei et al. 2016).

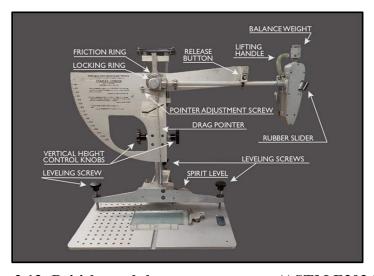


Figure 2.13: British pendulum test apparatus (ASTM E303 2022)

In the dynamic friction tester (DFT) (Figure 2.14a), a horizontally spinning disk is outfitted with three spring-loaded rubber sliders. When sliders contact the surface, the disk's rotational speed slows down because of the friction between the sliders and the disk. The sliders touch the pavement, and water is delivered when the tangential velocity reaches a certain threshold. As the sliders gradually slow to a halt, the resulting data for friction measurements is collected. The rotational forces on the sliders are used to quantify torque, which is then utilized to determine friction (DFT number) as a function of rotational velocity (ASTM E1911 2019). DFT, similar to BPT, may be used to measure friction in both the field and the laboratory. A major advantage of this method is that it permits friction to be measured at high speeds. On the other hand, this approach

has the limitations of necessitating traffic lane closure and providing point data rather than a certain area measurement (Ergin 2019).

The locked wheel test (LWT) (Figure 2.14b) apparatus comprises a vehicle with one or more test wheels built into it or as part of a suitable trailer pulled by a vehicle. The testing device is accelerated to the required speed. Water is supplied in advance of the test tire, and the braking system is activated to lock the tire. The resultant recorded force or torque is used to calculate the skid resistance of the paved surface, which is then reported as the skid number (SN) (ASTM E274 2015). This test procedure is practical and relatively safe in terms of operation; however, its operating and startup costs are high.

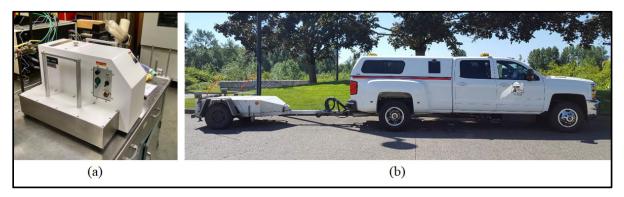


Figure 2.14: (a) DFT equipment (b) LWT setup (Buss et al. 2016)

Lee et al. (2012) conducted BPT, LWT, grip tester, and third scale model mobile loading simulator (MMLS 3) tests on chip seal samples. A strong correlation between BPNs and SNs was reported with a reasonably high coefficient of determination ( $R^2 = 0.74$ ). The authors asserted that the SN value could be accurately calculated from the BPN value acquired in the laboratory. In addition, BPT results exhibited a strong correlation with bleeding, i.e., the higher the bleeding, the lesser the BPN number obtained.

Buss et al. (2016) conducted the DFT test in conjunction with MTD measurements just after chip seal construction and a year after the construction. As expected, the MTD results showed a decreasing trend over time as aggregate embedment increased with traffic. However, the skid resistance values tend to increase over time. Therefore, the authors reported either no or poor correlation between the MTD results and skid resistance. This situation can be attributed to the fact that microtexture plays a more critical role than macrotexture, especially at slower speeds (Mataei et al. 2016; Schonfeld 1970). The conclusions reached by Buss et al. (2016) are similar to the findings of other investigations in the literature (Mataei et al. 2016).

The sand circle test is the primary performance test indicator in New Zealand (TNZ 2005). Although the skid resistance test remains essential in terms of providing a safe driving environment, it is doubtful to be used as a chip seal performance test since it does not provide direct information on aggregate and binder and their adhesion characteristics and is significantly affected by micro-texture, aggregate type, hardness and roughness values of aggregates and climate.

## 2.3.2 Chip Seal Aggregate and Binder Application Rate Measurement

Implementing the designed binder and aggregate rate in the field is of paramount importance to obtain a high-quality chip seal maintenance treatment (Gransberg and James 2005; Malladi and Castorena 2019; TNZ 2005). It should be emphasized that using an excessive amount of binder may cause bleeding, while an insufficient amount of binder may weaken the bond between the aggregate and the binder. Similarly, applying fewer chips to the binder may diminish skid resistance, while over-chipping often results in less embedding of the aggregate, which may result in less aggregate retention performance (Guirguis and Buss 2020). In both cases, the chip seal's service life is negatively impacted, i.e., early chip seal failure becomes inevitable. Hence, the binder and aggregate application rate measurements are essential to the quality assurance/quality control program.

The change in velocity and flow rates of the asphalt distributor can cause transverse and longitudinal non-homogeneous distribution of the asphalt emulsion along the way. In addition, the clogged nozzles may cause the asphalt binder not to be sprayed homogeneously (Figure 2.15). Therefore, regular distributor truck maintenance and calibration are required for the asphalt binder distributor trucks, and distributor truck drivers must receive fundamental training and certification to ensure that the equipment is operated effectively (Coleri et al. 2020b). Several methods and technologies have been developed to measure the asphalt emulsion application rate in the field for tack coat and chip seal applications (Coleri et al. 2017, 2020b; Malladi and Castorena 2019).



Figure 2.15: Examples of inconsistent asphalt binder applications (Mohammad et al. 2012)

ASTM D2995 (2014) is the only standard that addresses the measurement of the application rate of asphalt distributors. The summary of this test procedure is as follows:

- The pads are first weighed and positioned on the path the asphalt distributor will pass (Transversely or longitudinally oriented tarps may be employed to investigate the position dependence of emulsion application rate).
- A distributor of asphalt emulsion passes over the pads and sprays the asphalt emulsion on them.
- Option A: quickly remove the pads from the road and reweigh them instantly.

• Option B: oven dry the pads until a constant weight is reached to determine the residual asphalt in the emulsion.

Coleri et al. (2017) utilized ASTM D2995 (2014) to assess the uniformity and accuracy of tack coat application rates in the field and reported that the application rates for some of the distributor trucks were incoherent (Coleri et al. 2017). Additionally, it was claimed that ASTM D2995 (2014) is an impractical test due to its labor-intensive procedure and the safety risks associated with placing textile pads on the road (Coleri et al. 2020b). In addition, Coleri et al. (2020b) indicated that a significant portion of the applied emulsion could be lost when the pads were moved from the roadway to the side of the road for weighing. Muench and Moomaw (2008) also highlighted that when ASTM D2995 (2014) is used, there is a possibility that water would be lost from the emulsion before the weighing of the tarps, which may result in an inaccurate measurement. Moreover, Rawls et al. (2016) stated that the pavement surface's current texture influences the "effective" amount of emulsion available for bonding, which cannot be measured using the ASTM D2995 (2014) standard.

Rawls et al. (2016) introduced the 'Tack Lifter' device for the determination of 'effective' -(taking into account the quantity of binder that was absorbed by the substrate) emulsion application rate for tack coats and chip seal applications (Rawls et al. 2016; Rawls and Castorena 2019). The tack lifter device (Figure 2.16) is a device that has a certain weight and is placed on top of a layer of superabsorbent foam that has been applied to the surface of a pavement. The emulsion is absorbed by the absorbent sheet from the roadway surface. The weight of the emulsion soaked up by the superabsorbent may be used in conjunction with the area of the application surface to calculate the emulsion application rate. Without considering the amount of emulsion absorbed by the substrate, the approach calculates the effective application rate of the emulsion (Rawls et al. 2016). The field measurement results show a negative correlation between the MTD and the proportion of the applied emulsion absorbed by the tack lifter. The authors also mentioned that it was difficult to handle the ASTM D2995 (2014) sheets because of their large size, which was 12 inches by 12 inches. Besides, researchers concluded that emulsion leaked from the edges of the sheets as they were transported to the scale, which may lead to erroneous results (Rawls and Castorena 2019).

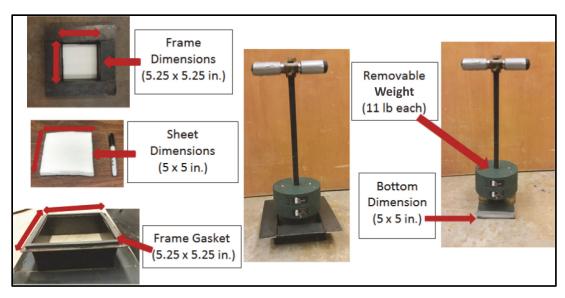


Figure 2.16: The tack lifter device for emulsion application rate measurements (Rawls et al. 2016)

To overcome the practicality issues of the ASTM D2995 (2014) standard, Coleri et al. (2020b) recommended using OreTackRate, i.e., using wireless scales controlled by a tablet computer application to measure the application rate of asphalt binder and uniformity of the distributor truck. The authors recommended that system for the certification and calibration of distributor trucks (Coleri et al. 2020b). The OreTackRate method consists of three wi-fi scales, one tablet computer, and asphalt shingles glued on plastic plates, as shown in Figure 2.17. A coefficient of variation value and a mean application rate error were calculated from the measured values to use for the certification and validation of the distributor truck.

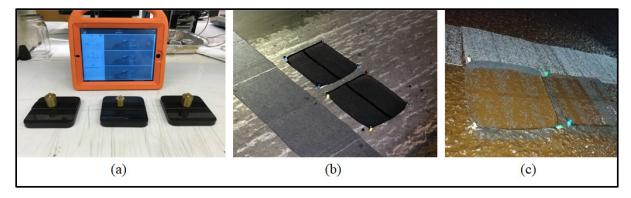


Figure 2.17: OreTackRate method to determine the asphalt binder application rate (a) The calibration of wi-fi scales and tablet computer (b) scales covered asphalt shingles next to textile pads used for ASTM D2995 (c) performing application rate and variability measurements in the field (Coleri et al. 2020b)

The measurements of the developed OreTackRate method were validated with the ASTM D2995 (2014) measurements (Figure 2.17b). The correlation between the two measurements is given in Figure 2.19. The results show a strong correlation between the two test methods utilized. The

higher error rates at high application rates are a result of the emulsion dripping from the ASTM D2995 pads. For this reason, OreTackRate measurements are expected to be more accurate (and also practical) than the ASTM D2995 measurements. Even though the OreTackRate technique is only utilized for tack coat applications, it appears promising for determining chip seal emulsion application rates.

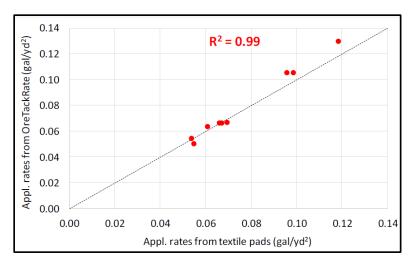


Figure 2.18: The correlation between application rate measurements obtained from OreTackRate and ASTM D2995 (2014)(Coleri et al. 2020b)

OreTackRate was developed by Coleri et al. (2017) to measure the total asphalt emulsion applied on the pavement surface. The tack lifter, on the other hand, was developed to determine the effective emulsion application rate on the pavement. By combining the OreTackRate and tack lifter, the emulsion absorbed by the existing substrate can be calculated. The research study presented herein aims to use both emulsion application rate measurement methods to determine the effective emulsion application rate and the emulsion absorbed by the substrate.

#### 2.3.3 Macrotexture Measurement Methods

For a chip seal, the term "texture" most commonly refers to the macrotexture or the texture that can be seen by the naked eye (from 0.5 mm to 10 mm). Microtexture, on the other hand, is known as the microscopic surface of the chip up to 1 mm (TNZ 2005). The definition of pavement macro texture was provided in ASTM E965; "the deviations of a pavement surface from a true planar surface with the characteristic dimensions of wavelength and amplitude from 0.5 mm up to those that no longer affect tire-pavement interaction". The spaces between particles determine macrotexture, whereas the surface irregularities of each aggregate determine microtexture. Figure 2.19 is provided to demonstrate these parameters. Micro and macrotexture significantly affect the skid resistance of the road (i.e., a rough macro texture and harsh microtexture combination provide the best skid resistance performance)(TNZ 2005).

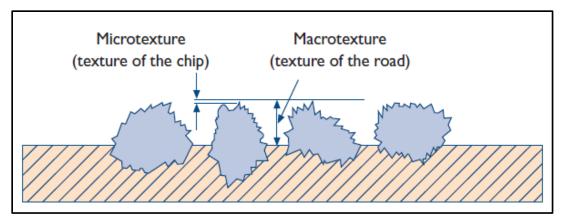


Figure 2.19: The illustration of microtexture and macrotexture terms (TNZ 2005)

The measurement of macrotexture can provide helpful information regarding the current performance of chip seal application. In many research projects, macrotexture was used as the primary performance indicator (Buss et al. 2016; Karasahin et al. 2015; Roque et al. 1991). In order to prevent the most prevalent form of chip seal failures, such as bleeding (Gransberg and James 2005), the macrotexture value must be greater than a particular threshold value. Nevertheless, a high macro texture value may indicate that the aggregates are not sufficiently embedded in the asphalt binder. A weak aggregate-binder bond may lead to the raveling problem in this case. Therefore, it should be aimed to keep the macro texture and aggregate embedment values at a certain level so that the chip seal can serve effectively throughout its designed service life. To satisfy that, Transit New Zealand (TNZ 2005) recommended measuring the macrotexture of the chip seal a year after the production via sand circle test according to TNZ T/3 (Transit New Zealand (TNZ T/3) 1981). The details of the test procedure are provided in Section 2.3.3.1. For chip seal roads with posted speed limits of 70 km/h or more, the macrotexture shall be at least 0.9 mm one year following chip seal construction. It is advised that chip seals that fall below this macrotexture value should be reconstructed (TNZ 2005).

Studies in the literature attempted to correlate macrotexture values and chip seal performance using various tests and visual inspection methods. Many reported a strong correlation between macrotexture measurement and chip seal performance (Adams and Kim 2014; Buss et al. 2021; Gransberg and James 2005; Haider et al. 2021; Karasahin et al. 2015; TNZ 2005). Shuler et al. (2011) provided a model to calculate the percent embedment of aggregate using macrotexture value and ALD of aggregate. Kutay et al. (2016) recently developed new methodologies for determining percent embedment from the field cores using image processing. The measured percent embedment was correlated with the macrotexture measurements. They also determined percent embedment thresholds for high-performance chip seals. A detailed explanation of that methodology, along with other widely used macrotexture measurement methods, will be provided in the following section.

#### 2.3.3.1 Sand patch test

In terms of methods for measuring macrotexture, the sand patch test is the only one that many states and countries agreed on (Gransberg and James 2005). ASTM E965 (2015), TNZ T/3 (1981), and BS EN 13036-1 (2010)) provide details of the sand patch test

procedure. The sand patch or sand circle test consists of a portable windshield, surface cleaning brushes, a sample container, a spreading tool, a ruler, and solid glass spheres with a roundness of 90 percent (ASTM E965 2015).

The test procedure is as follows:

- A known volume of sand (glass spheres) spread over a clean and dry pavement surface sheltered by a windshield.
- The glass beads are distributed by making a circle along the pavement's surface, achieving a smooth surface and filling all the voids between the aggregates on the pavement's surface.
- The texture depth of the pavement surface can be calculated using the volume of the sand and the circle area obtained.
- To obtain the average macrotexture depth, the same operator should perform the test at least four times at various random locations.

The average macrotexture depth can be calculated using Equation (2-12).

$$MTD = \frac{4V}{\pi D^2}$$

(2-12)

Where:

MTD = Mean texture depth (in)

V = Volume of sample (in<sup>3</sup>)

D = Average diameter of the area that the material covers (in)

The sand patch test method is suitable for both laboratory and field applications. The sand patch test method is practical and inexpensive. However, it has limitations, such as the inability to be utilized in rainy conditions, it provides macrotexture value for a limited area, and the fact that results might vary significantly from operator to operator depending on the shape of the created circle and the depth of the texture. When the surface texture is too high or too low, creating a reasonable circle shape can be challenging. Laboratory and field application of sand patch test is shown in Figure 2.20.

The MTD value obtained from the sand patch test can be used as an indicator for predicting the bleeding rather than aggregate retention performance. In other words, one can build a chip seal road with a relatively high MTD value, yet chip loss would be inevitable if the construction were to be done with inappropriate materials. Hence, although the MTD value is of critical importance as a performance index, adhesion strength tests are required to assess the chip seal performance more comprehensively.

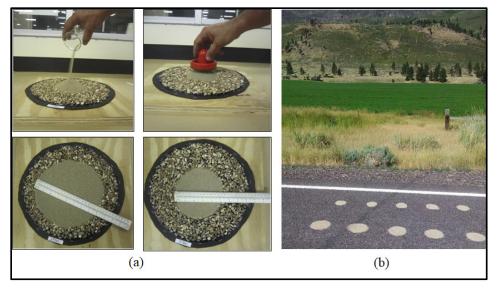


Figure 2.20: Sand patch test on (a)Laboratory samples (Gheni et al. 2017) and (b) Field pavement surface (Buss et al. 2016)

## 2.3.3.2 Outflow meter

The outflow test indirectly provides information regarding the macrotexture, i.e., the test is mainly used to determine the surface drainage characteristics of the pavement. The testing procedure involves monitoring the amount of time that has passed since a predetermined amount of water was allowed to escape between the surface of the pavement and the test device (ASTM E2380 2015). The time value obtained from the outflow test can be utilized to indirectly determine the macrotexture using Equation (2-13). However, ASTM E2380 (2015) stated that the outflow test only provides an indication of macrotexture properties. To obtain more reliable results, it was recommended to use the outflow meter in conjunction with other macrotexture measurement methods (i.e., ASTM E1845 (2015); ASTM E2157 (2015); ASTM E965 (2015)). Uz and Gokalp (2017) reported a strong correlation between the macrotexture measurements obtained from the sand patch test and the outflow meter. However, it should be noted that the permeability of the pavement layer can also affect the MTD values calculated by using the outflow meter measurements.

$$MTD = \frac{3.114}{OFT} + 0.636$$
(2-13)

Where:

MTD = Mean texture depth (in)

OFT = Outflow time (s)

The volumetric macrotexture measurement techniques (Sand patch and outflow meter) are vulnerable to local pavement texture fluctuations. Consequently, their repeatability is limited and highly operator-dependent. Hence, collecting multiple measurements at regular intervals is necessary to characterize a specific road section (Aktas et al. 2011). Despite these shortcomings, volumetric test methods are the most popular macrotexture measuring techniques due to their low cost, portability, and practicality (Choi 2008; Doty 1975). The outflow test, similar to the sand patch test, can be conducted both in the laboratory and in the field. Figure 2.21 illustrates an application of the outflow test in the field.



Figure 2.21: Outflow test meter application in the field (Aktas et al. 2011)

## 2.3.3.3 Laser profilers and texture scanners

Laser systems are one of the most commonly used methods for measuring the macrotexture of pavements in the United States. The core idea behind a laser system is that it sends out laser light particles that reflect off any aggregate or binders on the road surface before reaching a photosensitive receiver. Then, the texture depth is computed based on the distribution of signal-detection locations inside the receptor (Choi 2008). Laser systems (called laser profilers) are also used to measure surface texture, roughness, and profile. Compared to volumetric testing, the laser profiler's main advantage is that it can be mounted on a moving vehicle, allowing network assessments to be performed at highway speeds without a traffic closure. However, the cost of the laser profiler is significantly higher than that of volumetric measurement techniques. However, those technologies can provide data from a larger area (statistically more representative of the entire pavement surface) without creating operator or test material bias during the measurements.

ASTM E1845 (2015) details the test procedures to be followed. Mean profile depth (MPD) is the output obtained from the test, and MPD is linearly correlated with the MTD obtained from the sand patch test (ASTM E965 2015). In this test procedure, the average segment depth of each portion of pavement is determined first (Figure 2.22). The MTD

value is then generated by computing the average of all acquired mean segment depths. Adams & Kim (2014) stated that a three-dimensional map of the road's surface texture is generated by taking measurements of the distance between the laser sensor and the road's surface in both the longitudinal and transverse directions. Another laser-based technique is the laser texture scanner (ASTM E2157 2015).

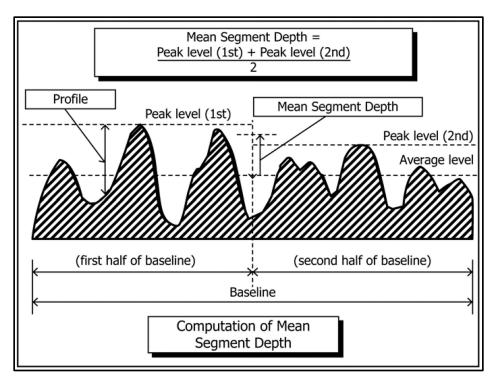


Figure 2.22: Mean segment (profile) depth introduced by ASTM E1845 (2015)

Equation (2-14) provided in ASTM E1845 (2015) to estimate MTD (a.k.a. Estimated texture depth (ETD)) value from MPD value.

$$MTD = 0.2 + 0.8 MPD$$
 (2-14)

In this study, the sand patch test, laser texture scanner, and high-speed profiler were utilized in conjunction before and after chip seal construction to measure macrotexture. The results obtained were then correlated to determine the most effective method.

## 2.3.3.4 Image processing

The assessment of the macrotexture properties of pavement surfaces using image processing techniques has significantly evolved within the last five years, particularly due to the recent technology advancements in computing technologies. Schonfeld (1970) conducted one of the first experiments to determine the textural characteristics of pavements using stereo photos (using two images from different angles to develop a 3D image). Using this technique, a correlation between the skid resistance of the pavement

and microtexture characteristics was established by Schonfeld (1970). Ergun et al. (2005) took cores from the field and used image processing methods to determine the micro and macrotexture features of different surface types (e.g., Chip seal, slurry seal, asphalt concrete, etc.). The micro and macrotexture results were used to estimate the road surface friction. The authors obtained images and performed image processing using an older technology. Therefore, it is debatable whether these procedures should be employed today.

Pidwerbesky et al. (2006) performed image processing on chip seal samples using fast Fourier transform (FFT) analysis. The theory behind the FFT technique is that, in comparison to seals that have been flushed or stripped, those in good condition will have more information (in the form of more sharply defined borders between aggregate particles and the surrounding binder). The FFT results were then correlated with the MTD results obtained from the sand patch test. Researchers found a fair relationship between FFT values and MTD; however, they stated that it was inaccurate over various chip seals with different nominal aggregate sizes. The methodology requires further improvement to quantify the chip seal's macrotexture accurately.

Image analysis techniques were employed by Kim and Lee (2008) to assess the textural changes in chip seals compacted using a variety of rolling patterns. First, the chip seal samples were sawn in the vertical direction, then images were obtained with a scanner from the core cross-section, and macrotexture profiles were obtained using algorithms developed in MATLAB. The major disadvantage of this method was that due to the problems with the image processing technique, some of the aggregates appear to float on the image as they are attached to the surface at different locations, which can lead to erroneous texture estimates.

Kutay et al. (2016) also performed image processing methods with recent technologies to quantify the texture of the chip seal treatments by focusing on percent embedment. Vertical cross-sections were produced in the laboratory by cutting the cores collected from the field. The peak valley method, the surface coverage area method, and each aggregate image processing method were developed in a MATLAB-based program to calculate the percent embedment. Figure 2.23 depicts the stages of sample preparation and image processing.



Figure 2.23: Stages of determination of percent embedment (Kutay et al. 2016)

Kutay & Ozdemir (2016) noted that the image processing approach they created compensated for shortcomings of conventional techniques such as sand patch and laser profilometer. (i.e., assuming that the pavement surface examined is flat, the aggregates do not sink into the substrate, etc.). In the continuation of this study, Boz et al. (2018) attempted to construct an aggregate embedding limit to utilize the percent embedment value as a performance criterion. This measured embedment value can be accepted as the reference (ground truth) embedment value for chip seal aggregates. Several laboratory test results were used to establish correlations between aggregate loss, bleeding parameters, and aggregate embedment value. According to the test results and analysis findings, the minimum and maximum percent embedment thresholds for chip sealing are set at 58 and 70 percent, respectively. In their research, they used smartphone-taken 2D images to derive the 3D surface topography of materials. Specimens with varying embedment depths were photographed to assess the bleeding performance (Boz et al. 2019).

Despite the high reliability of the percent embedment value acquired using image processing produced by Kutay et al. (2016), this approach is labor-intensive and destructive to be used in the field since it entails extracting a core from the field and cutting it horizontally to be able to observe the cross-section. Additionally, the recommended aggregate embedment depth limit has been determined by research conducted on a small number of laboratory samples. Therefore, further field and laboratory investigations are necessary to effectively apply these techniques during construction.

# 2.4 LABORATORY TEST METHODS TO PREDICT AND EVALUATE IN-SITU CHIP SEAL PERFORMANCE

Most chip seal failures can be categorized into two broad categories: bleeding and aggregate loss, and numerous laboratory test methods have been developed to investigate the sources of these issues. This section will outline the available test methods in the literature that are meant to assess the in-situ chip seal performance in the laboratory by conducting different types of experiments.

## 2.4.1 Third Scale Model Mobile Loading Simulator (MMLS3)

The third scale model mobile loading simulator (MMLS3) was first developed as an accelerated pavement testing method to evaluate the performance of hot mix asphalt surfaced pavements (Lee 2003). In addition, some studies have used this method to evaluate chip seal performance (Adams and Kim 2014; Lee et al. 2006; Lee and Kim 2008). For trafficking, the MMLS3 employs a continuous loop. The system is comprised of four bogies with one wheel per bogie. These wheels have pneumatic tires with a diameter of 11.8 inches, roughly one-third the diameter of a standard truck tire. A more comprehensive description of the system is available in the documents prepared by (Lee et al. 2006; Lee 2003).

MMLS3 device can be placed in an environmental chamber to perform the test at different temperature values (Lee and Kim 2014). Percent aggregate loss can be determined by periodically checking the surface of the chip seal layer after a different number of load applications to examine the aggregate retention performance. Moreover, some image processing methods can be employed before and after the MMLS3 test to evaluate the bleeding performance of chip seals (Lee and Kim 2008). A schematic illustration of the MMLS3 test setup is provided in Figure 2.24. Although this test method is effective in terms of simulation of traffic conditions and is presumed to be a good candidate for estimating the long-term performance of chip seals, the high cost of the test system is a significant drawback.



Figure 2.24: MMLS3 test setup: (a) mounting of samples on steel platform (b) MMLS3 device (c) placing the device in a climate chamber (d) MMLS3 test ready to perform a test (Adams and Kim 2014)

## 2.4.2 Accelerated Chip Seal Simulation Device (HSKSC)

Accelerated Chip Seal Simulation Device (HSKSC(acronym in Turkish)) was introduced by Aktas et al. (2013) and attempted to simulate in-situ traffic conditions at different temperatures, wheel passing, and vehicle load. The researchers used HSKSC to predict the long-term performance of chip seal samples in the laboratory. Similar to MMLS3, the HSKSC device can be run in an environmental chamber to control climate conditions. HSKSC operates on the basis that the device's pneumatic (48.5 mm diameter, 70 psi) wheel moves forward and backward. The device is capable of up to 1500 wheel passes per hour, with a load capacity of up to 1500 kg. The apparatus is made so that the testing may be conducted in wet and dry conditions (Aktas & Karasahin 2013).

According to the results of HSKSC tests (Figure 2.25) performed on chip seal specimens, the greatest aggregate loss occurs during the first phase of wheel loading, and the overall loss trend lessens as the number of wheel passes increases. Hence, the authors stated that traffic control procedures should be carefully considered following chip seal construction.(Aktas et al. 2013; Aktas & Karasahin 2013).

Although the HSKSC equipment attempts to simulate real traffic situations properly, it is considered that it would be hard for contractors or DOTs to acquire such costly and massive test equipment for chip seal quality control. In other words, the drawbacks of this procedure are the equipment cost and the test method's impracticability.

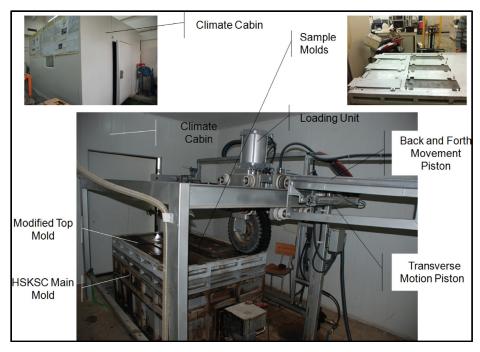


Figure 2.25: HSKSC test setup (Aktas and Karasahin 2013)

## 2.4.3 Hamburg Wheel Tracking (HWT) Test

The Hamburg wheel tracking (HWT) device is a useful and efficient instrument for evaluating the rutting resistance of asphalt pavements. HWT creates repeated loading on the specimens submerged in water and measures the accumulated rut depth on the surface of the asphalt concrete specimen as load cycles increase. It is one of the most widely acknowledged testing methodologies in the U.S. and other countries. Numerous agencies, DOTs, and asphalt pavement laboratories own HWT devices to perform rutting and moisture susceptibility tests. Hence, it might be efficient to use HWT equipment to assess in-situ chip seal performance. However, a limited number of studies are available in the literature in this regard. This situation may be attributed to the highly destructive loading of the steel wheels of the HWT device that can crush the aggregates located on the surface of the chip seal specimens.

Boz et al. (2018) utilized a modified HWT device to evaluate chip seal samples' bleeding and aggregate retention performance. They used rubber wheels (tire pressure of 34 psi) instead of steel wheels and reduced the load from 156 lbs. to 125 lbs. The illustration of the modified HWT device is provided in Figure 2.26. The authors determined the HWT cycles considering the service life of the chip seal (5 years) and proportioned it by considering the average service life of asphalt concrete (20 years). They also modified the test temperature based on trial tests. Image processing was conducted at varying HWT cycles to evaluate the bleeding performance. The percentage aggregate loss was selected as the aggregate retention performance criterion.

Rahman et al. (2020) also utilized HWT with a rubber wheel and investigated the aggregate loss percent and rutting parameters at 1,000 passes. The test was conducted on the core samples taken from the field. Different types of emulsion and application rate parameters were investigated according to ASTM D6372 (2015) standard. The authors reported that the average coefficient of

variation (COV) in the HWT test results was 1.3% which validates the repeatability of the data. Also, it was found that the rut depth increased with the increasing emulsion application rate for all emulsion types tested.

HWT test is a promising method to assess the reasons for common chip seal failures, i.e., aggregate loss and bleeding. However, these tests must be conducted with specimens that have various aggregate gradations and aggregate and binder types to demonstrate the variability of the results. Also, the findings obtained from the HWT device should be validated with field data. Hence, further investigations are required to determine the reliability and validity of this test method.

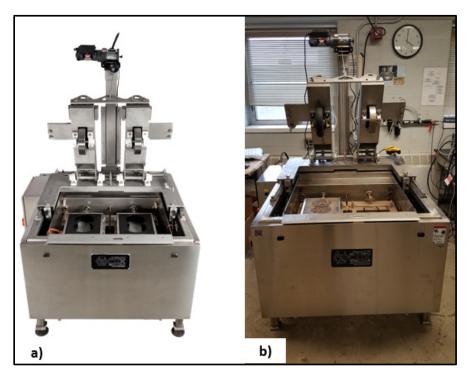


Figure 2.26: (a) Conventional HWT device (b) modified HWT device (Boz et al. 2018)

## 2.5 RECLAIMED ASPHALT PAVEMENT MODIFIED CHIP SEAL APPLICATIONS

Milled overlays or surface treatments can be processed to obtain recycled/reclaimed asphalt and aggregates. Utilizing reclaimed asphalt pavement (RAP) is a common practice in the hot mix asphalt (HMA) industry to reduce waste and improve the pavement's sustainability and cost. Researchers and agencies are seeking ways to increase the RAP content in HMA and widen the usage of RAP to other applications such as chip seals (Duncan et al. 2020; Robbins et al. 2021), microsurfacings (Garfa et al. 2016; Wang et al. 2019), slurry seals (Saghafi et al. 2019).

Los Angeles County was the first place to build a chip seal using RAP instead of virgin aggregate in 2008 (Updyke and Ruh 2016). RAP aggregates were crushed and screened to a required gradation and then used as aggregates in the chip seal construction. Los Angeles County claimed that once processed, RAP aggregate generally retains a residual asphalt content of 5-8%,

has a specific gravity of around 2.4, and has an absorption rate of around 1.5% (Updyke and Ruh 2016). It was highlighted that the RAP aggregates were used in many chip seal projects in Los Angeles County. Several projects used polymer-modified rejuvenating emulsions with RAP chips (Updyke and Ruh 2016).

According to a research project funded by the California Department of Resources Recycling and Recovery (CalRecycle), RAP aggregate (which has two different gradations with nominal maximum aggregate sizes-NMAS of 3/8 in. and 5/16 in.) was tested in two road sections with a hot applied tire rubber modified paving asphalt (PG 76-22) (Updyke and Ruh 2016). The aim was to investigate the performance of the hot-applied asphalt with ambient temperature (non-heated) RAP. The results showed that the road constructed with 5/16 in NMAS had moisture and dust issues. Therefore, it was concluded that RAP aggregates should be dry and clean before application. In addition, it was found that hot-applied asphalt has less moisture tolerance than emulsion. Moreover, no following placement issues were reported despite the unfavorable weather, and the project performed sufficiently well in the following years (Updyke and Ruh 2016).

Jahangirnejad et al. (2019) tested RAP aggregates (which cost 35% less for PennDOT) in chip seals in 1,000 or fewer ADT roads and concluded that the RAP-modified chip seals performed as well as chip seals constructed with virgin aggregates. The cost of RAP was highly dependent on the availability and transportation of the materials. As a result, RAP chip seal costs may vary from location to location. Tarefder & Ahmad (2018) conducted a life cycle cost analysis on chip seals constructed with RAP and virgin aggregates in New Mexico. The results showed that the chip seal constructed with RAP is 23-37% more cost-effective than the chip seals constructed with virgin aggregates. Ahmad & Tarefder (2020) conducted laboratory tests on chip seal specimens produced with RAP and virgin aggregates. The results show that the shear strength, skid resistance, and surface texture of specimens with and without RAP were similar. Robbins et al.(2021) also stated that chip seals could benefit from using 100% RAP if appropriately controlled and divided.

Using RAP instead of virgin aggregate in chip seals appears to be a promising technique based on the studies in the literature. However, it should be highlighted that adequate QA processes must be applied to the chip seal constructed with RAP for further validation. In addition, a life cycle cost analysis is also necessary to evaluate whether the chip seal should be constructed with RAP or local virgin aggregate. The price of the asphalt binder, RAP, and virgin aggregates at the time of the analysis can change the cost-effectiveness of RAP-modified chip seals.

#### 2.6 LITERATURE REVIEW SUMMARY

Chip seal is one of the most effective, economical, and practical road construction strategies to maintain and preserve pavements and increase the longevity of the roadway network. In the last decades, chip seal performance expectations have increased, notably due to the rising truck traffic on roadways and extending chip seal construction to higher traffic routes. To satisfy this ever-growing demand, various chip seal design and quality control strategies are being developed by many institutions. Previously, the quality of the chip seal was subjectively evaluated during design and construction (Gransberg and James 2005), while the aggregate and

binder application rates for the chip sealing were decided by experience and engineering judgment.

In SPR777 (Buss et al. 2016), an engineering concept was adapted for designing chip seals in Oregon. Although it is anticipated that the created design technique would improve the long-term performance of chip seals in Oregon, it is necessary to ensure that the chip seals are appropriately constructed by sticking to the new design method in order to attain significant long-term performance gains. However, current quality control methods are based on experience, judgment, and convenience rather than quantitative measurement methods. Hence, bringing the "engineering" concept into QA/QC and using higher quality materials and construction methodologies is expected to extend chip seals' durability. The main objective of this research study is to develop effective, practical, and economical engineering methods for building construction quality control strategies for chip seals in Oregon.

According to the literature review presented in this chapter, the overall factors affecting the quality of chip seals include but are not limited to the binder and aggregate application rate and uniformity, aggregate-binder bond properties, binder type and quality, aggregate properties, climate (mostly temperature), substrate condition, traffic conditions, and macrotexture properties (or aggregate embedment). The abovementioned parameters and test methods were summarized with their capabilities and limitations. There is a technological trend observed in the test methods, i.e., more computational, practical, automatic, and user-friendly tools/test setups were aimed to be developed to increase the overall quality and repeatability of QA/QC processes. To some extent, test tools were automated, the time required for tests tended to decrease, and safety concerns were prioritized over time.

Two typical chip seal problems were mainly reported in the literature: bleeding and aggregate loss. Adhesion tests are a good indicator of aggregate retention performance. It was also found that aggregate moisture level, density, and flakiness play an essential role in aggregate retention performance. To address the bleeding issues, test setups simulating actual truck traffic at smaller scales (MMLS3, HSKSC, etc.) were found to be effective; however, since they are expensive systems, using a slightly smaller scale HWT device for bleeding performance was concluded to be more suitable for chip seal performance assessment in the laboratory. However, further investigation is required to validate the effectiveness of the HWT test for chip seal performance assessment.

Macrotexture and aggregate embedment were considered to be important quality control parameters controlling long-term chip seal performance. The current methods to measure macrotexture were summarized in this literature review (Section 2.3.3). One conclusion that could be drawn is that the sand patch method is acknowledged worldwide and stands as an effective test, according to many researchers. However, the test method can be operator-dependent and does not consider aggregate penetration through the soft substrate. Laser systems (high-speed profilers and texture scanners) can be an effective option; however, there is a need to calibrate the mean profile depth (MPD) obtained using laser texture measurements and high-speed profiler measurements with mean texture depth (MTD) obtained from sand patch test. Correlation equations needed to be established between MPD and MTD results, and their performance in categorizing textures as low and high should be analyzed.

In-situ emulsion application rate (EAR) measurements are also an essential part of QA during field construction. The EAR determined during the chip seal design process should be applied consistently and uniformly in the field according to targeted levels. The wireless scale technology developed for tack coats in SPR 818 (Coleri et al. 2020b) presents a promising approach and could be tested in the field for chip seal applications.

Another important method to extend the service life of chip seals is increasing the material quality. Based on the literature review, some conclusions were drawn regarding the impact of material quality on performance. Generally, the results given in the literature revealed that polymer-modified emulsions are often better than non-modified emulsions. In addition, aggregate type, gradation, flakiness, dustiness, and maximum aggregate size were found to be important characteristics controlling aggregate retention and bleeding performance of chip seal samples.

Using RAP as a replacement for virgin (natural) aggregate in chip seals appears to be a sustainable technique. However, it should be noted that despite some field applications reported in the literature, none included any quantitative bleeding and aggregate retention performance, either in the field or in the laboratory. There is a need to quantitatively evaluate the aggregate retention performance of RAP in chip seal samples.

The literature review underscored the necessity for the development of practical and effective aggregate-binder adhesion tests suitable for both laboratory and in-situ settings. Additionally, improvements were required for laboratory bleeding tests utilizing the HWT device, which is already available in most research laboratories and the industry. Furthermore, conducting laboratory and field tests on RAP chip seals to accurately measure and monitor their performance was deemed essential.

## 3.0 AGGREGATE-BINDER ADHESION

## 3.1 INTRODUCTION

The adhesion between the aggregate and the binder is undeniably a crucial factor influencing chip seal performance. As indicated in the literature review, chip loss is considered to be a commonly observed failure mechanism in chip seals (Gransberg and James 2005). The dislodgment of chips from the pavement may result in windshield damage. The excessive chip loss can also lead to a reduction in friction and, ultimately, the failure of the section. In addition, the removal of the aggregates randomly along the pavement surfaces increases road roughness, which reduces user comfort and increases fuel consumption and tire wear (Haddadi et al. 2017). There is a need for a test method that is not only practical and effective but also cost-efficient, specifically designed to evaluate the aggregate retention performance of chip seals.

In this chapter of the study, the aim was to develop adhesion test methods that are practical, effective, economical, and suitable for both laboratory and field applications. When considering the tests outlined in the literature (Section 2.3.1), it was observed that the sweep test and the Vialit test are the most commonly utilized. The sweep test (Section 2.3.1.2), designed as a laboratory test to simulate the brooming effect in the field, was found to be limited by its inapplicability in the field and the lengthy phase of sample preparation. Therefore, this test was modified by the research team to enhance its practicality and applicability in the field. Similarly, the Vialit test, a ball-drop impact test (Section 2.3.1.1) conducted on chip seal samples prepared on metal plates, was also modified for in-situ execution. It is important to note that both tests have been subject to both positive and negative evaluations in the literature (See Section 2.3.1). A pull-off test (Section 2.3.1.4) was planned to be developed to validate the results obtained. Preliminary laboratory tests were carried out for the development of these test procedures, the determination of curing conditions, and the examination of their applicability, with the findings being presented in Section 3.2. After the testing procedures and parameters had been established, the developed methods were employed in the field (Section 3.3) and on laboratory-prepared samples using materials sourced from construction sites (Section 3.4). The test results from the modified sweep and Vialit tests were correlated with those from pull-off tests to assess their effectiveness in evaluating aggregate retention performance, with a high correlation noted for both modified sweep and Vialit tests. Additionally, factors influencing aggregate retention performance, including aggregate surface moisture, dustiness, binder type, and substrate conditions, were also reported in Section 3.4. Finally, in Chapter 3.5, the developed test methods were performed using aggregates sourced from four different regions in Oregon and evaluated with two commonly used emulsions (one anionic and one cationic).

## 3.2 PRELIMINARY LABORATORY TESTS

In this section, the tests developed to determine the adhesion properties between aggregate and binder -namely, the Modified Sweep, Vialit, and Pull-off tests- are described. The approach utilized in the development of these test methods was detailed. Based on the preliminary test results, the test method procedures, testing temperatures, and curing conditions were determined.

## 3.2.1 Objectives

The major objectives of this section are as follows:

- Develop practical, economical, and reliable adhesion tests that can be performed in the laboratory and in situ.
- Refine the testing procedures and parameters based on preliminary test results.
- Finalize testing and curing temperatures used in the tests.

## 3.2.2 Materials and Methods

Preliminary tests using modified sweep and Vialit methods were conducted on chip seal samples. The samples were obtained from four distinct aggregate sources in Oregon, including two from the eastern region and two from the western region, as illustrated in Figure 3.1. The physical properties of these aggregates are presented in Table 3.1, while their gradation curves are shown in Figure 3.2. Two commonly used polymer-modified emulsions, namely anionic high-float rapid set (HFRS-2P) and cationic rapid set (CRS-2P) emulsions, were evaluated in this study.

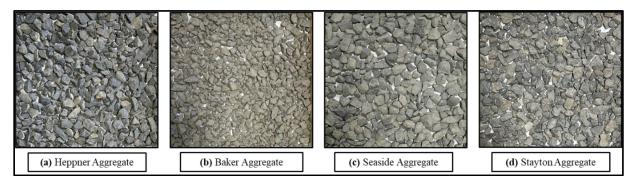


Figure 3.1: Aggregates acquired from different regions in Oregon

Table 3.1: Physical properties of aggregates

Aggregate Source	Unit Weight (kg/m³)	Specific Gravity	Absorption (%)	Flakiness Index (%)	Median Particle Size (mm)
Heppner	1,553.6	2.77	1.25	17.3	6.5
Baker	1,528.0	2.78	1.88	20.1	6.7
Seaside	1,616.8	2.86	0.83	18.7	7.8
Stayton	1,514.0	2.67	2.09	29.0	5.3

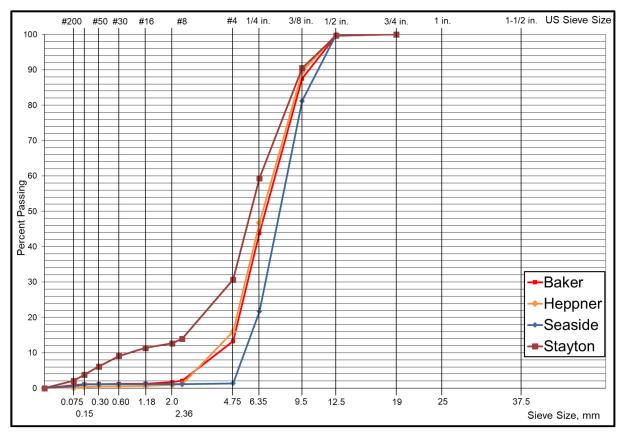


Figure 3.2: The gradations of aggregates from different regions of Oregon

Upon evaluating the gradation curves presented in Figure 3.2, it can be observed that the aggregates from Baker and Heppner exhibit almost identical gradations, while Seaside displayed a relatively coarser gradation, and Stayton features relatively finer aggregate gradations. It was found that Stayton has a relatively higher percentage of fine particles, with more than 10% passing through the 2 mm sieve.

The primary objective of this part of the research study is to develop/determine an effective, practical, and cost-effective test method to assess aggregate-to-binder adhesion for Oregon's chip seals. From this perspective, the Vialit test method was chosen as it is one of the most practical and economical methods for assessing aggregate-binder adhesion. In addition to the Vialit test, the modified sweep test and pull-off test were developed and performed to facilitate the comparison of test results and determine which method is the most effective and applicable.

#### 3.2.2.1 Modified sweep & Vialit tests

The Vialit test evaluates binder adhesion by dropping a metal ball from a specified height onto an inverted chip seal sample, subjecting it to an impact load (more details can be found in Section 2.3.1.1). The adhesivity is determined by counting the aggregates remaining on the plate after the ball-drop process. In addition, the specification requires an application rate that is dependent on aggregate size. In this study, instead of strictly adhering to the standard protocol, a replication of the chip seal construction process was

carried out in the laboratory. The actual emulsion and aggregate application rates used in construction were applied to the Vialit plates rather than the rates mentioned in the standard. The major advantage of the Vialit test is its practicality. Vialit plates can be brought to the construction site and placed on the pavement surface, and the emulsion and aggregates can be applied during construction. The plate with aggregates and emulsion can be removed for compaction and curing on the side of the road. The test can be rapidly conducted afterward. In addition, rather than counting the aggregates recommended in BS EN 12272-3 (2003), in this study, the plates were weighed before and after the ball drop, with the percentage weight loss documented as the test result (chip loss by weight).

As previously stated, the chip seal construction involved the application of an asphalt layer, followed by the compaction of aggregates using pneumatic and steel compactors. Typically, the surplus aggregates were then swept off the surface on the subsequent day. To simulate the construction, the Vialit plates underwent brooming prior to testing, thereby replicating conventional chip seal construction procedures. The chip loss that occurred due to sweeping is recorded as % chip loss (modified sweep test).

The sweep test evaluates chip seal aggregate loss by simulating brooming on a chip sealcoated asphalt disc, measuring aggregate retention after abrasion with a nylon brush (Section 2.3.1.2). The sweep test methodology outlined in ASTM D7000 (2019) requires using a laboratory mixer, asphalt felt disc, and clips, which can be costly and laborintensive. Furthermore, its application is constrained to laboratory settings. In this study, a more practical and cost-effective approach was employed by utilizing a readily available rechargeable electric spin scrubber with a maximum rotational speed of 380 revolutions per minute (RPM) for conducting the sweep test. One notable advantage of this tool is its ability to operate on battery power, rendering it suitable for field applications in chip seal construction. To further enhance the practicality of the test method, the sweep test was conducted on 20 cm × 20 cm Vialit plates. It should be noted that the Vialit test protocol requires inverting the plates prior to the ball-drop process. This step could result in the loss of aggregates with minimal to no contact with the binder, potentially yielding inaccurate test results. Hence, performing the sweep test before the Vialit test can increase its reliability. In actual construction, all the chip seals are subjected to rotational forces generated by power brooms employed at the end of construction. During the sweep test, it was observed that aggregates with minimal or no contact with the binder were effectively removed. Therefore, sweeping is not expected to significantly impact the results of the Vialit tests.

The aggregates were conditioned at room temperature (25±2°C) for 3 days before being utilized in chip seal test samples, i.e., air-dry aggregates were utilized. After emulsion and aggregate were spread on the Vialit plates (20 cm × 20 cm) (Figure 3.3 a, b, and c) using the apparatus developed by Weaver et al. (2023), the plates were compacted with a standard 25-kg rubber wheel in both perpendicular directions 3 times as recommended in BS EN 12272-3 (2003) (Figure 3.3d). Once compacted, the samples underwent a curing process in an environmental chamber (Figure 3.3e).

In these preliminary tests, the curing temperature and duration for the samples were set at 25°C and 24 hours, respectively. The selection of these temperature and duration parameters is based on previous studies (Adams et al. 2017; Aktas and Karasahin 2013; Estakhri et al. 2017; Howard et al. 2011; Kim et al. 2023; Zheng et al. 2022). The sweep test was performed after this complete curing process. Initially, 5 °C and 40°C were selected as testing temperatures to assess aggregate retention. As summarized in the literature, it is generally expected that chip loss is more likely to occur during the first winter term following chip seal construction (Gransberg and James 2005). At lower temperatures, the binder tends to behave more brittle, and under the influence of traffic, aggregates may be dislodged, especially if the adhesion between aggregate and binder is insufficient (Kim et al. 2017). On the other hand, it is also anticipated that the binderaggregate adhesion may be weakened at high temperatures. Hence, it was determined that a relatively high temperature (40°C) should also be tried for adhesion tests.

After curing the samples at 25°C for 24 hours, the sweep test was performed at 25 °C (Figure 3.3f). The samples were then conditioned at 40 °C and 5 °C (3 plates per testing temperature) for 20 minutes. Subsequently, a 500-gram steel ball is dropped onto the upside-down Vialit plates on the platform (Figure 3.3g). The distinct phases of the experimental procedure are depicted in Figure 3.3. The experimental plan for the sweep and Vialit test is given in Table 3.2.

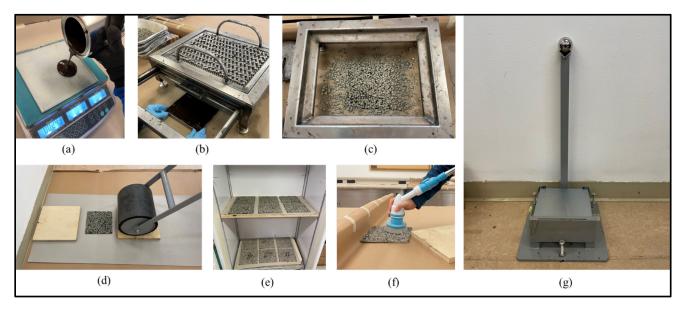


Figure 3.3: Experimental process stages of the sweep and Vialit tests: (a) emulsion application on the plates, (b-c) spread of chips on the emulsion using the apparatus developed by Weaver et al. (2023), (d) sample compaction using a rubber wheel, (e) sample curing at 25 °C for 24 hours, (f) conducting the modified sweep test on the plates (25 °C), (g) execution of the Vialit test after conditioning the samples at 5 °C and 40 °C

Table 3.2: Experimental plan for preliminary tests (HFRS-2P: anionic polymer-modified high-float rapid set, CRS-2P: cationic polymer-modified rapid set emulsion)

Test	Aggregate sources	Emulsion type	Emulsion application rate (gal/yd²)	Testing temperature (°C)	Replicates	Total tests
Modified	4	HFRS-2P	0.38	25	6	96
sweep test		CRS -2P	0.48			
Vialit test	4	CKS -2P	0.40	5 and 40	3	96

## 3.2.2.2 Pull-off test

In this study, various test systems were evaluated to assess their effectiveness in quantifying the adhesion properties of chip seals. Initially, the Oregon Field Tack Coat Tester (OFTCT) device, designed for tack coats (Coleri et al. 2017), was utilized to assess its applicability as a chip seal pull-off test (Figure 3.4). The pull-off tests aimed to detach chips (aggregates) from the binder at a specific displacement rate and temperature while measuring the force necessary to pull the aggregates off. The value of the pull-off force, along with the contact area, was used to calculate the bond strength.

The initial challenge involved identifying a suitable adhesive to adhere the pull-off platens to the aggregates. This adhesive needed to possess sufficient strength to establish a secure bond with both the platen and the aggregates. Simultaneously, it was desirable for the adhesive to set relatively quickly for practicality. After experimenting with different adhesives, a fast-setting epoxy adhesive that solidifies in just 5 minutes was selected for the testing process in the present study. The epoxy adhering to the aggregate surface and not being in contact with the binder is of critical importance for accurately measuring the bond strength between the aggregate and the binder. To meet this requirement, a standard sand (conforming ASTM C778) was applied over the chip seal sample. As the binder was covered with sand, the epoxy was prevented from adhering to the binder, thereby ensuring that the epoxy's adhesion was confined to the aggregates only.



Figure 3.4: Trial tests with the OFTCT on chip seal samples

The initial trial tests were carried out on a granite plate, and tests were conducted at 40°C. One significant challenge that emerged was the difficulty of conducting tests at 5°C. This challenge stemmed from the size of both the plate and the testing device, which made it impractical to place them inside the environmental chamber. Furthermore, achieving such low temperatures, specifically in the field where chip seal construction predominantly occurs during the summer, would be highly challenging. For these reasons, an alternative device for the pull-off tests has been employed.

The PosiTest is a device designed to evaluate the adhesion properties of coatings on metal surfaces, and it is commonly used for adhesion testing on bridge decks. An attempt has been made to test the feasibility of using the PosiTest device on chip seal samples (Figure 3.5). This device, noted for its compact size and battery-operated capability, is suitable for in-situ use. For testing chip seals, dollies with a diameter of 50 mm have been selected. This was the largest diameter available for the device, and the nearest alternative to 50 mm was 20 mm dollies; considering the aggregate size (Table 3.1), 20 mm dollies may provide a limited area for assessing adhesion properties.

During the trial tests conducted at room temperature (25±2°C), it was noted that failures frequently occurred between the plate and the epoxy, as illustrated in Figure 3.6. To increase the contact area between the dolly and epoxy, circular threads with a thickness of 1 mm were integrated into the dollies, as shown in Figure 3.7. The PosiTest activator is positioned within an environmental chamber and conditioned in accordance with the established protocols prior to testing (Figure 3.8).



Figure 3.5: Trial tests with PosiTest on chip seal samples



Figure 3.6: Adhesive failure between the dolly and epoxy

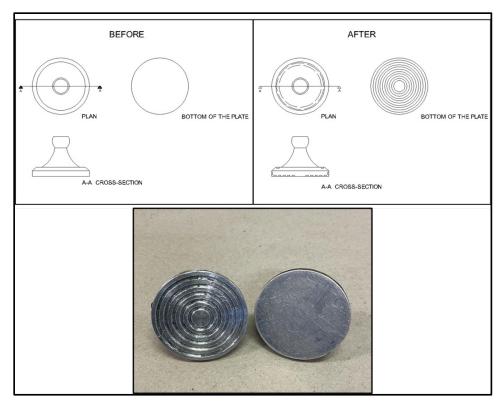


Figure 3.7: Introducing threads in dollies to increase the contact area with epoxy

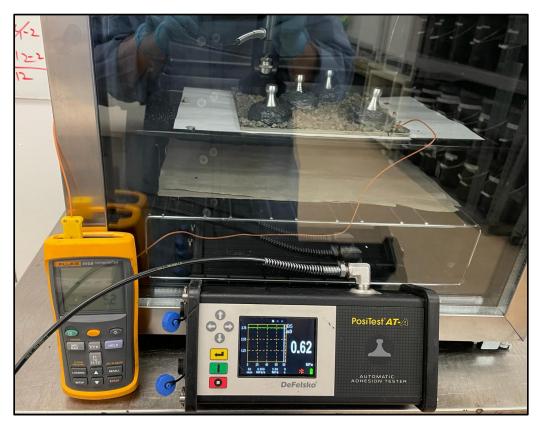


Figure 3.8: Performing pull-off test via PosiTest in the environmental chamber (5°C)

The trial tests showed that the device could not measure the adhesion properties of aggregate and binder effectively. This is because the device was designed for testing metal coatings, which are typically brittle materials. Its actuator can only move 4 mm, which was not long enough to dislodge the aggregates from the binder in various cases. Hence, it was decided to use a 30kN Universal Testing Machine (UTM-30) test system for pull-off tests.

The UTM-30 device has a loading capacity of 30 kN and can precisely control the sample's temperature within a broad range. A specialized actuator and clamping system were designed and manufactured at a machine shop to facilitate successful pull-off tests. The test setup is depicted in Figure 3.9. Using this system, the Vialit plates can be securely clamped onto the base plate. Following the completion of a test, the Vialit plate can be rotated in any direction and can be secured with clamps to facilitate subsequent tests. The tests were performed at a displacement rate of 0.5 mm/min. Despite the limitation of being unable to perform this test in the field, field samples can be transported to the laboratory for testing. This way, samples that were exposed to the effect of field curing could be tested. The primary advantage of using the UTM-30 device is its accurate temperature control, along with displacement-controlled loading, ensuring high precision.

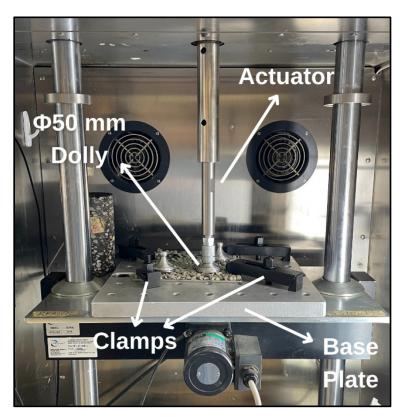


Figure 3.9: Performing pull-off test with the UTM-30 test system

Another question that arose within this test method is the calculation of bond strength. The UTM-30 device provides the force needed to detach aggregates from the binder. To determine the contact area, three different approaches were introduced:

- Circular Area: The circular area of a 50 mm diameter dolly is used to calculate the bond strength.
- Pline Area: The cross-section area of each dolly is calculated with a polyline (Pline) drawn around the perimeter of the cross-section and used for bond strength calculations.
- Sand Area: The net binder area (black area) is calculated using the sand method.

In Figure 3.10, the circular area is shown in red. Its area is 1962.5 mm<sup>2</sup>, while the exact cross-section of the chip seal samples can be calculated with a polyline, which is shown in green in Figure 3.10.



Figure 3.10: Pull-off test dolly after the test. The red circle shows the area for the circular method, while the green lines show the Pline method

To determine the effective area (black binder area) by the sand method, materials in regular geometric shapes were obtained. These objects, characterized by their regular geometrical forms, were coated with asphalt emulsion and allowed to cure at 25°C for 24 hours. Following the curing period, the weights of these shapes were recorded. Subsequently, these objects were subjected to heating with a fan and immersed in standard sand before being reweighed (same sand used in the pull-off test- conforming ASTM C778 (2021)). Figure 3.11 displays the objects submerged in sand.



Figure 3.11: Steps for calibration of effective binder area measurement

The amount of sand adhered to the binder is calculated, and a correlation between the weight of sand adhering to the object and the object's area is determined. This relationship is presented in Figure 3.12.

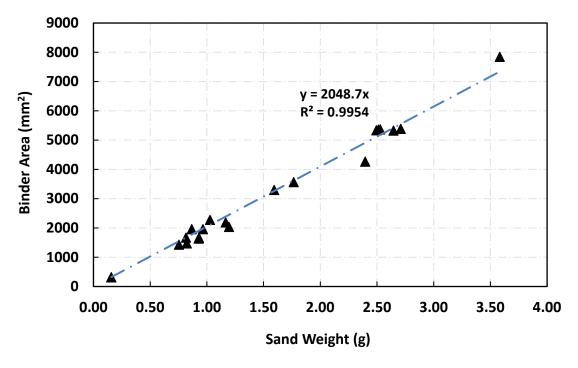


Figure 3.12: The correlation between sand weight and binder area

As shown in Figure 3.12, there is a strong correlation between sand weight and binder area. Therefore, the effective binder loading area can be calculated for each dolly after the pull-off test by following this indirect method. The steps followed in the pull-off test are shown in Figure 3.13.

First, the chip seal sample is prepared as described in Figure 3.3. Excess aggregate on the chip seal is removed by brooming (Figure 3.13b). Standard sand (ASTM C778 (2021)) is then applied to the binder of the chip seal sample (Figure 3.13c). Dollies are attached to the chip seal samples using epoxy (Figure 3.13d). After conditioning at the testing temperatures for 20 minutes, the dollies are pulled off from the chip seal sample (Figure 3.13e).

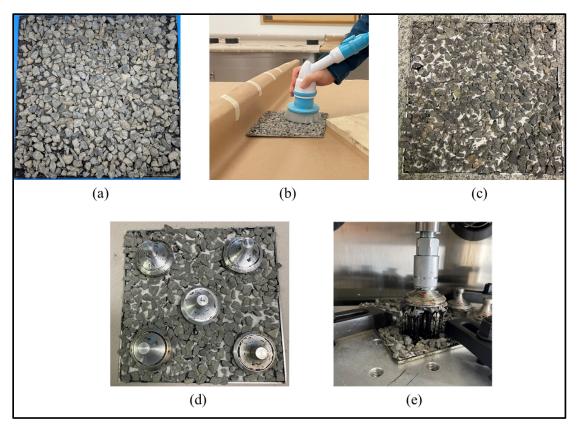


Figure 3.13: The experimental process stages for pull-off tests: (a) chip seal samples on Vialit test (cured), (b) sweeping excessive aggregate, (c) spread of standard sand to cover binder, (d) adhering dollies on the chips using epoxy, (e) conducting the pull-off test

It should be highlighted that the circle area method yielded reasonable results and provided the highest correlations with the results of the modified sweep and Vialit tests. Therefore, a contact area of 1962.5 mm² has been utilized in the calculation of bond strength between the aggregates and the binder. It should be noted that no preparatory processing was conducted around the dolly prior to its detachment from the chip seal specimen, meaning the test area was not cut or altered. Consequently, an attempt was made to peel off a region of the chip seal specimen, corresponding to a 50 mm diameter

circle, adhered to the metal plate. This approach might have confined the resistance offered by the chip seal specimen to an area equal to a 50 mm diameter circle. Moreover, the polyline and sand measurement methods had a higher likelihood of human error, which could have led to inaccuracies in the results of the Pline and sand approaches. Ultimately, the bond strength test results were calculated by dividing the ultimate force required to pull the aggregates off by a cross-sectional area of 1962.5 mm<sup>2</sup>.

## 3.2.3 Results & Discussion of Preliminary Laboratory Tests

The modified sweep test (conducted at 25°C) results are displayed in Figure 3.14Error! **Reference source not found.**. Note that all the error bars in this report represent a length equivalent to one standard deviation.

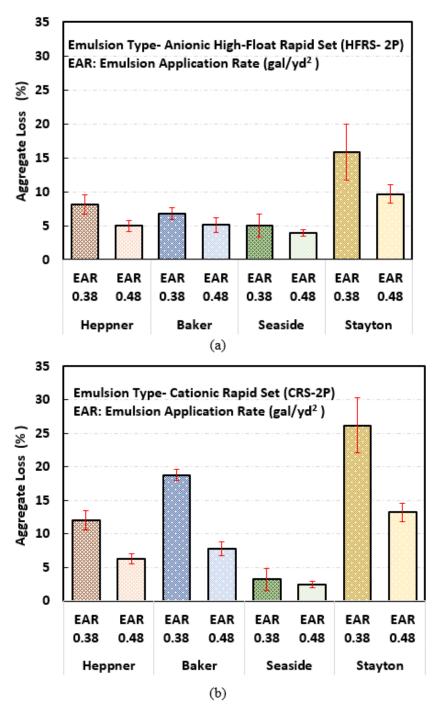
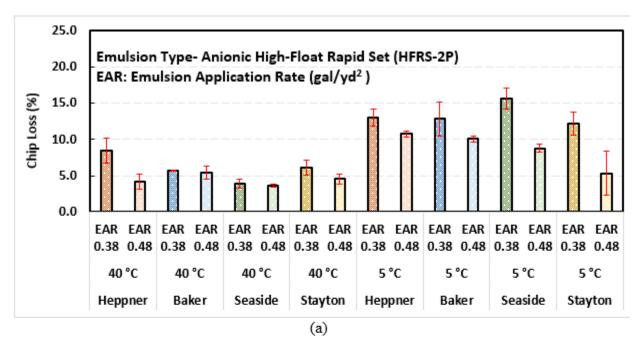


Figure 3.14: Sweep test results (average) at 25 °C testing temperature (a) HFRS-2P (b) CRS-2P (Error bars are one standard deviation height)

Upon evaluating the results presented in Figure 3.14, it was observed that Stayton aggregates exhibit the highest chip loss, irrespective of the emulsion type. As shown in Figure 3.2, the Stayton aggregate exhibited the highest fine material content (dust), which likely contributed to increased chip loss. A reduction in chip loss is noted for both emulsions with an increase in binder content, indicating the sweep test's sensitivity to change in binder content. It is reasonable

to anticipate that higher binder contents will result in greater aggregate embedment and enhanced adhesion. This increase in adhesion is expected to lead to a reduction in chip loss. It can be inferred that the sweep test effectively captures the adhesion properties. When comparing binders, it was found that aggregates from Heppner, Baker, and Stayton show lower chip loss with anionic emulsion (HFRS-2P) as compared to cationic emulsion (CRS-2P). In contrast, Seaside aggregates demonstrate improved performance with the cationic binder (CRS-2P). ODOT authorities have also reported compatibility issues observed in the field for the Seaside aggregates and the anionic binder (HFRS-2P). Thus, preliminary tests suggest that the sweep test can be an effective methodology for addressing aggregate-binder compatibility problems.

Figure 3.15 presented the Vialit test results at both 40°C and 5°C. The graphic in the upper section (Figure 3.15a) depicts the results for anionic emulsion (HFRS-2P), while the lower section (Figure 3.15b) corresponds to the results for cationic emulsion (CRS-2P).



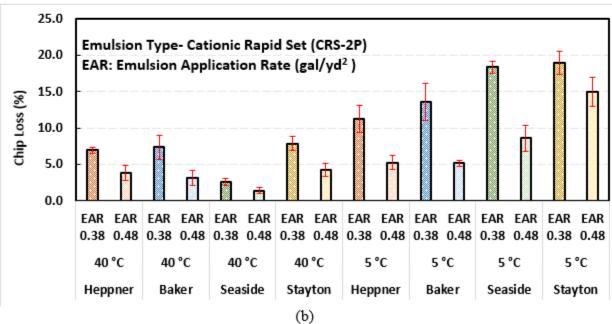


Figure 3.15: Vialit test results (average) at 40°C and 5°C testing temperatures (a) HFRS-2P (anionic binder) (b) CRS- 2P (cationic binder) (Error bars are one standard deviation height)

Vialit test results revealed that the chip loss was lower at 40°C compared to 5°C. This trend is consistent for both the emulsion types. This phenomenon can be attributed to the brittleness of the binder at the lower test temperature. For both temperatures (40°C and 5°C), increasing the binder amount from 0.38 gal/yd² to 0.48 gal/yd² resulted in less chip loss. This effect was more pronounced at 5°C compared to 40°C for all aggregate types. Furthermore, it was challenging to perform the test at 40°C due to the binder's excessive softness, leading to some aggregates falling

under their own weight rather than from impact force. Considering that high temperatures in chip sealing tend to cause bleeding rather than chip loss, it was decided to adjust the testing temperature to 25°C, aligning with the standard temperature for fatigue cracking tests for asphalt concrete materials (Coleri et al. 2020a).

It should also be noted that the samples conditioned at 40°C necessitated only 3-5 N of force for dislodgement in the pull-off test, consistently resulting in cohesive binder failure. Therefore, testing at 40°C was omitted from the experimental plan, aligning with the protocol for sweep and Vialit tests. In addition, during the testing of samples conditioned at 5°C, indications of uncured emulsions, such as a brown color, were observed. It was known that the emulsions are initially brown upon application and turn black as the water evaporates. Figure 3.16 shows photos of these samples tested at 5°C.



Figure 3.16: Samples after the pull-off tests (5°C) (brown color showed insufficient curing)

As seen in Figure 3.16, the emulsion is not fully cured. This result indicates that pull-off tests can visually identify partially cured areas of chip seals. However, in preliminary tests, uncured sections led to variations among samples. This is because water evaporation of emulsions in chip seals depends on factors such as binder type, aggregate size, absorption capacity, and environmental conditions (Kim et al. 2017). To ensure all samples are sufficiently cured, it was decided to increase the curing temperature. Overall, the laboratory testing process has undergone the following changes:

- The curing temperature increased from 25 °C to 45 °C to ensure all the water in the emulsion is evaporated.
- An additional flip-over process has been introduced before conducting the sweep test. This step helps eliminate aggregates with no contact with the binder and effectively neutralizing variations in the aggregate application rate.
- It was decided to test aggregate-binder adhesion at 5 °C and 25 °C.
- The emulsion is preheated in a closed container at 60°C for 2 hours before testing to better simulate the in-situ application process.
- In the field, damp aggregates are commonly used in emulsion-based chip seal applications. Consequently, the aggregates decided to be wetted with water before being spread over the emulsion.

#### 3.3 FIELD TESTS

In this section, the in-situ adhesion tests have been discussed. In the summer of 2023, the research team visited two chip seal construction projects in Oregon: one in Pendleton in the eastern region and one in Woodburn in the western region. Chip seal samples were collected from these sites and cured under field conditions on the same day. The developed adhesion tests (Modified Sweep, Vialit, and Pull-off) were performed on these samples, and the results were reported.

## 3.3.1 Objectives

The major objectives of this section are as follows:

- Determining the field applicability of the developed adhesion test methods (Modified sweep, Vialit, and pull-off tests).
- Examining the impact of curing samples under field conditions on aggregate-binder bond properties.
- Monitoring environmental conditions (temperature, humidity, wind speed) in the field and observing their impact on the evaporation of water within the emulsion.

## 3.3.2 Materials and Methods

During the summer of 2023, the research team visited two chip seal construction projects in Oregon. One in the eastern region (Pendleton) and one in the western region (Woodburn). Table 3.3 provides a summary of chip seal construction details, including dates, highway locations, target emulsion application rates (EAR), and aggregate application rates (AAR).

**Table 3.3: Chip Seal Construction Details** 

Project Location	Highway(s)	Date of Construction	Emulsion Type	Target EAR (gal/yd²)	Target AAR (lb/yd²)
Pendleton	OR-11 and US-730	June 2023	CRS-3P*	0.47	27.0
Woodburn	OR-219	July 2023	HFRS-2P**	0.44	18.5

<sup>\*</sup> Cationic rapid set emulsion (CRS-3P)

The gradation of the field aggregates is presented in Figure 3.17, while their physical properties are detailed in Table 3.4.

<sup>\*\*</sup> Anionic high-float rapid set emulsion (HFRS-2P)

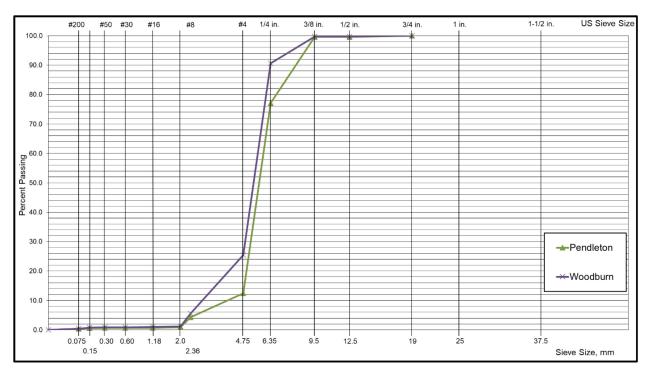


Figure 3.17: The gradation of field aggregates

Table 3.4: Physical properties of the aggregates sampled from the field

Project Location	Specific Gravity	Absorption (%)	Flakiness Index (%)	Median Particle Size (mm)
Pendleton	2.78	1.12	25	8.2
Woodburn	2.67	1.07	16	7.5

At both of these locations, Vialit plates were transported to the field and positioned on the road shoulder to prevent any potential negative impact on the actual construction on the main mat. Alongside the Vialit plates, 3 cm (1.18 in) thick asphalt concrete (AC) samples were also placed on the shoulder to assess the effect of substrate on adhesion characteristics between the aggregate and the binder. Hamburg test samples and asphalt shingles (to measure EAR) were also placed at the shoulder. The emulsion is applied to the samples using a distributor truck, followed by the spreading of aggregates with the equipment utilized in construction. Photographs of the test sections can be seen in Figure 3.18 (Pendleton) and Figure 3.19 (Woodburn). Note that asphalt shingles were also placed in Woodburn; however, they were promptly removed to the side after the emulsion was sprayed.

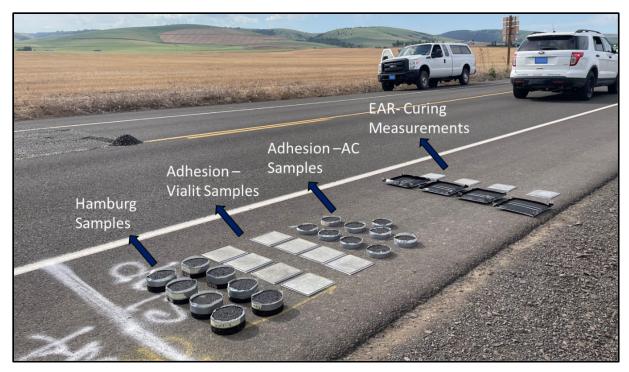


Figure 3.18: Pendleton chip seal sampling section



Figure 3.19: Woodburn chip seal sampling section

Once the emulsion and aggregates were applied to the adhesion and Hamburg test samples, the samples were compacted using a 25 kg rubber wheel compacter on the side of the road, as depicted in Figure 3.20.



Figure 3.20: Compacting samples after emulsion and aggregate application

Following the compaction, the samples were left to cure on the shoulder of the test section. It was well-established that environmental conditions can significantly impact chip seal performance, and it is not always possible to simulate the field curing temperatures in the laboratory (Gransberg and James 2005; Pierce and Kebede 2015). Hence, the research team exposed samples to field conditions before testing them in the field and laboratory. For both projects, the decrease in emulsion weight (water evaporation) was monitored periodically, and when no significant change in weight was observed for about 30 minutes, the curing process ended (meaning all the water in the emulsion evaporated). The samples were cured for approximately 10 hours in Pendleton and 9 hours in Woodburn. The test section's temperature, humidity, and wind speed were measured with a handheld weather station, and the data collected are shown in Figure 3.21. The average values measured are given in Table 3.5.

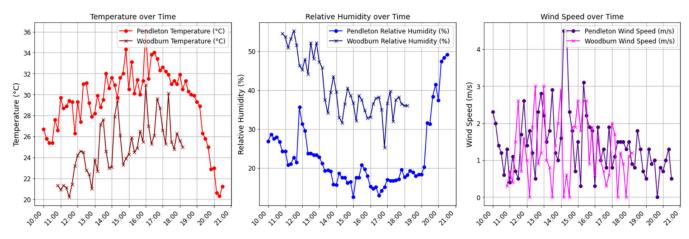


Figure 3.21: Temperature, Relative humidity, and wind speed measured in Pendleton and Woodburn

**Table 3.5: Weather Station Data (Average of all data points)** 

Location	Average Temperature (°C)	Average Relative Humidity (%)	Average Wind Speed (m/s)
Pendleton	29.4	22.7	1.4
Woodburn	24.9	40.8	1.3

The emulsion consisted of bitumen, water, and emulsifying agent. The adhesion properties of the emulsion increased with the evaporation of water, as established in the literature (Howard et al. 2011; Shuler 2011). This evaporation rate is dependent on temperature, wind speed, relative humidity, and type of emulsion, among other factors (Gransberg and James 2005). In chip sealing, determining the appropriate time to sweep excess aggregate on a newly constructed chip seal is critical. Early sweeping with power brooms may result in excessive aggregate loss. Given the known correlation between the water content in the emulsion and its adhesion properties (Shuler 2011), monitoring the moisture loss in the emulsion is vital for quality control. When a specific amount of water has evaporated, power brooms can be used to sweep the road. Subsequently, the section may be opened to uncontrolled traffic. In both field tests, the evaporation of water from the emulsion was monitored. The results are given in Figure 3.22 (The evaporation data is collected from the shingles placed on small wireless scales in the field). As illustrated in Figure 3.22, water evaporation occurred more rapidly in Pendleton compared to Woodburn. Despite the differences in the EAR and emulsion types between these chip seal projects, the lower humidity and elevated temperatures in Pendleton likely contributed to rapid water evaporation. Additionally, Pendleton experienced more sunny weather conditions than Woodburn, suggesting that increased ultraviolet light (UV) exposure may have further accelerated water evaporation in Pendleton compared to Woodburn. Also, under identical environmental conditions, laboratory evaporation tests indicated that the water in cationic CRS-3P emulsion evaporated faster than in anionic HFRS-2P.

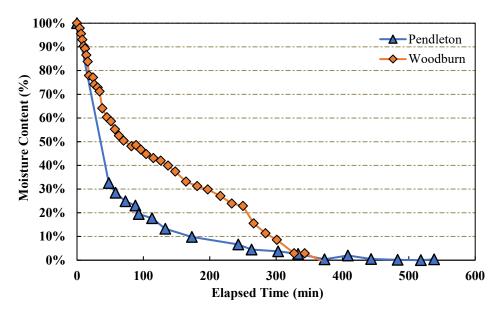


Figure 3.22: The change in moisture loss in emulsions over time (Field evaporation measurements)

The specimens were allowed to cure in the field until no weight change was observed. Subsequently, they were covered with bubble plastic wrap and transported to the laboratory for testing. It is important to note that in Pendleton, the sweep test was conducted in the field due to the long transportation distance, which could have potentially damaged the specimens.

#### 3.3.3 Results & Discussions

The field samples were transported to the laboratory for testing (in Pendleton, the modified sweep test was performed in situ). They were first conditioned at 25°C for 30 minutes in an environmental chamber. The Vialit plates were then rotated perpendicular to the ground and gently brushed to remove aggregates not in contact with the binder (Flip-over test – See section 2.3.1.3). This was followed by the sweep test. Post-sweep test, three Vialit plates were conditioned at 25°C and another three at 5°C for 20 minutes. Following conditioning, the Vialit test was conducted on these plates. For the pull-off tests, two Vialit plates were utilized, one conditioned at 5°C and the other at 25°C for 20 minutes. Figure 3.23 presents the results of the sweep and Vialit tests.

The flip-over test (which is performed before the sweep test to eliminate aggregates that are not in contact with the binder) results indicate the quantity (in percent weight) of excess aggregate spread on the samples. Since the chip loss is higher in Woodburn, it exhibited a higher amount of excess aggregate. On the other hand, the sweep test outcomes show that chip loss in Pendleton was significantly greater than in Woodburn. As noted in Table 3.3, different binders and aggregates were utilized in these two projects. Additionally, varied environmental conditions were recorded at these locations (Figure 3.21), complicating direct comparisons between samples. Nevertheless, the marked difference in sweep test results could be attributed to the fact that the sweep tests in Pendleton were conducted in the field, where environmental conditions

were less controllable. The higher temperatures recorded in Pendleton might have contributed to increased chip loss in the sweep test.

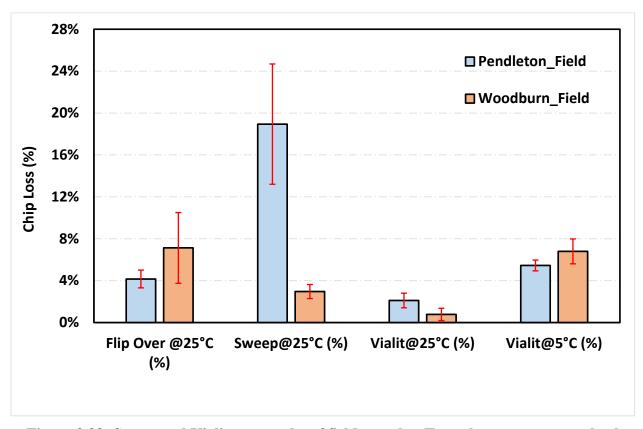


Figure 3.23: Sweep and Vialit test results of field samples (Error bars are one standard deviation height)

It should be noted here that in this study, a Welch-modified two-sample t-test was employed to statistically evaluate the significance of the observed differences between two distinct testing results. The mean outcomes of these tests are denoted as  $m_1$  and  $m_2$ , respectively. The hypotheses framed for this evaluation were as follows:

- Null Hypothesis ( $H_0$ ): There is no significant difference between the mean outcomes of the two testing methodologies ( $m_1=m_2$ ).
- Alternative Hypothesis (H<sub>1</sub>): There is a significant difference between the mean outcomes of the two testing methodologies  $(m_1 \neq m_2)$ .

The criteria for making a decision based on the t-test were established as follows:

- Reject (H<sub>0</sub>): If the p-value is less than 0.05, indicating a statistically significant difference between the mean outcomes of the two methodologies.
- Fail to Reject  $(H_0)$ : If the p-value is 0.05 or higher, indicating that the difference between the mean outcomes is not statistically significant.

In the case where the null hypothesis was rejected (p-value < 0.05), it was concluded that the mean outcomes of the tests under investigation were significantly different.

Upon comparing the Vialit test results, it is observed that at 5°C, both Woodburn and Pendleton exhibit higher chip loss compared to 25°C, i.e., at lower temperatures, higher chip loss can be expected due to more brittle behavior of the binder. When comparing the results from Pendleton with those from Woodburn, at both temperatures, no significant difference in chip loss is recorded (p=0.29 at 25°C and p= 0.44 at 5°C according to the t-test).

In each designated location, a pair of Vialit plates were prepared to conduct pull-off tests. These tests were executed at temperatures of 25°C and 5°C. On each plate, five pull-off dollies were affixed to chip seal samples for testing by following the process described in Section 3.2.2.2. The test results are given in Figure 3.24. The results demonstrated that samples from Woodburn exhibited higher bond strength at both 5°C and 25°C. As anticipated, higher bond strength values were obtained at 5°C compared to those at 25°C due to an increase in brittle behavior of the binder.

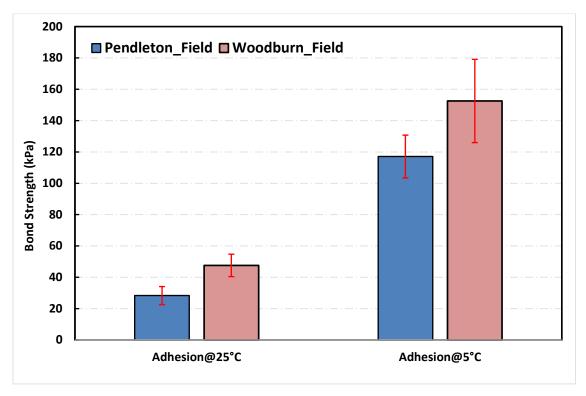


Figure 3.24: Pull-off test results (Field samples) (Error bars are one standard deviation height)

To assess the accuracy of the pull-off test, the research team decided to conduct tests on samples prepared with field-sampled materials in the laboratory at various curing durations. It is known that increasing the curing time enhances the binder's strength. Laboratory tests using field-sampled aggregates and emulsions were conducted at different curing times and presented in Section 3.4. Similarly, sweep and Vialit tests were also performed, and correlations among the results (sweep-pull-off and Vialit pull-off) were established to determine the reliability of the test

methods. Those correlations also provided valuable information regarding the performance of the tests utilized in this study. In addition, the sensitivity of the three test methods to varying curing times was analyzed in Section 3.4.

# 3.4 ADHESION TESTS ON LABORATORY-PREPARED SAMPLES USING MATERIALS SAMPLED FROM CONSTRUCTION

In this section, the results of the laboratory tests conducted using aggregates and emulsion sampled from two chip seal construction projects (Pendleton & Woodburn) in Oregon were presented. The initial phase involved preparing chip seal samples with various curing times (3 hours, 24 hours, and 48 hours), followed by conducting sweep, Vialit, and pull-off tests. The results obtained were then compared with field-cured samples. Correlations were established between the modified sweep-pull-off and Vialit-pull-off tests to assess their reliability in determining the aggregate retention performance of chip seal samples. Based on these results, final recommendations have been formulated. The investigation also extended to the effect of surface conditions on aggregate retention performance, where dry and damp aggregates with clean and dusty surfaces were tested to assess their effect on aggregate retention. Following that, the difference in bond strength between chip seal samples on metal plates and those on compacted asphalt concrete (AC) discs was compared using the pull-off test. Lastly, various aggregates and binders commonly used in Oregon were tested using recommended test methods.

## 3.4.1 Objectives

The major objectives of this section are as follows:

- Conduct modified sweep, Vialit, and pull-off tests on chip seal samples prepared at various curing times using aggregates and emulsion sampled from Pendleton & Woodburn chip seal construction projects.
- Compare the aggregate retention performance of laboratory-cured samples with field-cured samples.
- Assess the reliability of modified sweep and Vialit tests in determining aggregate retention by correlating results obtained in pull-off tests. Formulate final recommendations based on established correlations.
- Apply the proposed test methodologies to examine the impact of different surface conditions of aggregates (dry compared to damp and clean compared to dusty) on adhesion between the aggregate and the binder.
- Assess the influence of emulsion type on aggregate retention performance.
- Evaluate the bond strength difference between chip seal samples on metal plates and compacted AC discs.
- Test various aggregates and binders used in Oregon with recommended test methods and report their adhesion performance.

#### 3.4.2 Materials and Methods

Aggregates and emulsion were sampled from both construction sites and transported to the laboratory for testing. The most suitable curing time and temperature were aimed to be

determined. Preliminary laboratory tests revealed that 25°C and a 24-hour period were insufficient to complete the evaporation of water in the emulsion. Consequently, the research team conducted evaporation tests at 35°C and 45°C. The samples were placed in an environmental chamber, and the weight loss was monitored periodically for 48 hours. The evaporation data indicated that the moisture loss in the field occurred significantly faster than in laboratory conditions at 35°C and 45°C. This discrepancy could be attributed to factors such as ultraviolet (UV) radiation, humidity, and wind conditions in the field. The evaporation rate at 45°C was found to be closer to that observed in the field. The research team decided against increasing the curing temperature further to avoid significant changes in the binder's viscosity due to higher oxidative aging at high temperatures, eventually causing aggregate embedment and adhesion issues. Therefore, the curing temperature was set at 45°C. The samples underwent curing for durations of 3 hours, 24 hours, and 48 hours, after which modified sweep, Vialit, and pull-off tests were conducted. The reason for choosing the curing times in a gradual manner is that it is known as the curing time increases, the amount of water in the emulsion decreases due to evaporation, and the adhesive properties of the binder improve (Adams et al. 2018). The aim was to observe whether the developed adhesion test methods could demonstrate this rising trend in adhesion properties. Moreover, for a robust correlation to be established between the pull-off test and the results of the modified sweep and Vialit test results, it is critical to test the binder at a wide range of adhesion levels (both low and high).

Initially, the emulsion brought from the field was heated to 60°C for 2 hours. The aggregates sampled from the field were moistened before being spread on the emulsion, replicating field conditions. The emulsion application rate (EAR) measured as 0.47 gal/yd<sup>2</sup> for Pendleton and 0.44 gal/yd<sup>2</sup> for Woodburn, along with the Aggregate Application Rate (AAR) values, recorded as 22 lb/yd<sup>2</sup> for Pendleton and 16 lb/yd<sup>2</sup> for Woodburn, were applied as per the measurements obtained from both field sites. The heated emulsion was then spread onto a 20cm x 20cm metal Vialit plate using a spatula. Subsequently, aggregates were dropped onto the Vialit plate using an aggregate spreader apparatus developed by Weaver et al. (2023)(See Figure 3.3b). The sample was then compacted by passing a 25 kg rubber wheel over it three times from both directions (See Figure 3.3d). Afterward, the sample was cured at 45°C for predetermined durations. The cured samples were then allowed to rest at ambient temperature (25±2°C) for 30 minutes. This was followed by a flip-over process to remove excess aggregates, and a sweep test was performed afterward. The sample was then conditioned at 5°C and 25°C for 20 minutes each before performing the Vialit test. It should be noted that the maximum aggregate loss observed in the sweep test occurred in the samples cured for 3 hours. Due to an excessive loss of aggregates from these plates in the sweep test, it was challenging to use the same plate for the Vialit test. Consequently, new samples were prepared for the Vialit tests at the same curing duration. Following the flip-over process, these samples were conditioned at both 25°C and 5°C, after which the Vialit tests were conducted. Similarly, pull-off tests were conducted on separate Vialit plates. The process followed is detailed in Section 3.2.2.2.

## 3.4.3 Results & Discussions

The sweep test results are given in Figure 3.25. It is evident that the chip loss due to sweeping is significantly greater in samples cured for 3 hours than in those cured for 24 and 48 hours. This observation held true for both Woodburn and Pendleton samples and can be attributed to the water content in the emulsion; as water evaporates over time, adhesion between the binder and

aggregates is increased, enhancing aggregate retention. While the influence of curing duration on chip loss for the 24 and 48-hour samples is less pronounced, a trend of decreasing chip loss with increased curing time can be observed. Pendleton samples exhibit higher chip loss across all curing durations than Woodburn samples. However, comparing these samples directly is challenging due to differences in the binders and aggregates used, notably in their gradation and physical properties as well as environmental conditions to which they were exposed. One possible explanation for Woodburn's superior aggregate retention performance could be its smaller median particle size (the sieve size corresponds to 50% passing-Pendleton 8.2 mm – Woodburn 7.5 mm) (Table 3.4). The chemical bond between the aggregate and binder, or the performance of the binder itself, might have also played a key role. When comparing field samples with those cured in the laboratory for 24 and 48 hours, it becomes apparent that the field samples exhibit higher chip loss, except when compared to the 3-hour lab-cured samples. This discrepancy can likely be attributed to the different curing durations; the field samples were cured for 8-9 hours. The more controlled curing conditions in the laboratory could have significantly contributed to the observed differences in chip loss between the laboratory and field samples.

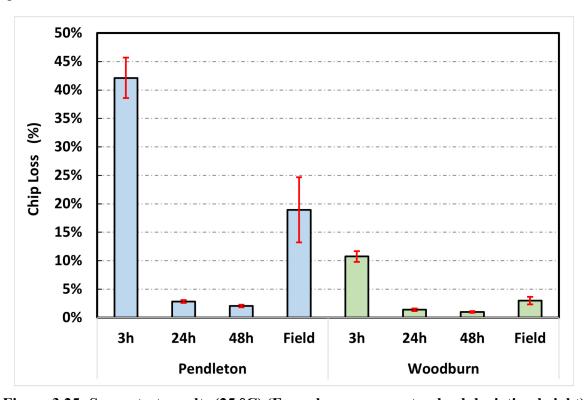


Figure 3.25: Sweep test results (25 °C) (Error bars are one standard deviation height)

Figure 3.26 presents the results of the Vialit tests conducted at 25°C. As illustrated in the figure, paralleling the results of the Sweep test, the highest chip loss is observed in samples cured for 3 hours, followed by those cured in the field. These results show that both the modified sweep and the Vialit test can differentiate between the curing times of samples at 25 °C (higher chip loss at shorter curing times). Given that the adhesion properties of the binder improve with longer curing times, it can be said that these tests accurately assess the adhesion characteristics. The difference in chip loss between the 24-hour and 48-hour cured samples is statistically

insignificant (p=0.82 for Pendleton and p=0.40 for Woodburn). Consistent with previous findings, Pendleton samples exhibited greater chip loss compared to Woodburn across each curing condition.

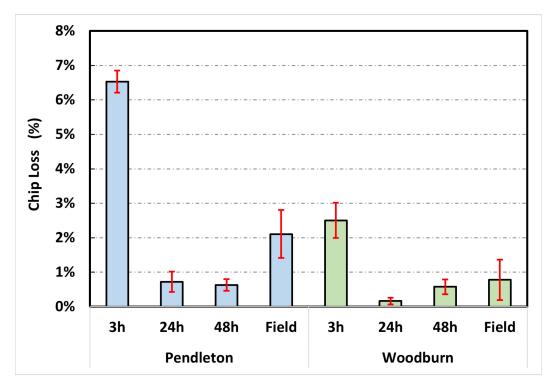


Figure 3.26: Results of the Vialit test conducted at 25°C (Error bars are one standard deviation height)

Figure 3.27 displayed the 5°C Vialit test results. Higher chip loss values were observed at 5°C compared to 25°C, which can be attributed to the increased brittleness of the binder at lower temperatures, where it stiffened and behaved more like a brittle, glassy material. Similar to other tests (Sweep and 25°C Vialit), the highest chip loss was noted in samples cured for 3 hours, followed by field-cured samples. Contrary to the 25°C Vialit test results, the 48-hour cured samples exhibited more chip loss than the 24-hour cured samples at 5°C, a difference that is statistically insignificant (p=0.13 for Pendleton and 0.052 for Woodburn). In this regard, it can be said that the results show a parallel trend with the Sweep test and 25°C Vialit test results. When the field samples are compared, it can be observed that a higher variability was reported for both projects. This can be attributed to a less controlled curing environment in the field when compared to the laboratory. For both projects, field samples exhibited higher chip loss compared to samples cured for 24 and 48 hours but lower chip loss compared to samples cured for 3 hours. Considering that the field samples were cured for 9-10 hours, the higher chip loss compared to samples cured for 24 and 48 hours can be related to differences in curing times. Overall, Woodburn chip seal samples provided better aggregate retention compared to Pendleton chip seal samples.

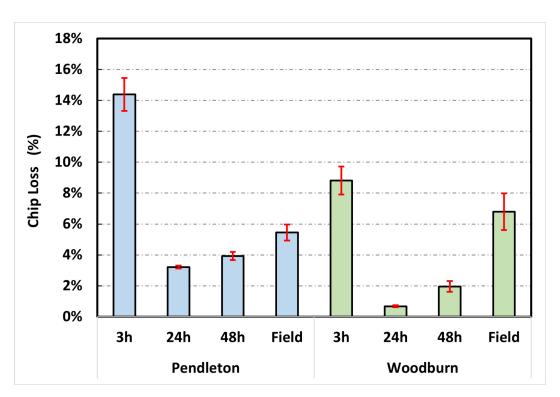


Figure 3.27: Results of the Vialit test conducted at 5°C (Error bars are one standard deviation height)

Figure 3.28 shows the results of the pull-off tests at 25°C. As described in Section 3.2.2.2, the circular area method is used in calculating the bond strength; the maximum load obtained is divided by the circular cross-sectional area of the dolly (1,962.5 mm²). The results given in Figure 3.28 align with expected outcomes and demonstrate a strong correlation between curing times and bond strength. Considering Woodburn chip seal specimens exhibited better aggregate retention in both sweep and Vialit tests, enhanced bond strength in Woodburn specimens during pull-off tests can be anticipated. This expectation is confirmed across all curing conditions in the pull-off test results. It is important to highlight that all failures observed at 25°C were cohesive failures of the binder material. In other words, the failures were within the binder itself (binder-binder), with no instances of aggregate-binder separation observed.

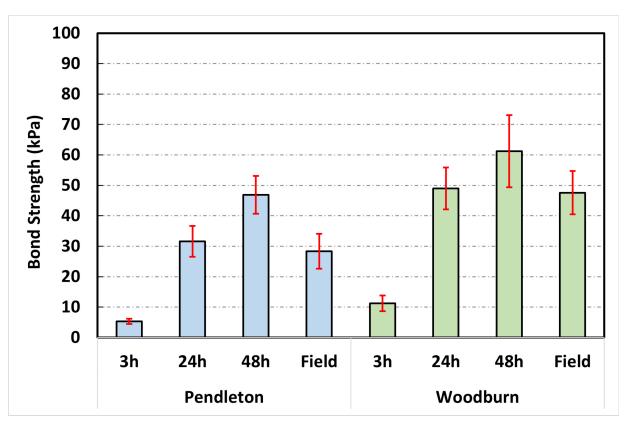


Figure 3.28: Pull-off test results at 25°C (Error bars are one standard deviation height)

The results of the pull-off tests conducted at 5°C are presented in Figure 3.29. According to these results, both Pendleton and Woodburn samples demonstrated higher bond strength values at 5°C compared to 25°C. As previously discussed, this can be attributed to the glassy behavior observed in the binder at lower temperatures, where the binder exhibits a more brittle response. This finding is also in line with the findings from the Vialit test. In the samples, a hybrid occurrence of both binder-binder and binder-aggregate failures was observed. Therefore, it can be suggested that 5°C is a suitable temperature for assessing the adhesive properties of aggregate-binder interactions, while the cohesive properties of the binder can be more accurately determined at 25°C. Similar to the results obtained at 25°C, it was observed in the pull-off test conducted at 5°C that the bond strength values increased as the curing time increased.

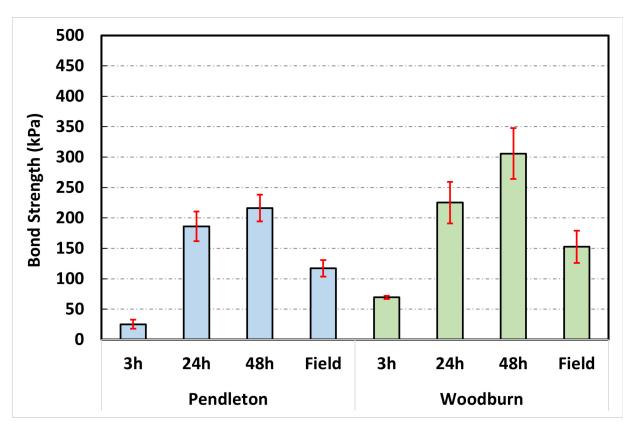


Figure 3.29: Pull-off test results at 5°C (Error bars are one standard deviation height)

To assess the reliability of the test methods developed, it was decided to establish correlations between adhesion results obtained from pull-off tests and chip loss results from the modified sweep and Vialit tests. While the pull-off, Vialit, and sweep tests differed in their operational mechanisms—for instance, dynamic impact loads are predominant in the Vialit test, shear loading was dominant in the sweep test, and static tension loading was significant in the pull-off test—they collectively evaluated adhesive properties. A certain degree of correlation among these tests can be anticipated, though it may not be distinctly pronounced. For the chip loss distress mode, the tensile strength of the binder-to-aggregate adhesion from the pull-off test can be considered to be the ground truth (reference) value. However, unlike the pull-off test, the Vialit test is more practical and can also be conducted during construction.

Figure 3.30 illustrates the correlation between sweep test results and pull-off test results. The  $R^2$  value displayed on the graph represents the coefficient of determination, which ranges from 0 to 1. An  $R^2$  value closer to 1 indicates that the model explains a significant portion of the variance in the dependent variable based on its independent variables, suggesting a strong fit. Conversely, an  $R^2$  value closer to 0 suggests that the model explains little of the variance in the dependent variable, indicating a weak fit. A higher  $R^2$  value also suggests a stronger relationship between the dependent and independent variables. An exponential function was fitted to the data, yielding the highest  $R^2$  values compared to other correlation functions. Analysis of these results indicated a relatively strong correlation ( $R^2 = 0.73$ ) between sweep test results and the bond strength values derived from the pull-off test. Within the graphs, an outlier was readily identifiable-Pendleton's field sweep test result (Figure 3.30a). As previously noted, the sweep test in

Pendleton was conducted in situ, where environmental conditions were less stringently controlled. Excluding this outlier significantly enhanced the R<sup>2</sup> value of the correlation to 0.79 (Figure 3.30b). Given this relatively high correlation curve, it can be concluded that the sweep test at 25°C can be effectively and practically used to determine the adhesion between the aggregate and the binder, considering the complexity, lack of practicality, and cost associated with the pull-off test.

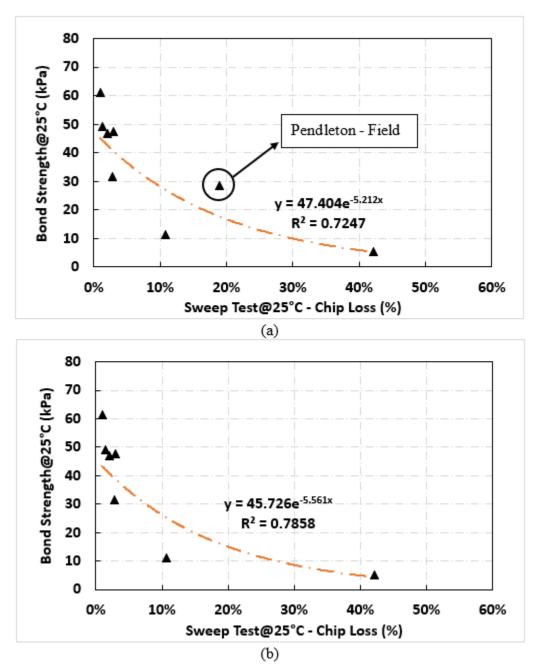


Figure 3.30: The correlation between the sweep test (25°C) and Pull-off test results (25°C) (a) with the outlier, (b) without the outlier

Figure 3.31 displayed the correlation between the results of the pull-off test and the Vialit test conducted at 25°C. Similar to the sweep test, a strong correlation can be observed between the pull-off test results and the Vialit test results at 25°C (R²=0.79). The high correlation obtained suggests that the Vialit test (at 25°C) can also serve as a practical and reliable test method for assessing the aggregate retention of chip seal samples. While the sweep and Vialit tests can be practical methods for evaluating binder adhesion properties, they have limitations, particularly in differentiating performance when chip loss is zero or near zero. In such instances, the pull-off test can be performed to ascertain the binder's adhesion characteristics.

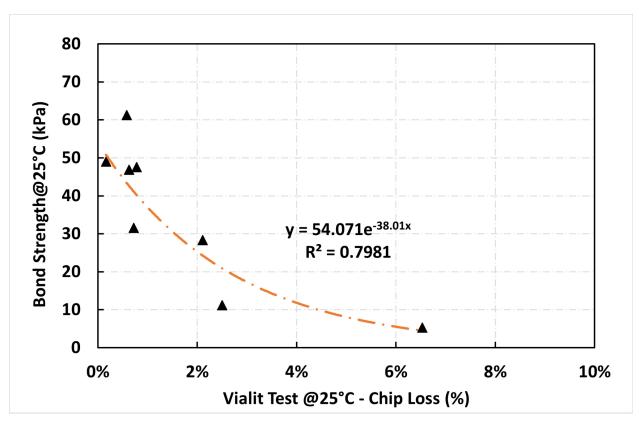


Figure 3.31: The correlation between the Vialit test (25°C) and Pull-off test results (25°C)

Figure 3.32 presents the correlation between the pull-off test results and the Vialit test outcomes, both conducted at 5°C. Similar to the patterns observed in the sweep and Vialit tests (25°C), the 5°C Vialit test results show a high R² value when correlated with the pull-off test at 5°C. An R² value of 0.76 is considered robust, particularly considering the variations in loading conditions between the pull-off (constant displacement rate tension) and Vialit (dynamic impact load) tests. These findings suggest that the Vialit test can yield reliable results when conducted at 5°C. Furthermore, in scenarios with no or minimal chip loss, the pull-off test can be employed to assess the adhesive properties between the aggregate and the asphalt binder.

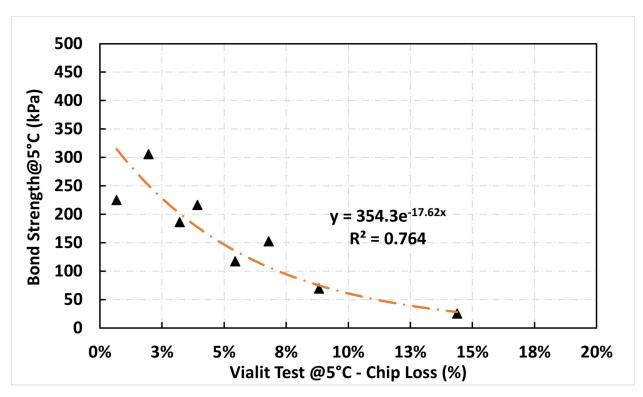


Figure 3.32: The correlation between the Vialit test (5°C) and Pull-off test results (5°C)

The established correlation demonstrated that at 25°C, the sweep test is suitable for evaluating within-binder adhesion characteristics (cohesive failure), while at 5°C, the Vialit test is appropriate for assessing aggregate-binder adhesion characteristics. In this manner, three Vialit samples can be prepared, and a sweep test can subsequently be performed at 25°C. Following this, the same samples can be conditioned at 5°C, and the Vialit test can then be conducted. This approach allowed for the practical determination of both binder-binder cohesion and aggregate-binder adhesion properties.

Based on the results presented in Figure 3.30 and Figure 3.32, a critical threshold can be established to differentiate between poor and good adhesion clusters for the sweep, Vialit, and pull-off tests. As observed in Figure 3.30 and Figure 3.32, samples cured for 3 hours have formed a distinct cluster. Figure 3.25 shows these 3-hour cured samples exhibited significantly high chip loss. As discussed in the literature review of this report (Section 2.1.1), it was recommended that the percent wastage for aggregate loss in chip seal design was 5% for rural and residential areas and 10% for relatively high-volume roads. Also, many research studies used a 10% limit for the sweep test (Guirguis and Buss 2019; Im and Richard Kim 2016; Lee and Kim 2014). Given these insights, 10% is selected as a reasonable threshold to separate the 3-hour cured (low adhesion) samples from fully cured (high adhesion) samples, as shown in Figure 3.33a. For tests conducted at 25°C, the adhesion value corresponding to 10% is determined to be 25 kPa using correlation equations. For the pull-off and Vialit tests conducted at 5°C, the thresholds that separate the clusters, as illustrated in Figure 3.33b, are set at 8% for the Vialit test and 100 kPa for the pull-off test. If samples perform below these established values, it can be interpreted that sufficient adhesion between the aggregate and binder is not observed.

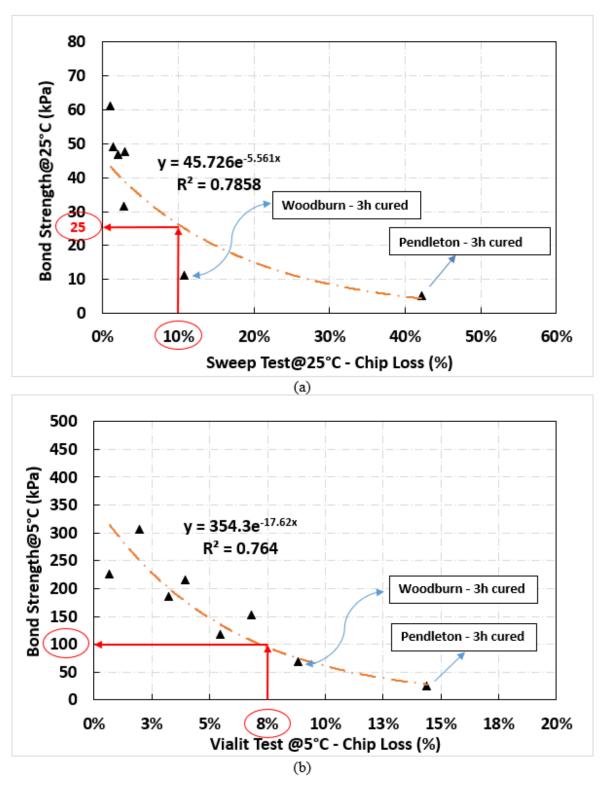


Figure 3.33: The threshold values determined (a) sweep & pull-off test (25°C), (b) Vialit & pull-off (5°C)

## 3.4.3.1 The effect of aggregate surface moisture condition on aggregate-binder adhesion characteristics

In the construction of emulsion-based chip seals, it is common practice to moist aggregates with water before being spread over the emulsion (Joslin et al. 2019; Shuler et al. 2011). Ignatavicius et al. (2021) reported enhanced aggregate retention of chip seal samples when the aggregate surface was moist. To evaluate the effectiveness of this wetting process on aggregate retention and determine whether it can be captured using the test methods developed in this study, the research team conducted an additional set of experiments using dry aggregates. For this purpose, Pendleton and Woodburn aggregates were applied to the emulsion in an air-dried state (conditioned in the laboratory for three days before spread over the emulsion). Subsequently, sweep, Vialit, and pull-off tests were conducted on these samples after they had been cured at 45°C for 24 hours. The results of the sweep tests are presented in Figure 3.34. It was found that damp aggregates showed enhanced aggregate retention compared to dry aggregates for both Pendleton and Woodburn samples. This difference is more pronounced in Pendleton samples than in Woodburn samples, which could be attributed to Pendleton's higher aggregate application rate (AAR) of 22 lb/yd² compared to Woodburn's AAR of 16 lb/yd².

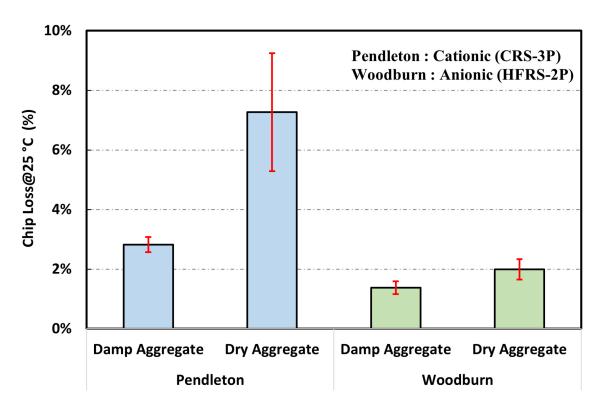


Figure 3.34: Sweep test results of damp and dry aggregates (Error bars are one standard deviation height)

It should also be noted that before conducting the sweep test, a flip-over process was executed to remove aggregates lacking contact with the binder. During this process, dry samples tended to lose a greater quantity of aggregates compared to damp ones. The

results of the flip-over test for dry and damp aggregates are presented in Figure 3.35. It can be inferred from this figure that aggregates pre-moistened with water demonstrate improved adhesion to the binder. It was considered that the cohesive force of water covering the surface of the aggregate may have enhanced the bonding between the emulsion and aggregates due to the water's more suitable electric charge.

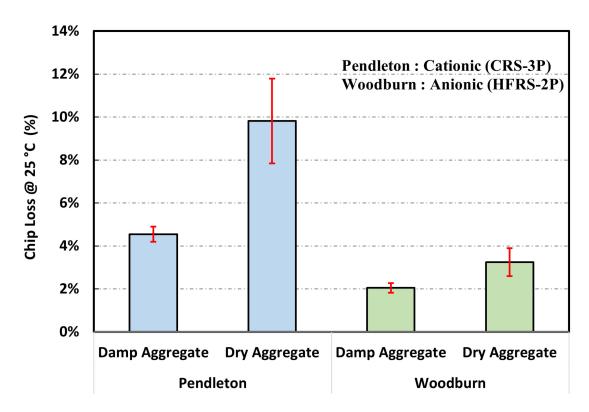


Figure 3.35: Flip-over test results of damp and dry aggregates (Error bars are one standard deviation height)

Figure 3.36 presents the results of the Vialit test conducted at 5°C. These results indicate that wetting the aggregate improves the chip seal's aggregate retention at low temperatures and underscores the significance of a proper wetting process before applying aggregate over emulsion. However, it is crucial to note that excessive wetting may lead to binder flushing. If the aggregates are overly wet, the emulsion can become excessively diluted with water, decreasing its viscosity and enabling it to flow more easily to the aggregate's surface (flushing). Therefore, the over-wetting of aggregates should be avoided in the field.

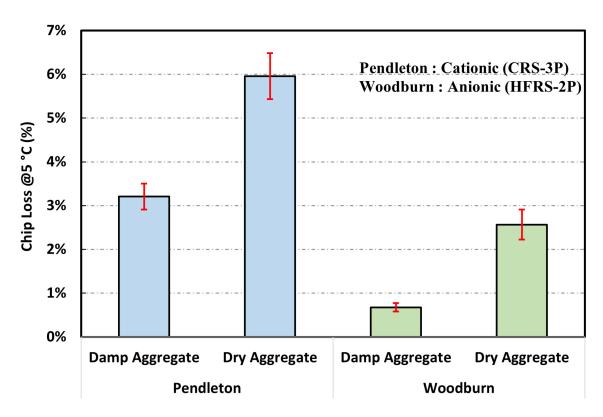
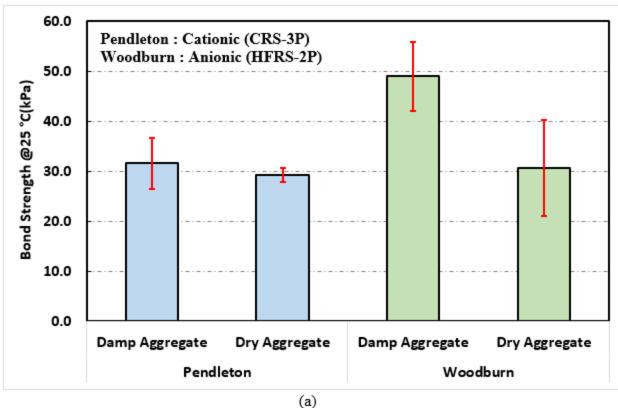


Figure 3.36: Vialit test (5°C) results of damp and dry aggregates (Error bars are one standard deviation height)

The pull-off test results for damp and dry aggregates are presented in Figure 3.37. Upon evaluating the results, it was observed that at both temperatures (25°C and 5°C), damp aggregates exhibited higher bond strength compared to dry aggregates. This difference was more pronounced in tests conducted at 5°C than at 25°C. Given that 25°C provides insights into the cohesive (binder-binder) properties and 5°C into the adhesion properties between aggregate and binder, it can be concluded that wetting the aggregates helps to improve the bond between the aggregate and the emulsion binder. This result suggested that wetting the aggregates is a reliable strategy for improving the adhesion between the asphalt binder and the aggregate surface, resulting in high resistance to chip loss.



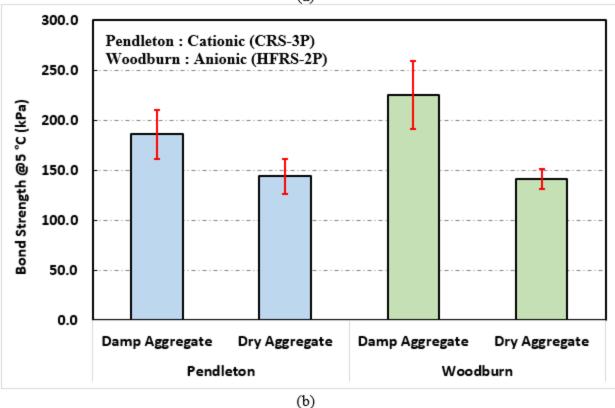


Figure 3.37: Pull-off test results of damp and dry aggregates (a) at 25°C (b) at 5°C (Error bars are one standard deviation height)

Considering that the results obtained for damp and dry aggregates align with the findings reported in the literature (Ignatavicius et al. 2021; Shuler et al. 2011), it can be concluded that the Modified Sweep, Vialit, and Pull-off tests are effective methods for determining the adhesion properties between aggregates and binder.

### 3.4.3.2 The effect of aggregate dustiness on aggregate-binder adhesion characteristics

It is known that the dust on the aggregate surface decreases the adhesion between aggregates and the binder by breaking the bonding (Aktas et al. 2013; Gurer et al. 2012). This raised the question: "Can the reduction in the adhesion between aggregate and the binder due to the dustiness of aggregates be mitigated through the wetting process?" To explore this, the research team planned to perform similar damp-dry experiments with cleaned aggregates. A certain amount of aggregates was washed multiple times in the laboratory to remove all surface dust from the aggregates and then allowed to dry. Chip seal samples using both dry-cleaned (first washed with water and then air-dried) and damp-cleaned aggregates (first washed and used without drying them) were then prepared for both projects. In addition, with 1 kg samples from both aggregates, the dust content was determined. First, 1 kg of aggregates in an air-dry state was weighed. These aggregates were then placed in an oven at 110°C for 48 hours to achieve a dry state and were weighed again. Afterward, the aggregates were washed several times with clean water in a bucket and sieved through a No. 200 (75µm aperture) sieve. The aggregates were then returned to the oven at 110 °C for another 48 hours and reweighed. The weight loss compared to the initial dry weight was reported as dustiness. The dustiness of the aggregates was determined to be 0.44% for Pendleton aggregate and 0.5% for Woodburn aggregate by the total weight of aggregates. Given the high correlation observed between pull-off tests and both Vialit and Sweep tests (Figure 3.30, Figure 3.32), for practicality, only the sweep test at 25°C and Vialit tests at 5°C were conducted for this assessment, omitting the pull-off test. The results of these experiments are presented in Figure 3.38.

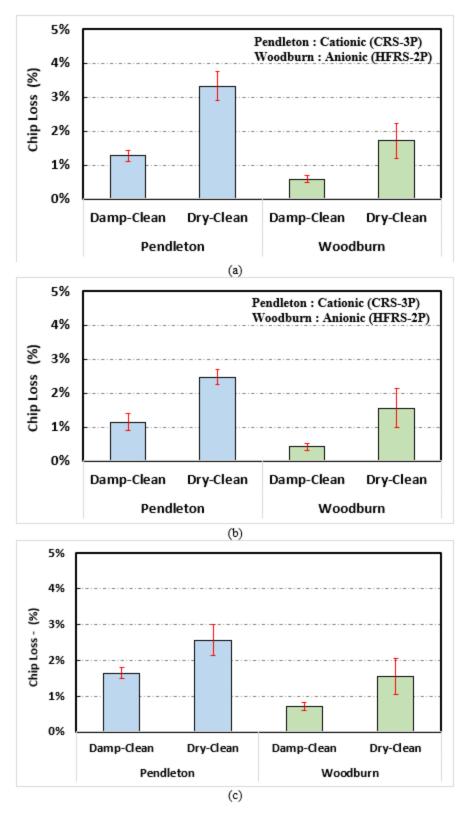


Figure 3.38: Cleaned aggregate tests (a) Flip-over (b) Sweep test at 25°C (c) Vialit test at 5°C (Error bars are one standard deviation height)

As shown in Figure 3.38, a consistent trend was evident across all tests. Damp aggregates led to reduced chip loss in both projects. In this setup, dust had been cleaned from the surfaces of the aggregates. Therefore, it can be concluded that the cohesive forces in water played a key role in improving the adhesion of the aggregates to the emulsion. To assess the impact of dust and determine if wetting can mitigate the bond loss caused by dust, Damp-Dusty aggregates were compared with Damp-Clean aggregates under both dry and damp conditions. The flip-over test results are given in Figure 3.39. As anticipated, the lowest chip loss values were observed for the damp-clean condition in both projects. It can be inferred that aggregates with a clean surface and a slight degree of moisture were less prone to dropping, even when their contact with the binder was minimal. Wetting dusty aggregate can mitigate the tendency of chip loss, but not to the fullest extent.

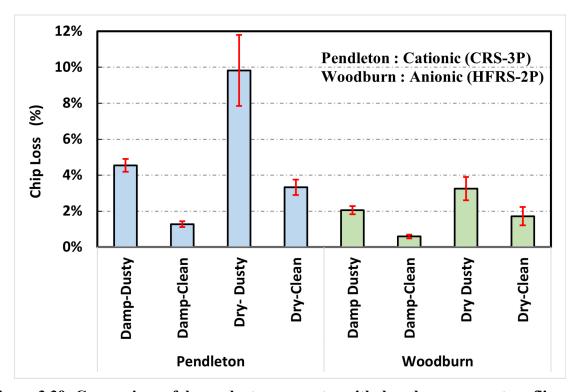


Figure 3.39: Comparison of damp-dusty aggregates with dry-clean aggregates - flip-over test at 25°C (Error bars are one standard deviation height)

The comparisons of sweep test results for dusty and clean aggregates under both damp and dry conditions are presented in Figure 3.40. In line with the flip-over test findings, the best aggregate retention was observed in the damp-clean condition for both projects. Generally, chip loss was recorded at less than 3% in all conditions (which is significantly lower than the 10 % limit determined), with the exception of the Pendleton Dry-Dusty condition, which is still deemed reasonable. As noted previously, AAR for Pendleton is significantly higher than for Woodburn (Table 3.3), and alterations in aggregate surface conditions affected Pendleton more markedly. The pull-off test results indicated a lower bond strength for Pendleton, suggesting that dustiness drastically impacts the bond strength in this case. Another explanation could be the susceptibility of the binder used;

for instance, CRS-3P was observed to be more vulnerable to dust effects compared to HFRS-2P. Based on the analysis of the sweep test results, it can be concluded that while wetting the aggregates proves effective, washing them might not be a cost-effective or sustainable method, as it did not result in a considerable change in chip loss values. In other words, if the dust content is around 0.5%, just wetting them can be a good choice to increase aggregate retention. However, the use of aggregates with higher dust contents for chip sealing should be avoided.

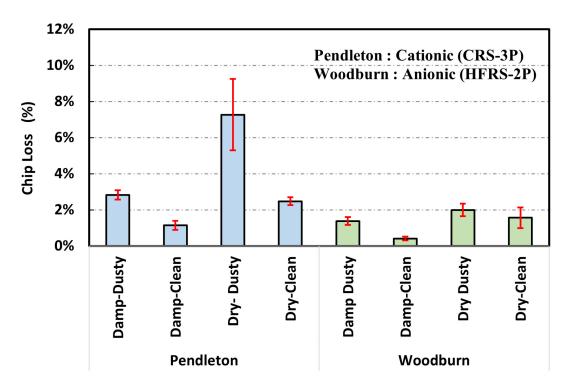


Figure 3.40: Comparison of damp-dusty aggregates with dry-clean aggregates - sweep test at 25°C (Error bars are one standard deviation height)

The comparisons of Vialit test results at 5°C for dusty and clean aggregates under both damp and dry conditions are depicted in Figure 3.41. The results indicated that cleaning the aggregates did not significantly alter the outcomes for Woodburn aggregates, while it significantly reduced chip loss for Pendleton samples. The dustiness levels of aggregates were determined to be 0.44% and 0.5% by weight for Pendleton and Woodburn, respectively (values that are nearly identical). Hence, the results given in Figure 3.40 suggested that the CRS-3P binder is more susceptible to dust effect compared to the HFRS-2P binder. Ignatavicius et al. (2021) also reported that anionic emulsions performed better than cationic emulsions in the presence of dusty aggregates. Thus, for aggregates with high dust content, HFRS-2P emulsion should be preferred. These results also suggest that the test method recommended in this study reliably captures the impact of aggregate dustiness and moisture on aggregate retention. Overall, damp aggregates exhibited chip loss values of less than 3%. Therefore, it can be concluded that wetting the aggregates is an effective method for enhancing aggregate retention in these projects.

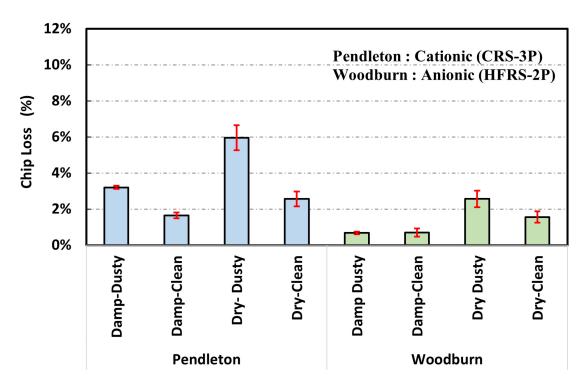


Figure 3.41: Comparison of damp-dusty aggregates with dry-clean aggregates - Vialit test at 5°C (Error bars are one standard deviation height)

#### 3.4.3.3 The effect of binder type on aggregate-binder adhesion characteristics

The selection of binders is critically important for a successful chip seal application (Pierce and Kebede 2015). It is known that some aggregates work better with negatively charged anionic emulsions, while others perform better with positively charged cationic emulsions depending on the surface charge of the aggregates (Ignatavicius et al. 2021). The physical and chemical properties of the binders have a significant impact on aggregate retention (Kim et al. 2017). In this context, the research team prepared samples combining Pendleton aggregates with the anionic emulsion used in Woodburn and Woodburn aggregates with the cationic emulsion used in Pendleton to investigate the effects of charge mismatch between the aggregates and binders on the aggregate retention performance of the chip seals. These samples were produced in their original (uncleaned) and damp states. After curing for 24 hours at 45°C, the samples were tested. The test results are given in Figure 3.42. In general, the Woodburn aggregate yielded lower chip loss values compared to Pendleton, which could be attributed to factors such as AAR or the size and gradation of the used aggregates (Table 3.3, Table 3.4).

Based on the flip-over test results as shown in Figure 3.42a, it can be said that the HFRS-2P binder demonstrated slightly higher, yet statistically significant (p=0.01 < 0.05) aggregate retention with Pendleton aggregate compared to the CRS-3P binder used in the field. In contrast, with Woodburn aggregate, the CRS-3P binder showed a higher aggregate retention. Upon examining the sweep test results given in Figure 3.42b, a similar trend was noted i.e., Pendleton aggregates exhibited better aggregate retention

when used with anionic (HFRS-2P) binder, compared to cationic binder (CRS-3P) used in construction. Likewise, the Vialit test results (Figure 3.42c) suggest that both aggregates performed better with an anionic (HFRS-2P) binder. It should be noted here that all aggregate-binder combinations exhibited acceptable performance, meeting the threshold values of 10% for the sweep test and 8% for the Vialit test. Based on these consistent results, the test methods developed in this report can be used before starting a project to determine which type of emulsion is suitable for a specific type of aggregate, assessing aggregate-binder compatibility.

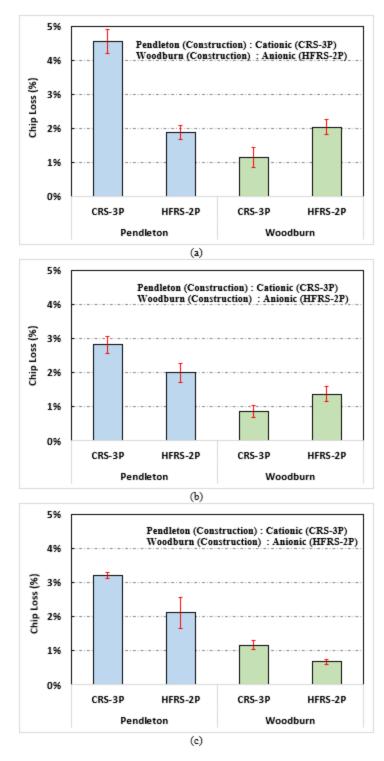


Figure 3.42: The test results of Pendleton and Woodburn aggregates with CRS-3P (cationic) and HFRS-2P (anionic) binders (a) Flip-over (b) Sweep test at 25°C (c) Vialit test at 5°C (Error bars are one standard deviation height)

#### 3.4.3.4 The effect of substrate type on aggregate-binder adhesion characteristics

Previously, sweep, Vialit, and pull-off test outcomes were primarily derived from samples on Vialit metal plates. To facilitate a comparative study between a metal surface and asphalt surface, the research team compacted and brought 3 cm thick laboratory-prepared asphalt concrete (AC) cores to both Pendleton and Woodburn constructions to acquire chip seal samples on these discs (See Figure 3.18). These specimens, alongside the metal plates, were subjected to similar field curing conditions. Additionally, chip seal samples were produced in a laboratory setting, utilizing emulsions and aggregates obtained from the field and applied to AC discs. These discs underwent a curing process at 45°C for 24 hours, followed by the execution of pull-off tests at temperatures of 25°C and 5°C. The results are presented in Figure 3.43.

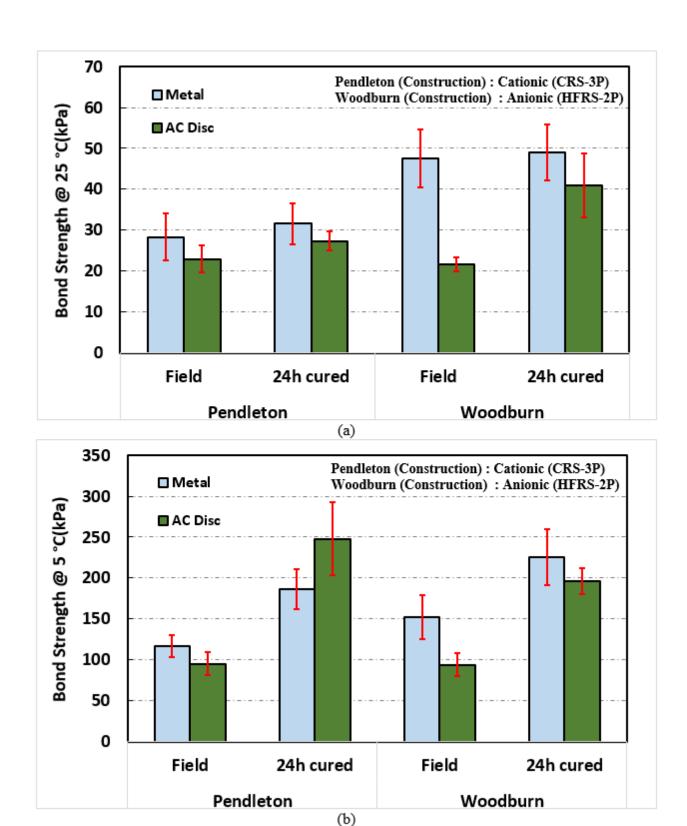


Figure 3.43: Pull-off test results of chip seal samples on metal plates and AC discs (a) 25°C (b) at 5°C (Error bars are one standard deviation height)

It was found that AC disc samples generally exhibit lower bond strength values compared to metal plates, as depicted in Figure 3.43. This could be attributed to the partial absorption of emulsion by the AC material. When examining the results specifically for Pendleton, no statistically significant difference was observed between metal and AC at both temperatures. Field samples displayed slightly lower values for AC at both temperatures, yet laboratory-prepared samples, cured for 24 hours, showed consistent averages across temperatures. Hence, it can be said that the disparity in bond strength between AC and metal diminished following the complete curing of the emulsion.

A similar trend can be observed in the Woodburn samples. In Woodburn 25°C samples, a statistically significant difference was found in field samples between metal and AC plates. Overall, AC discs demonstrated lower bond strength values for both field and laboratory samples. However, this difference was more pronounced in Woodburn samples than in Pendleton, potentially due to Woodburn's lower EAR (0.44) compared to Pendleton's (0.47). Consequently, the emulsion absorbed by the AC may have had a more significant impact on the Woodburn samples since the EAR was lower. Furthermore, the lower viscosity of the Woodburn emulsion compared to Pendleton's might have contributed to this increased absorption. Given the discrepancy in bond strength results obtained for AC and metal, the employment of metal plates is considered more advantageous as the preparation of AC is time-consuming and costly.

For the adhesion tests on AC discs, the edges of the discs were wrapped with waterproof tape (Figure 3.18, Figure 3.19). It's worth noting that during laboratory experiments, no significant binder accumulation was observed around the tape for the high-viscosity CRS-3P binder. However, for the low-viscosity HFRS-2P emulsion, a substantial amount of binder adhered to the tape, and in some cases, it even leaked. Consequently, the emulsion applied in experiments on AC discs did not fully contribute to the formation of binding characteristics. Therefore, it is believed that conducting experiments on metal plates can yield more consistent results and provide a clearer picture of the impact of binder, aggregate, and their interaction on adhesion and performance.

To account for the different absorption tendencies of emulsions, the Tack-Lifter mentioned in Section 4.0 can be used. The Tack-Lifter allows for quantification of the amount of emulsion absorbed by the pavement. Using the EAR and absorbed EAR, effective EAR (the emulsion retained on the pavement) can be calculated. The calculated effective EAR can then be utilized to conduct tests on metal plates.

## 3.5 ADHESION PERFORMANCE OF OREGON'S AGGREGATES AND BINDERS

## 3.5.1 Objectives

The major objective of this section is to test various aggregates and binders used in Oregon with recommended test methods and report their adhesion performance.

#### 3.5.2 Materials and Methods

In this section, the developed adhesion test methods were applied to chip seal samples that were prepared using aggregates and binders commonly utilized in Oregon. Furthermore, the EAR and AAR values were determined using chip seal designs developed by Buss et al. (2016) (See Section 2.1.1). The physical properties of aggregates are given in Table 3.1. One anionic (HFRS-2P) and one cationic (CRS-2P) emulsion were utilized. The EAR and AAR utilized in the study were provided in Table 3.6, and assumptions made in determining the application rates were given in Table 3.7. Those assumptions were kept constant for all types of aggregate and binder combinations.

Table 3.6: Chip seal design rates for each aggregate

Aggregate Source	EAR (gal/yd²)	AAR (lb/yd²)
Heppner	0.44	23
Baker	0.44	23
Seaside	0.44	28
Stayton	0.40	16

Table 3.7: Assumptions made during chip seal design

Condition	Number
AADT	5,000
Design life (years)	5
Percent truck	15
Aggregate percent allowed for waste	10
Surface condition factor (gal/yd²)	0.09

Initially, emulsion was applied onto the Vialit plate according to the quantities specified in Table 3.6. Then, pre-moistened aggregates were spread over the Vialit plates in the predetermined design ratio. Then, the sample was compacted by rolling a 25 kg rubber wheel on the sample. Subsequently, the sample was cured at 45°C for 24 hours. Upon removal from the environmental chamber, the sample was allowed to condition at 25°C for 30 minutes before being flipped over to remove aggregates not in contact with the binder. Following this, the sweep test was performed. After conditioning the samples at 5°C for 20 minutes, the Vialit test was conducted.

#### 3.5.3 Results & Discussions

The results of the sweep test are presented in Figure 3.44. It is observed that, across all types of aggregates and binders, the chip loss values were below the threshold determined for the sweep test, which was set at 10%.

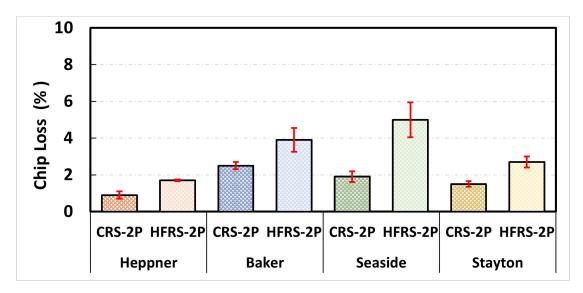


Figure 3.44: Sweep test results (25°C) of aggregates with anionic HFRS-2P and cationic CRS-2P emulsions (Error bars are one standard deviation height)

Regardless of the aggregate type, the CRS-2P binder exhibited slightly better aggregate retention performance compared to the HFRS-2P binder. While further research is needed to confirm this, the reason may be that the surface charge of Oregon's aggregates is better suited to cationic binders. The Vialit test results are given in Figure 3.45. Similar to sweep test results, the chip loss obtained for all the aggregate and binder combinations was less than 8%, which was determined as the threshold value for the Vialit test conducted at 5°C.

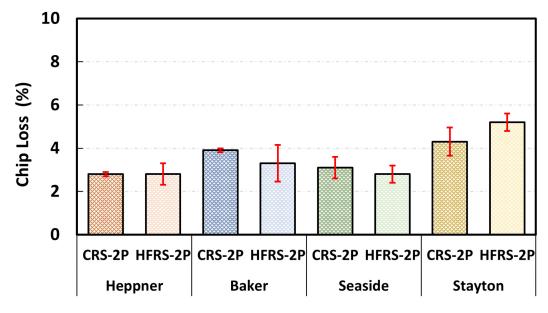


Figure 3.45: Vialit test results (5°C) of aggregates with HFRS-2P and CRS-2P emulsions (Error bars are one standard deviation height)

When the results presented in Figure 3.45 were analyzed, it can be concluded that no statistically significant differences were observed between the HFRS-2P and CRS-2P emulsions for all the aggregates. The data obtained shows that chip loss was 8% for the Vialit test (Figure 3.45) and less than 10% in the sweep test (Figure 3.44), suggesting that these aggregates can effectively work with either type of binder, although it can be said that they generally perform better with cationic binders.

#### 3.6 CONCLUSIONS

In this section, the adhesion properties between the aggregates and the binders were discussed. Modified sweep and pull-off tests were developed to evaluate aggregate loss in chip seals, and their effectiveness was compared with the Vialit test. Samples from chip seal construction projects in two distinct regions of Oregon (Pendleton and Woodburn) were collected and tested in the laboratory to assess adhesion performance. Aggregates and binders from these projects were used to prepare specimens in the laboratory, which underwent various curing times to evaluate their aggregate retention performance. The results from all three experimental methods were then compared and correlated to determine the most effective and practical testing approaches. Threshold limits were established based on the results to differentiate between good and poor adhesion characteristics. The recommended methods were then applied to explore the effects of dustiness and surface moisture on the aggregate retention performance of the chip seal samples. Lastly, the developed adhesion tests were performed on chip seal samples using aggregates from four distinct areas of Oregon, along with an anionic and a cationic emulsion, to assess their aggregate retention performance. Within the limits of this study, the following conclusions can be drawn:

- 1. The modified sweep, Vialit, and pull-off tests have shown sensitivity to the curing times of chip seals, with a high correlation among these methods suggesting their effectiveness in evaluating aggregate retention or aggregate-binder adhesion performance.
- 2. Modified sweep and Vialit tests can be performed in situ with minimal equipment requirements. For practicality, it was recommended to perform the sweep test at 25°C and the Vialit test at 5°C where no equipment is available for pull-off tests (based on high correlations established). In cases where chip loss is negligible or almost zero, the pull-off test can be employed to further quantify adhesion levels.
- 3. The modified sweep test can be conducted in the field to assist in determining the optimal timing for initiating the power brooming process in chip seal construction. The modified sweep test offers greater practicality compared to the sweep test delineated in ASTM D7000. Furthermore, it could be used in situ with minimal equipment requirements.
- 4. The test methods developed in this study allowed for the evaluation of adhesion properties between the aggregate and binder using specimens sampled directly from the field with negligible disruption to ongoing construction.
- 5. For the sweep test conducted at 25°C, a threshold value for distinguishing good from poor performance has been established at 10% chip loss, based on correlation curves. This threshold corresponds to a bond strength of 25 kPa for the pull-off test at the same temperature. Given that binder-binder failure consistently occurs at 25°C, this temperature is suitable for assessing the cohesive properties of the binder. To evaluate the adhesion characteristics between the aggregate and binder, the Vialit test and pull-off test at 5°C are

- recommended. The threshold for the Vialit test is set at 8%, and for the pull-off test at 5°C, it is recommended to be 100 kPa.
- 6. The sweep, Vialit, and pull-off tests successfully distinguished between samples with dusty surfaces and those with dry or wet aggregate surfaces. This indicated that these tests are sensitive to the surface condition of the aggregate, whether dry, wet, clean, or dusty. As expected, samples with dusty surfaces showed lower aggregate retention performance compared to those with clean surfaces, while samples with wet surfaces exhibited superior adhesion properties compared to those with dry surfaces. It was considered that the cohesive forces between water droplets on the wet surface and the water within the emulsion played a significant role in this enhanced adhesion. The ability of the developed test methods to make this distinction can be considered as an indicator of the effectiveness of the test methods developed.
- 7. The CRS-3P binder is found to be more susceptible to dust effect compared to the HFRS-2P binder. Thus, for aggregates with high dust content, HFRS-2P emulsion should be preferred since anionic emulsions are more resistant to the negative effects of high dust content (Ignatavicius et al. 2021).
- 8. The pull-off tests performed on AC discs and metal plates revealed that AC disc samples generally demonstrated lower bond strength relative to metal plates, presumably owing to the absorption of emulsion by the AC discs. It was concluded that the emulsion with lower viscosity absorbed more into the AC disc. Therefore, these findings favored the use of metal plates in bond strength evaluations due to their consistent performance and operational advantages over AC discs. In addition, the metal plates eliminate the absorption effect and provide a clearer picture regarding the performance of aggregates, emulsions, and their interaction.
- 9. Chip seal samples prepared according to the design developed for ODOT using commonly used aggregates and emulsions demonstrated adequate aggregate retention performance with both anionic and cationic binders. Overall, these aggregates exhibit better aggregate retention with cationic binders.

# 4.0 A FIELD WIRELESS SCALE SYSTEM TO MEASURE EMULSION APPLICATION RATES

#### 4.1 INTRODUCTION

In SPR777, a design method for Oregon's chip seals was developed (Buss et al. 2016). A critical aspect in attaining a high-performance chip seal lies in verifying that the appropriate quantity of emulsion is applied during field construction, i.e., the actual emulsion application rate (EAR) should closely align with the designed EAR. Monitoring EAR before construction is an important component of the QA/QC process for successful chip seal construction. In this section, the methodology proposed for measuring the EAR in the field is discussed. The research team decided to utilize asphalt shingles and wireless scales for EAR measurement by following a method and tools that were initially developed for tack coats in SPR 818 (OreTackRate)(Coleri et al. 2020b).

Furthermore, the research team aimed to quantify the amount of effective EAR, which refers to the quantity of emulsion remaining on the pavement surface after accounting for the portion absorbed by the existing pavement. The tack lifter introduced by Rawls et al. (2016) was developed in OSU-AMaP and utilized for this purpose.

### 4.1.1 Objectives

The major objectives of this section are as follows:

- To develop and refine a practical method for accurately measuring the actual EAR in field conditions, ensuring it aligns closely with the designed EAR.
- To quantify the effective EAR, which is defined as the amount of emulsion remaining on the pavement surface after subtracting the portion absorbed by the existing pavement.

#### 4.2 MATERIALS & METHODS

First, a lightweight plastic plate was cut to the dimensions of 1 ft x 1 ft (30.48 cm x 30.48 cm) (Figure 4.1a). Then, asphalt shingles, with dimensions of 32.5 cm x 32.5 cm, were attached to the plastic plate (Figure 4.1b). Following that, the edges of the asphalt shingles were folded, and clips were affixed to the corners to form an asphalt shingle tray (Figure 4.1c). These trays were then attached to a wireless scale with the help of Velcro (Figure 4.1d-e). The preparation steps for the OreTackRate system are detailed in Figure 4.1. It should be noted here that the emulsion is sprayed onto the pavement in a triangular shape from the distributor truck's nozzles, with these triangles overlapping each other on the pavement's surface (Figure 4.2). For this reason, a particularly thin wireless scale is used to ensure the shingle trays remain close to the pavement surface to achieve the most accurate results (Figure 4.1f).

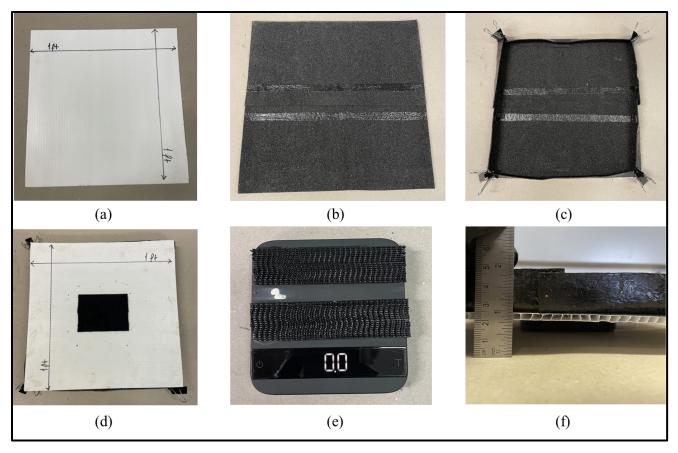


Figure 4.1: The preparation steps for the OreTackRate system: (a) cutting 1 ft x 1 ft (30.48 cm x 30.48 cm) plastic plate, (b) attaching shingle plates (32.5 cm x 32.5 cm) on the plastic plate, (c) folding the corners of shingles and securing with clips, (d-e) attaching shingle tray to the wireless scale using Velcro, (f) side view of OreTackRate system

The asphalt shingles were subsequently placed perpendicularly to the direction of travel on the road's shoulder. For each of the two projects, four asphalt shingles with wireless scales were prepared. The emulsion distributor truck sprayed emulsion on the shingle plates, and the weight measurements were recorded via an application installed on a tablet computer connected to wireless scales. Photos from the Pendleton project are illustrated in Figure 4.2.



Figure 4.2: OreTackRate system for measuring EAR of chip seal

As illustrated in Figure 4.2, the emulsion distributor truck uniformly sprayed the emulsion onto three shingle plates out of four. In both projects, three measurements were successfully obtained. Following the initial readings, the asphalt shingles were allowed to cure on the shoulder, and weight changes were periodically recorded to determine the evaporation rate to calculate curing time.

To measure effective EAR, the research team built a tack lifter device as described by Castorena & Rawls (2016). The tack lifter consisted of a metal apparatus resembling a weighted rod (15 kg) and a metal frame (Figure 4.3). A predetermined amount of emulsion was applied to the non-absorbent metal frame surface. A superabsorbent foam was cut and placed inside the metal frame (13 cm x 13 cm). Subsequently, pressure was applied to the foam surface using the rod apparatus, ensuring the absorption of the emulsion on the surface by the foam (Figure 4.3). This process allowed for the quantification of the effective EAR that had remained on the surface.

Trial tests were conducted in the laboratory with various superabsorbent pads at varying EARs  $(0.1, 0.2, 0.3, 0.4, \text{ and } 0.5 \text{ gal/yd}^2)$  to a square area  $(10 \text{ cm} \times 10 \text{ cm})$ , as depicted in Figure 4.3. Immediately after the emulsion was applied to the square area, the tack lifter was placed over the metal plates, and the pre-weighted foam, and the rod was placed over the emulsion. After waiting for 30 seconds to let the foam absorb the emulsion, the rod was removed from the foam, and the weight of foam was measured again. The weight differences noted for the foam were recorded as absorbed emulsion. This process was repeated for each EARs  $(0.1, 0.2, 0.3, 0.4, \text{ and } 0.5 \text{ gal/yd}^2)$ . The trial test results are shown in Table 4.1.

Table 4.1: Tack Lifter trial/sensitivity test results

No	EAR (gal/yd²)	Area of Foam (cm <sup>2</sup> )	Emulsion Absorbed (g)	Emulsion Absorbed (gal/yd²)	The difference between Applied EAR-Absorbed EAR (gal/yd²)	Average (gal/yd²)
_1	0.1	100	3.50	0.086	0.014	
2	0.2	100	7.58	0.186	0.014	
3	0.3	100	11.56	0.284	0.016	0.015
4	0.4	100	15.65	0.384	0.016	
5	0.5	100	19.82	0.483	0.017	

The trial test results suggest that about 0.015 gal/yd² of emulsion (average) could not be absorbed by the foam, regardless of the EAR value. Hence, this value should be added as a correction factor. It was planned to take the Tack Lifter device to the field, and once the emulsion is sprayed by the distributor truck, the metal frame with the foam will be quickly placed, and the absorbed emulsion will be measured. Since it was also planned to use asphalt shingles and wi-fi scales for EAR measurements, effective EAR (the emulsion amount not absorbed by the pavement surface) can be determined.

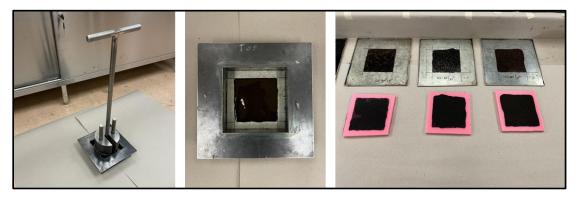


Figure 4.3: Tack Lifter device and trial tests

#### 4.3 RESULTS & DISCUSSIONS

The EAR measurements obtained from the Pendleton and Woodburn projects are presented in Figure 4.4. It was found that EAR measurements for both projects closely align with the target EAR. The measured average EAR values, along with their corresponding standard deviation values, are provided in Table 4.2.

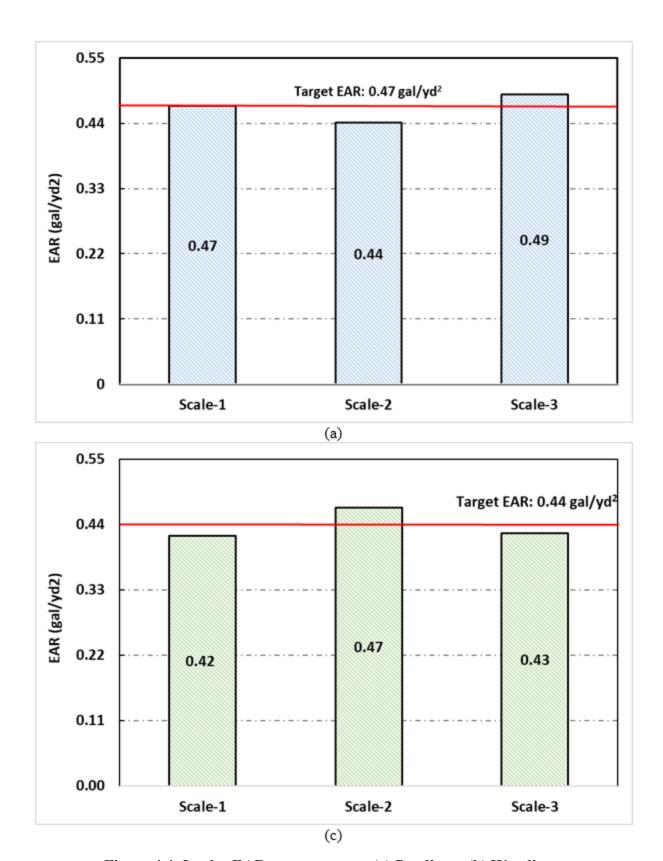


Figure 4.4: In-situ EAR measurements (a) Pendleton (b) Woodburn

**Table 4.2: In-situ EAR measurements** 

Location	Target EAR (gal/yd²)	Measured EAR (gal/yd²)	Standard Deviation (gal/yd²)			
Pendleton	0.47	0.47	0.02			
Woodburn	0.44	0.44	0.03			

The tack lifter measurements could only be obtained from Pendleton, as in Woodburn, the shoulders were narrow, and therefore, measurements were taken on a soil surface. Tarps were placed on the soil, followed by the application of emulsion and aggregate spreading using construction equipment. Due to the absence of an asphalt substrate in Woodburn, an effective EAR measurement could not be taken. The effective EAR measured for Pendleton is given in Table 4.3.

**Table 4.3: Tack lifter measurements** 

Location	Target EAR (gal/yd²)	Effective EAR (gal/yd²)	Absorbed EAR (gal/yd²)
Pendleton	0.47	0.39	0.08

Based on the results provided in Table 2.1, approximately 17 percent of the emulsion sprayed on the surface was absorbed by the AC substrate. The chip seal design method developed for ODOT takes into account the substrate condition (Buss et al. 2016), and the tack lifter device with the wireless scale system can be employed to evaluate the accuracy of design methods in estimating how effectively the emulsion is absorbed by the substrate. Also, it can be used as a QA tool in the field to determine the effective EAR.

#### 4.4 **CONCLUSIONS**

In this chapter, EAR measurements using OreTackRate and effective EAR measurements obtained using the tack lifter were discussed. Based on the results obtained, the following conclusions can be drawn:

- 1. OreTackRate could be used in chip seal construction for QA purposes to determine the actual EAR in situ. The EAR measurements taken from both chip seal projects were close to the target EARs with minute error rates.
- 2. The tack lifter can be used to determine the effective in-situ EAR. The results obtained in this study show that 17% of the emulsion sprayed was absorbed by the AC substrate for the Pendleton project.

As a part of future work, a correlation between MPD and absorbed EAR could be established to determine the extent to which the binder would be absorbed by the substrate.

# 5.0 IN-SITU MACROTEXTURE MEASUREMENTS USING DIFFERENT TECHNOLOGIES

#### 5.1 INTRODUCTION

One of the primary advantages of chip seals is that they offer a skid-resistant surface. As mentioned in the literature review, there are two main failure mechanisms in chip seals: chip loss and bleeding. Bleeding typically occurs during the summer when aggregates can fully embed in the soft binder. This phenomenon can result in a glass-like surface texture on the pavement, characterized by minimal to no textural depth, and this can pose a danger to vehicles due to reduced skid-resistance.

The susceptibility of chip seals to bleeding is often assessed through macrotexture measurements. One of the most commonly used macrotexture measurement methods is the sand circle (or sand patch) test (detailed in section 2.3.3.1). The sand patch test method is currently being employed by ODOT (Buss et al. 2021). Nevertheless, this test necessitates a traffic closure for its execution. Moreover, it can be heavily operator-dependent and may lead to inaccurate results (Praticò and Vaiana 2015). To address these challenges, macrotexture measurements were obtained using the sand circle method, the laser texture scanner developed by the Oregon State University Asphalt Materials and Pavements (OSU-AMaP) research group, and a high-speed profiler. These results were then correlated with one another to evaluate the efficacy of the laser texture scanner and high-speed profiler system for measuring pavement macrotexture. A high correlation was obtained between the results of the sand circle test and those obtained using laser systems (laser texture scanner and high-speed profiler). This suggests that macrotexture measurements can be performed in a more practical, accurate, and safer fashion using laser systems.

### 5.1.1 Objectives

The major objectives of this section are as follows:

- Conducting in-situ macrotexture measurements using the sand patch method, laser texture scanner, and high-speed internal profiler system to assess the bleeding susceptibility of chip seals before and after the construction.
- Establishing correlations between the mean texture depth (MTD) determined using the sand patch test and the mean profile depth (MPD) obtained from the laser texture scanner and high-speed profiler.
- Determining the efficiency and accuracy of the laser systems in determining the macrotexture of chip seal sections and making recommendations to improve the practicality, reliability, and safety of macrotexture measurements.

#### 5.2 MATERIALS & METHODS

#### **5.2.1** Sand Patch Test

The sand patch test (as described in Section 2.3.3.1) assesses pavement texture by distributing a known volume of sand over a dry surface, using the spread area and total volume to calculate the mean texture depth (MTD) (ASTM E965 (2015)). For the sand patch test, a standard-graded sand that complies with ASTM C778 (2021) is employed. In this test, 75 ml of sand is evenly spread over the pavement surface, forming a conical shape. Subsequently, a standard disc is used to spread the sand across the pavement, and the resulting diameter of the sand circle is measured (3 different diameter measurements were averaged for one sand circle test result). Assuming it forms a cylindrical shape, the average height of this cylinder can be calculated using volumetric principles. This calculated average height is then recorded as the mean texture depth (MTD) of the pavement. The photographs from the sand patch test from the field are given in Figure 5.1.

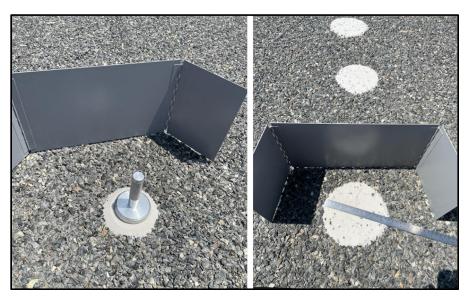


Figure 5.1: Sand patch test performed after chip seal construction (Pendleton-OR 11)

In a typical chip seal construction, a high MTD is initially observed following the first days of construction. However, with the influence of temperature and traffic, the aggregates gradually embed in the binder, causing the MTD to decrease over time. According to the New Zealand chip seal specifications, if the MTD value in a chip seal section falls below 0.9 mm, it is considered as a failure (TNZ 2005). Given that the typical chip seal service life is 5 to 7 years, it is expected that chip seals should maintain an MTD of 0.9 mm or above throughout their service life. Periodically measuring the macrotexture of the chip seal is critically important for evaluating the bleeding susceptibility of the chip seals.

## 5.2.2 Mean Profile Depth Measurements with Laser Texture Scanner

It is known that the sand patch test can be greatly dependent on the operator (Ergun et al. 2005; Praticò and Vaiana 2015). In response, the research team decided to use a laser texture scanner to establish a correlation between MTD measurements and the mean profile depth (MPD) obtained

from the laser texture scanner. However, the high cost of commercial laser texture scanners was a challenge to adopt it as a QC tool. A cost-effective laser texture scanner system, including hardware and software, was developed at OSU-AMaP to address this. Building this laser system costs around \$9,000, which is significantly less than the laser texture scanners available in the market. The developed laser texture scanner system is shown in Figure 5.2.

The laser texture scanner has been developed, featuring a three-support frame designed to securely hold the laser (Figure 5.2). This frame includes adjustable feet, allowing precise leveling of the laser. Movement control of the laser is achieved through a high-precision stepper motor, which enables adjustments in the sampling interval—the space between each measurement. The control over this stepper motor, including its speed, sampling rate (the number of readings taken per second), and sampling interval (the distance measured between readings), is managed through software developed at OSU-AMaP. This software allows for control over the laser's operational parameters.

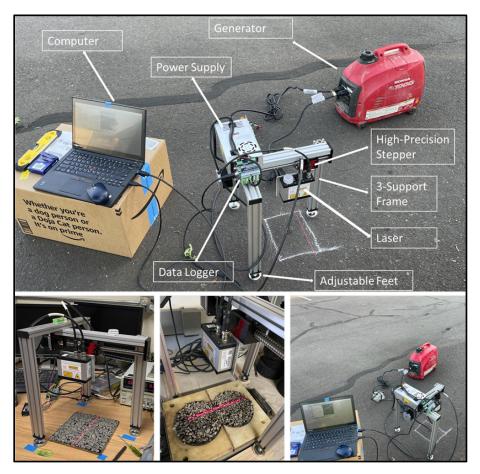


Figure 5.2: Laser texture scanner developed at OSU-AMaP

The laser texture scanner has the capability to scan an area of approximately 6 inches ( $\approx$ 15 cm) in width and 12 inches ( $\approx$ 30 cm) in length. This scanning process captured the surface profile and exported it as x and y coordinates. The calculation of the MPD was performed following guidelines outlined in the ASTM E1845 (2015) (Figure 5.3). It was suggested that at least 10

different segment depths be calculated, and the average of these segment depths be considered as the MPD (ASTM E1845 2015).

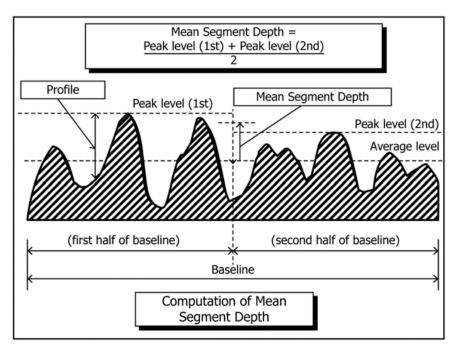


Figure 5.3: Mean segment depth calculation (ASTM E1845 2015)

One of the challenges in calculating MPD was the pavements with superelevation. A correction algorithm was developed in Python to remove the superelevation effect from the texture data. A linear fit is performed on the profile-x location graph, and the profile was updated (normalized). The normalization process is detailed in Figure 5.4.

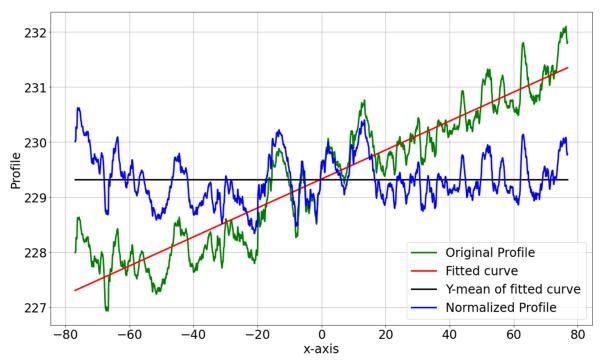


Figure 5.4: Normalization of an elevated surface for MPD calculation

## 5.2.3 Mean Profile Depth Measurements with High-Speed Profiler

The high-speed inertial profiler system, equipped with lasers, accelerometers, GPS, and other sensors mounted on a vehicle, is commonly deployed by agencies to quantify road smoothness via the International Roughness Index (IRI), as outlined by ASTM E950 (2022). The raw data obtained from the inertial profiler can also be used to calculate the Mean Profile Depth (MPD) value as per ASTM E1845 (2015), following the equation provided in Figure 5.3. A photograph of the high-speed inertial profiler system utilized in this study is shown in Figure 5.5.



Figure 5.5: High-speed profiler system used in this study (Photo credit: Alejandro Rosales of Idaho Asphalt)

The high-speed inertial profiler offers advantages such as not requiring traffic closure and rapidly acquiring measurements. The high-speed profiler employed in this study features a line laser with a sampling rate of 5 kHz (5000 readings per second), captures measurements at every 1-inch interval (sampling interval), and operates effectively at speeds of up to 100 mph (Surface Systems & Instruments Inc. 2023). However, it should be noted that MPD measurements obtained using a high-speed profiler could be affected by weather conditions, including sunlight (lasers work more effectively in shaded areas), precipitation, or strong winds, which may introduce airborne debris (FHWA - InfoTechnology 2022). In this study, along the same sections, the sand patch, laser texture scanner, and high-speed profiler were utilized before and after chip seal construction, and their results were compared and correlated with each other.

#### 5.2.4 Field Macrotexture Measurement Test Plan

The research team conducted field macrotexture measurements in Pendleton, arriving before the initiation of chip seal construction (31 May 2023) and right after the chip seal construction (15

June 2023). (Note: One-year post-construction measurements were taken on 22 July 2024, and the results are given in Appendix A). Before the construction phase, measurements were taken for 12 sections on US-730 and 5 sections on OR-11, as shown in Figure 5.6. The construction schedule and the sections designated for chip sealing are presented in Figure 5.7. The ODOT crew also collected macrotexture data using the sand patch test on May 31, 2023, as it was recommended in SPR 777. They conducted the sand patch test following the guidelines specified in SPR 777 (Buss et al. 2016). The MTD results obtained by the ODOT crew were compared with those from the OSU-AMaP research team to explore potential operator-related biases.

Before the chip seal construction, the ODOT crew and OSU AMaP research team initiated macrotexture measurements starting from US-730 near the Washington state border at post-mile (PM) 203 southbound (SB). Initially, the plan was to conduct macrotexture measurements (the sand patch test and the laser texture scanner) at one-mile intervals. However, it was noted that the macrotexture variation was minimal at these intervals, which limited the ability to develop robust correlation curves due to a lack of a wide range of macrotexture values. Also, considering time constraints, the decision was made to adjust the measurement strategy to focus on locations where there was a change in pavement history. In US-730, a total of 12 measurements (sand patch and laser texture scanner) were taken by the research team, and 11 measurements (only sand patch) by the ODOT crew (Figure 5.6). The next day, the research team proceeded to measure macrotexture on OR-11, starting from PM 26 southbound (SB). On OR-11, a total of 5 macrotexture measurements were taken (Figure 5.6).

Following the construction phase, a wildfire impacted US-730, resulting in the closure of sections to traffic. Consequently, macrotexture data was collected from three sections on US-730 and 5 sections on OR-11 for post-chip seal construction. The post-construction macrotexture measurements were performed only by the research team.

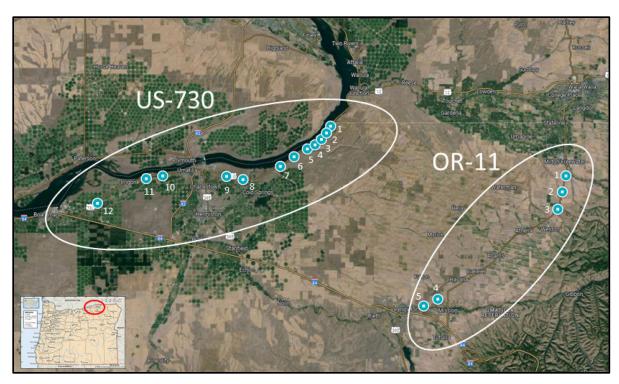


Figure 5.6: Macrotexture measurement sections on US-730 and OR-11 highways (Google Maps 2024; Map of US 2023)

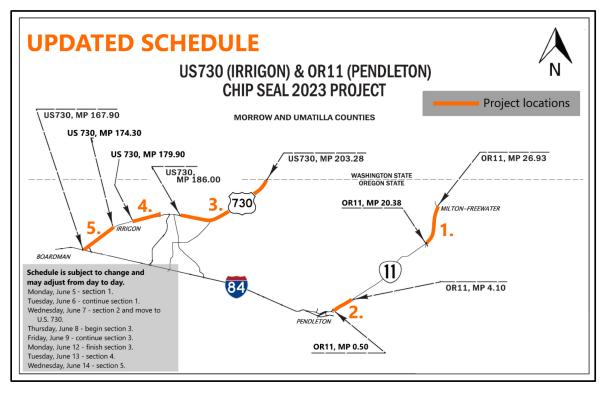


Figure 5.7: Chip seal locations and schedule (ODOT 2023)

The test plan for each road section is outlined in Figure 5.8, and a photograph of one of the test segments is given in Figure 5.9. In each section, five sand patch tests were performed on the wheel path (WP), and an additional five tests were conducted between the wheel paths (BWP). Due to time constraints, the laser texture scanner was run once on the WP and once on the BWP. For each laser texture measurement, the mean segment depth was averaged from five readings. The section's location was recorded using a Global Positioning System (GPS). High-speed profilers were employed throughout the project; however, data from a 50 ft around the section's location were utilized to calculate the average mean profile depth (MPD) for each section (increasing the interval to 100 and 200 ft did not significantly affect the average MPD obtained).

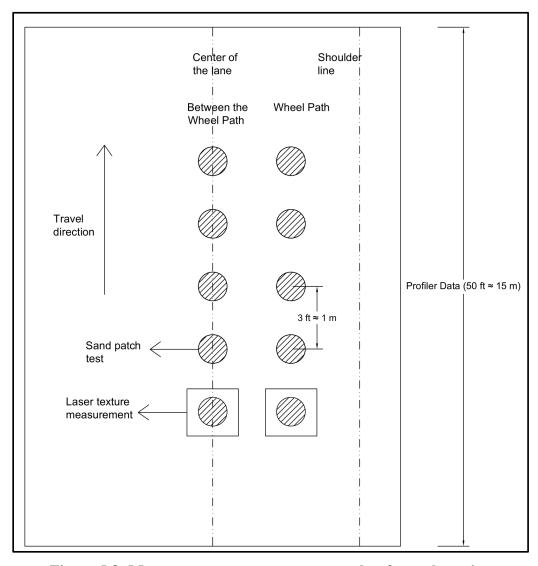


Figure 5.8: Macrotexture measurement test plan for each section

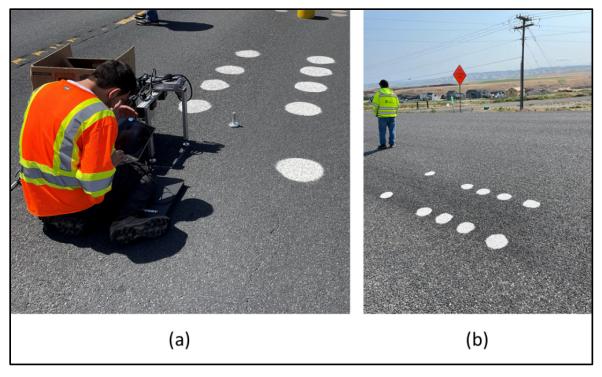


Figure 5.9: Macrotexture measurements from the field (a) before construction (b) after construction (Pendleton, OR-11)

#### 5.3 RESULTS & DISCUSSIONS

Table 5.1 displayed MTD measurements obtained from the sections. Significant differences were observed in WP and BWP values, particularly in areas where the existing substrate was chip seal. The influence of traffic, which pushed aggregates into the binder and existing surface, dramatically reduced the macrotexture. According to the research team's macrotexture results given in Table 5.1, for both OR-11 and US-730, no failure was noted in WP or BWP as per New Zealand standards (except section 12-marked in red color in Table 5.1); the MTD values were above 0.9 mm but close to this threshold.

Following construction, there was a significant increase in MTD values, as expected. Variations in MTD measured post-construction could be attributed to traffic effects. When measurements were taken post-construction, some sections had already been trafficked for a few days, which may have led to a decrease in MTD. The MPD measurements from the pavement surface are provided in Table 5.2 for the laser texture scanner and in Table 5.3 for the high-speed profiler. It is worth noting that certain missing post-construction data points in these tables are a result of the wildfire incident.

Table 5.1: MTD measurements of sections along US-730 and OR-11 (STD is the standard deviation).

Table 5.1: M				Substrate	ı		nstructio		After Construction			
Highway	Section	Direction	PM		WP		BWP		WP		BWP	
	Number	Direction	1 1/1	Substrate	MTD	STD	MTD	STD	MTD	STD	MTD	STD
					(mm)	(mm)	(mm)	(mm)	(mm)	(mm)	(mm)	(mm)
	1	SB	203	Chip Seal	1.04	0.06	1.24	0.11	-	-	-	-
	2	SB	202	Chip Seal	1.03	0.09	1.29	0.09	-	-	-	-
	3	SB	201	Chip Seal	1.03	0.08	1.39	0.06	-	-	-	-
	4	SB	200	Chip Seal	1.04	0.08	1.32	0.09	-	-	-	-
	5	SB	199	Chip Seal	1.06	0.09	1.21	0.03	-	-	-	-
110 720	6	SB	197	Chip Seal	1.17	0.04	1.74	0.13	-	-	-	-
US-730	7	SB	195	Chip Seal	0.96	0.05	0.94	0.12	-	-	-	-
	8	SB	190	AC	0.78	0.13	0.51	0.04	2.86	0.11	3.12	0.14
	9	SB	188	AC	0.63	0.04	0.55	0.01	2.84	0.17	3.12	0.14
	10	SB	180	AC	0.73	0.07	0.73	0.05	2.87	0.12	3.08	0.19
	11	SB	178	Chip Seal	0.94	0.06	1.15	0.15	-	-	-	-
	12	SB	171	Chip Seal	0.83	0.06	1.60	0.09	-	-	-	-
	1	SB	26	AC	0.67	0.02	0.85	0.07	2.48	0.19	2.77	0.17
OR-11	2	SB	24	AC	0.96	0.04	0.73	0.07	2.65	0.19	2.90	0.10
	3	SB	22	AC	0.63	0.04	0.70	0.04	2.67	0.14	2.75	0.16
	4	SB	3	AC	0.70	0.11	0.58	0.09	3.03	0.21	3.63	0.19
	5	NB	1	Chip Seal	1.63	0.06	1.07	0.08	3.05	0.13	3.65	0.21

Note: Values in red denote chip seal bleeding failures, with measurements below 0.9 mm.

Table 5.2: MPD measurements from laser texture scanner along US-730 and OR-11 (STD is the standard deviation)

				Substrate	В	efore Co	nstructio	n	A	After Co	nstructio	n
Highway	Section	Direction	PM		WP		BWP		WP		BWP	
	Number	Direction	FIVI	Substrate	MPD	STD	MPD	STD	MPD	STD	MPD	STD
					(mm)	(mm)	(mm)	(mm)	(mm)	(mm)	(mm)	(mm)
	1	SB	203	Chip Seal	-	-	-	-	-	-	-	-
	2	SB	202	Chip Seal	1.13	0.23	-	-	-	-	-	-
	3	SB	201	Chip Seal	1.13	0.09	1.61	0.23	-	-	-	-
	4	SB	200	Chip Seal	1.26	0.07	1.70	0.17	-	-	-	-
	5	SB	199	Chip Seal	1.25	0.14	1.44	0.27	-	-	-	-
110 720	6	SB	197	Chip Seal	1.51	0.09	2.10	0.11	-	-	-	-
<b>US-730</b>	7	SB	195	Chip Seal	1.04	0.12	1.27	0.13	-	-	-	-
	8	SB	190	AC	0.98	0.13	0.70	0.08	3.17	0.45	3.86	0.39
	9	SB	188	AC	0.77	0.16	0.82	0.13	2.85	0.39	3.22	0.60
	10	SB	180	AC	0.83	0.09	0.87	0.07	2.90	0.48	2.85	0.26
	11	SB	178	Chip Seal	1.22	0.26	1.33	0.11	-	-	-	-
	12	SB	171	Chip Seal	0.85	0.09	2.01	0.25	-	-	-	-
	1	SB	26	AC	0.92	0.08	1.02	0.11	2.78	0.49	2.62	0.16
	2	SB	24	AC	1.27	0.14	0.74	0.13	2.49	0.14	2.87	0.33
OR-11	3	SB	22	AC	0.86	0.04	0.96	0.04	3.11	0.62	2.55	0.31
	4	SB	3	AC	0.88	0.07	0.81	0.11	2.66	0.45	3.17	0.35
	5	NB	1	Chip Seal	1.81	0.16	1.44	0.12	2.79	0.37	2.74	0.49

Note: The missing data is due to a wildfire incident.

Table 5.3: MPD measurements from high-speed profiler along US-730 and OR-11 (STD is the standard deviation)

			PM	Substrate	В	efore Co	nstructio	on	After Construction			
Highway	Section	Direction			V	/ <b>P</b>	BWP		WP		BV	VP
	Number	Direction	1 1/1	Substrate	MPD	STD	MPD	STD	MPD	STD	MPD	STD
					(mm)	(mm)	(mm)	(mm)	(mm)	(mm)	(mm)	(mm)
	1	SB	203	Chip Seal	0.79	0.21	-	-	-	-	-	-
	2	SB	202	Chip Seal	1.05	0.21	-	-	-	-	-	-
	3	SB	201	Chip Seal	0.87	0.18	-	-	-	-	-	-
	4	SB	200	Chip Seal	1.00	0.20	-	-	-	-	-	-
	5	SB	199	Chip Seal	0.85	0.18	-	-	-	-	-	-
US-730	6	SB	197	Chip Seal	1.38	0.26	-	-	-	-	-	-
08-730	7	SB	195	Chip Seal	0.86	0.20	-	-	-	-	-	-
	8	SB	190	AC	0.76	0.16	-	-	3.28	0.71	3.16	0.87
	9	SB	188	AC	0.83	0.19	-	-	2.54	0.52	2.72	0.65
	10	SB	180	AC	0.67	0.19	-	-	-	-	-	-
	11	SB	178	Chip Seal	1.59	0.29	-	-	-	_	-	-
	12	SB	171	Chip Seal	1.37	0.25	-	-	-	-	-	-
	1	SB	26	AC	-	-	-	-	-	-	-	-
	2	SB	24	AC	-	-	-	-	-	-	-	-
OR-11	3	SB	22	AC	-	-	-	-	-	-	-	_
	4	SB	3	AC	-	-	-	-	2.51	0.49	2.51	0.49
	5	NB	1	Chip Seal	-	-	-	-	2.32	0.60	2.29	0.51

Note: The missing data is due to a wildfire incident.

As mentioned in the literature review (Section 2.3.3.1), the sand patch test results can be operator-dependent. To assess this variability, sand patch measurements from the ODOT crew were analyzed alongside those conducted by the OSU-AMaP research team. The ODOT crew carried out the sand patch test at 11 of 12 locations on US-730 before chip seal construction. From these 11 measurements, those taken on asphalt concrete (AC) sections were excluded. The data for the remaining 8 measurements along US-730 are detailed in Table 5.4 and illustrated in Figure 5.10.

Table 5.4: Comparison of MTD measurements conducted by the ODOT crew and the OSU-AMaP research team along US-730 before chip seal construction (*STD* is the standard deviation)

Highway	Section Number	Direction	PM	Location	MTD (mm)- ODOT Crew	MTD (mm)- OSU- AMaP	STD- ODOT Crew	STD- OSU- AMaP	p- values
	1	SB	203	WP	0.90	1.04	0.06	0.06	0.0061
	1	SD	203	BWP	1.10	1.24	0.10	0.11	0.0686
	2	SB	202	WP	0.90	1.03	0.07	0.09	0.0359
	2	SD	202	BWP	1.11	1.29	0.02	0.09	0.0097
	3	SB	201	WP	0.89	1.03	0.05	0.08	0.0136
				BWP	1.33	1.39	0.07	0.06	0.1846
	4	SB	200	WP	0.90	1.04	0.07	0.08	0.0189
US-730				BWP	1.25	1.32	0.05	0.09	0.1773
03-730	5	SB	199	WP	0.90	1.06	0.01	0.09	0.0160
	3			BWP	1.51	1.21	0.06	0.03	0.0001
	6	SB	197	WP	0.99	1.17	0.11	0.04	0.0182
	U	SD	19/	BWP	1.63	1.74	0.07	0.13	0.1457
	7	SB	195	WP	0.75	0.96	0.06	0.05	0.0004
	/	SD	193	BWP	0.75	0.94	0.06	0.12	0.0199
	11	SB	170	WP	0.82	0.94	0.07	0.06	0.0201
	11	מנ	178	BWP	1.28	1.15	0.22	0.15	0.3108

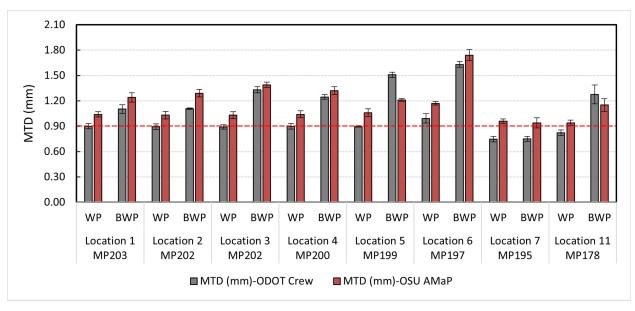


Figure 5.10: MTD measurement comparison between ODOT Crew and OSU AMaP team along US-730 (The error bars represent one standard deviation in height)

Upon examining the results in Table 5.4, a significant difference (p<0.05 according to the t-test, highlighted in bold in Table 5.4) is identified in the measurements conducted by different operators at 11 out of 16 locations. The OSU-AMaP team's measurements did not reveal any instances of bleeding failure, whereas the ODOT crew's data indicated bleeding failures in the wheel paths at 3 (PM 178, 195, and 201) of the 8 assessed locations, as emphasized in bold within Table 5.4. On PM 199, 200, 202, and 203, the ODOT crew recorded an MTD of 0.9 mm (illustrated in Figure 5.10), which is the failure threshold according to New Zealand specifications (TNZ 2005).

The difference in measurements between the two groups is likely due to the operator-dependent nature of the test, which involves creating a circular shape with sand on the pavement surface—a process that can be challenging and subjective for the operator. The data presented in Table 5.4 indicates that the OSU AMaP consistently recorded higher Mean Texture Depth (MTD) values across all locations, except for Location 11 (MP 178), in comparison to the ODOT crew's results. This variation in results could be due to the different types of sand used in the tests: OSU-AMaP utilized standard-graded sand, compliant with ASTM C778 standards, while the ODOT crew used conventional multi-purpose sand. Van Zyl and Van der Gryp (2015) reported that sand with a coarser grade tends to produce lower MTD measurements. It can be concluded that sand patch tests should be performed by the same operator using standard materials and equipment for reliable test results. However, the MTD results obtained by the ODOT crew were correlated with MTDs obtained by the OSU-AMaP research team, as shown in Figure 5.11. The scatter in the data is thought to arise from operator-dependent phenomena. The linear relationship observed is thought to deviate from the x=y curve due to the use of different types of sand.

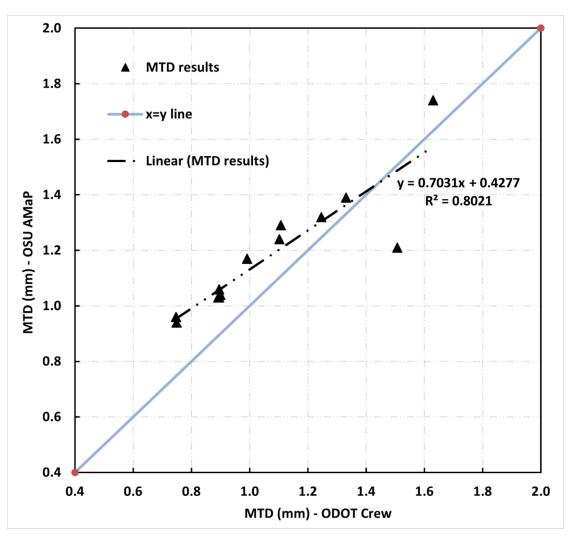


Figure 5.11: Correlation of MTD results between ODOT crew and OSU-AMaP research team

The results given in Table 5.1, Table 5.2, and Table 5.3 were correlated for comparison. The correlation between MTD and MPD provided by the laser texture scanner is given in Figure 5.12.

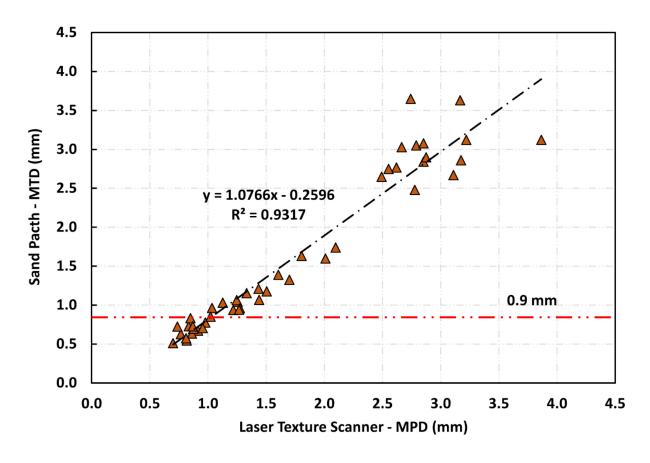


Figure 5.12: MTD (sand patch-MPD (laser texture scanner) correlation

When the results were analyzed, it was observed that there was a strong correlation between MTD and MPD obtained from the laser texture scanner. This correlation seemed stronger for the measurements taken before construction, i.e., specifically on surfaces with relatively lower texture. In low-textured areas, a more consolidated data cluster was observed, while in high-textured areas, a broader spread of data was observed. Several reasons could account for this variation in data. One such factor is the 'shadow effect' seen in laser scans of highly textured surfaces. The laser beams, when reflected off the pavement surface back to the receiver, may not return efficiently in high-textured areas due to scattering among the aggregates. This could lead to sampling loss and incorrect measurement of texture. In addition, when the sand patch test was performed on high-textured surfaces, achieving a perfect cylindrical shape was found to be challenging. The sand, particularly around the edges, tended to form more of a cone-like shape in these high-textured areas, which may have eventually led to variable and less accurate MTD results.

The MTD-MPD data obtained from the high-speed profiler is presented in Figure 5.13. The high-speed profiler recorded fewer data points than the laser texture scanner due to a software malfunction that occurred while collecting data. Upon analyzing the results given in Figure 5.13, it can be concluded that, although relatively weaker compared to the laser texture scanner, there still exists a noticeable correlation between MTD and MPD values obtained from the high-speed profiler. It can be said that this outcome was expected, given factors such as sunlight and

airborne debris carried by wind may affect the macrotexture (MPD) data obtained by the high-speed profiler to some extent.

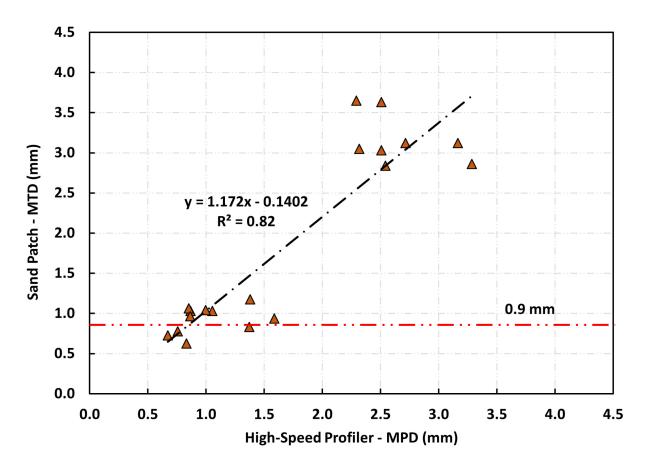


Figure 5.13: MTD (sand patch)-MPD (high-speed profiler) correlation

To evaluate the efficacy of laser-based methods (laser texture scanner and high-speed profiler) as alternatives to the sand patch test, a cluster analysis was conducted. Initially, the MTD values were categorized into three groups: values less than 0.9 mm were considered a "fail", values between 0.9 mm and 1.5 mm were marked as "close to fail", and values greater than 1.5 mm were designated as "good". The threshold of 0.9 mm was chosen based on the New Zealand specification for chip seal bleeding criteria (TNZ 2005). The value of 1.5 mm was determined considering that the last chip seal treatment on the US-730 highway occurred in 2014, and the latest treatment on OR-11 was conducted in 2009. Given these roads are at the end of their service lives, their MTD values were used as references. As seen in Figure 5.10, most MTD measurements taken by both groups fall between 0.9 mm and 1.5 mm, hence classified under the "close to fail" category. Measurements above this range were considered "good." Considering only one chip seal data point was below 0.9 mm (Table 5.1), which was deemed insufficient for robust analysis, measurements taken on asphalt concrete (AC) surfaces were also included in the analysis.

After completing the classification process, the sand patch MTD values were used as a reference to categorize the measurements under "fail," "close to fail," and "good" classifications.

Subsequently, the Mean Profile Depth (MPD) values obtained from the laser texture scanner were converted to MTD values using the correlation equation (Equation (5-1)) between the laser texture scanner (MPD) and sand patch (MTD), as shown in Figure 5.12. These converted MTD values were then classified using the same threshold values applied for the sand patch. The results of this classification are presented in Table 5.5.

$$MTD = 1.08MPD - 0.26$$

(5-1)

Table 5.5: Cluster analysis of laser texture scanner data

Cluster	Limits (mm)	# of MTD values (Sand Patch)	# of MTD values (calculated using Eq. (5-1))	Performance	# of False Positive
Fail	0-0.9	14	15	100%	N/A
Close to Fail	0.9-1.5	14	12	86%	1
Good	1.5+	18	19	100%	N/A

According to the sand patch test results (Table 5.1), 14 measurements fell into the "fail" category (when AC sections were also taken into account). Utilizing the laser texture scanner-sand patch test correlation equation given in Equation (5-1), the MTD values for all these 14 locations were classified correctly into the "fail" category, indicating a 100% match accuracy. These accuracy rates are provided in the "performance" column of Table 5.5, showing an 86% accuracy for the "close to fail" category and 100% for the "good" category.

Considering the "close to fail" classification, 14 measurements were categorized as "close to fail" for the sand patch test, while according to the laser texture scanner results, 12 measurements were classified in this category. Upon closer examination of the two mismatched measurements, one was categorized as "close to fail" by the sand patch test but deemed a "fail" according to Equation (5-1). This suggests that a section not yet failing but close to failing was identified as a "fail". Such a situation could be considered as a false negative, which is acceptable since it favors safety. However, for the other mismatched measurement, a location classified as "close to fail" by the sand patch test was categorized as "good" according to Equation (5-1). This misclassification is a false positive, wrongly marking a section that, according to the sand patch, was "close to fail" as being in "good" condition. (It's important to note that no measurement classified as a "fail" by the sand patch was ever categorized as "good" by Equation (5-1)-laser texture scanner). Out of 46 measurements conducted with both the laser texture scanner and sand patch, only one was identified as a false positive. This can be seen as an acceptable error. The high accuracy of the laser texture scanner in clustering demonstrates its effectiveness as a method for macrotexture measurements.

Table 5.6 presents the cluster analysis for the high-speed profiler, displaying MTD values from the sand patch test alongside MTD results derived using the sand patch-high speed profiler correlation equation shown in Figure 5.13 (also provided in Equation (5-2)). Analysis of the results in Table 5.6 reveals that of the 4 locations classified as "fail" according to the sand patch test, 3 were accurately predicted by the high-speed profiler. The location that was mislabeled was classified as "close to fail" using Equation (5-2) (a false positive). Upon examining the "close to

fail" classification, it is observed that the high-speed profiler, with a 43% accuracy, performs less reliably in predictions compared to the laser texture scanner, which has an 86% accuracy. A closer look at this mislabeling shows that for three measurements, areas labeled as "close to fail" by the sand patch were marked as "fail" according to profiler data (false negatives). Only in one area, a measurement classified as "close to fail" by sand patch results was mislabeled as "good" according to high-speed profiler results (a false positive). Despite obtaining relatively few data points (due to equipment malfunction during data collection), observing only two instances of false positive mislabeling among a total of 19 measurements can be considered as noteworthy accuracy. This indicates that the high-speed profiler is a promising, practical, and reliable method for macrotexture measurements. It should also noted that obtaining more data would enhance the reliability of the analysis, specifically for the high-speed profiler.

$$MTD = 1.17MPD - 0.14$$

(5-2)

Table 5.6: Cluster analysis of high-speed profiler data

Cluster	Limits (mm)	# of MTD values (Sand Patch)	# of MTD values (calculated using Eq. (5-2))	Performance	# of False Positive
Fail	0-0.9	4	6	75%	1
Close to Fail	0.9-1.5	7	4	43%	1
Good	1.5+	8	9	100%	N/A

When solely assessing the laser texture scanner and high-speed profiler for their precision in identifying the 1.5 mm threshold—that is, their ability to accurately classify sections according to sand patch test outcomes as either below or above 1.5 mm—it has been determined that the laser texture scanner ascertains whether a section falls below this threshold with 98% accuracy, while the high-speed profiler accomplishes this with 95% accuracy. Therefore, it can be concluded that both laser systems are highly reliable in detecting sections susceptible to bleeding.

The correlation between MPD values from the laser texture scanner and MPD values obtained from the high-speed profiler is depicted in Figure 5.14. A strong correlation has been observed between the two methods. It can be suggested that utilizing the high-speed profiler may offer advantages over the laser texture scanner, provided that the margin of error is kept within acceptable limits. This approach allows for the rapid measurement of pavement macrotexture without requiring a traffic closure, thus effectively simplifying the data collection process.

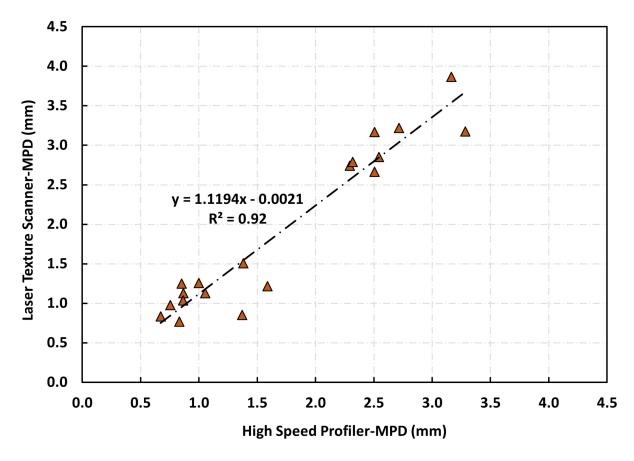


Figure 5.14: MPD (laser texture scanner)-MPD (high-speed profiler) correlation

As mentioned in the literature section (Section 2.3.3.1), the sand patch test is the most widely used macrotexture measurement method, but it has drawbacks: it requires traffic closure, the values measured can vary significantly from operator to operator, and it provides macrotexture information of a limited area. To address operator dependency, the laser texture scanner can be adapted as a macrotexture measurement method. Given the high accuracy obtained from the high-speed profiler system, the chip seal sections' bleeding susceptibility can be monitored using the high-speed profiler, and in those locations where the macrotexture is below 1.5 mm, either the laser texture scanner or the sand patch test can be performed. This way, the locations where there is a need for a sand patch test/laser texture scanner can be effectively determined. In addition, the entire section can be scanned using a high-speed profiler in a short period of time. This can potentially decrease the number of sand patch tests required for sections and can contribute to more practical, reliable, and safer macrotexture measurements for ODOT.

A comparison of the MPD-MTD data obtained in this study along with other studies in the literature (Castorena and Rawls 2016; Ozdemir et al. 2018; Plati et al. 2017; Praticò and Vaiana 2015; Van Zyl and Van der Gryp 2015) is presented in Figure 5.15. As seen in that figure, the MPD-MTD data obtained in this study was found to be aligned with the cluster observed in other research studies. It was observed that surfaces with higher macrotexture displayed a broader spread, while those with lower macrotexture were confined to a narrower range. Given that the low texture is considered a critical scenario for chip seal, it can be said that the application of

correlations established in Figure 5.12 and Figure 5.13, particularly for surfaces with low texture, would not result in significant errors. Furthermore, the formula recommended by ASTM E1845 (2015) (Equation (5-3)) was found to perform reasonably well for surfaces with low textures. For regions where the macro texture value exceeded 1.5 mm, this formula was concluded to underestimate the MTD value.

$$MTD = 0.2 + 0.8 MPD$$
 (5-3)

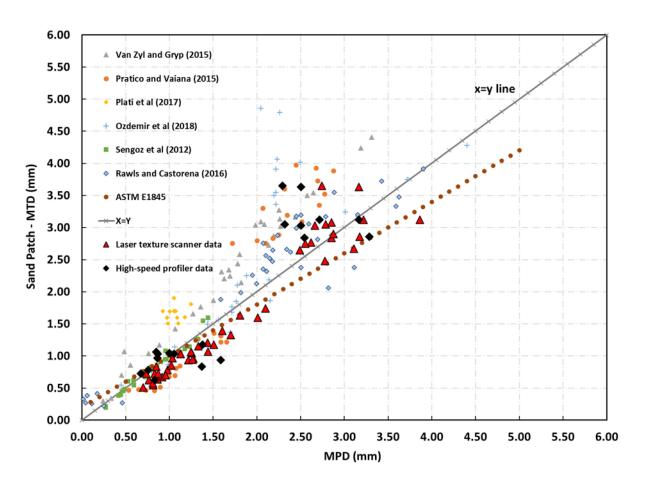


Figure 5.15: Comparison of MPD-MTD data with other studies

#### 5.4 CONCLUSIONS

In this chapter, the macrotexture measurements were obtained from a sand patch test, a laser texture scanner developed by OSU-AMaP, and a high-speed profiler. Measurements were taken before construction and a few days after its completion. Within the limits of this study, the following conclusions can be drawn:

1. High correlations have been observed between the Mean Profile Depth (MPD) data from both the laser texture scanner and the high-speed profiler and the Macrotexture Depth

- (MTD) data from the sand patch test ( $R^2$ =0.93 for laser texture scanner sand patch test and  $R^2$ =0.82 for high-speed profiler sand patch test). These correlations suggest that laser systems can be an excellent alternative to sand patch tests.
- 2. When comparing the sand patch MTD data collected by the ODOT crew and the OSU AMaP research team, a statistically significant difference was observed between the values. This difference has been attributed to the operator-dependent nature of the sand patch test and the use of different types of sand. However, the correlations between the two sets of measurements were high.
- 3. In the classification analysis conducted using the derived MPD-MTD correlation equations, the laser texture scanner accurately classified all sections that failed according to the sand patch test. The high-speed profiler accurately classified 75% of the failing sections. Assuming a critical macrotexture value of 1.5 mm for susceptibility to bleeding in chip seal, the laser texture scanner accurately classified sections with a 98% rate, while the high-speed profiler achieved a 95% accuracy rate.
- 4. Based on the analysis of the results, it is recommended that the high-speed profiler initially collects data on chip seal sections. In light of the collected data, measurements with the sand patch or laser texture scanner are recommended for sections with macrotexture values below 1.5 mm. This approach will enable a practical, rapid, accurate, and effective scanning of the entire chip seal section for bleeding susceptibility, thus facilitating a faster and more efficient bleeding susceptibility screening.

As part of future work, it was planned to periodically take macrotexture measurements every year, aimed to assess the bleeding susceptibility of chip seal sections over time (*Note: One-year post-construction measurements were taken on 22 July 2024, and the results are given in Appendix A*). This approach will enable the accumulation of more data points for correlations, thereby allowing for the generation of more reliable correlation curves and the improvement of classification analysis.

#### 6.0 BLEEDING TESTS

#### 6.1 INTRODUCTION

The bleeding susceptibility of chip seals can be monitored with macrotexture measurements in the field, as discussed in Section 5.0. Conducting bleeding tests on chip seal samples in the laboratory is crucial for selecting the appropriate materials for the project. The devices developed for laboratory bleeding tests, detailed in the literature review (Section 2.4), are highly costly. Therefore, the research team modified the Hamburg Wheel Tracker (HWT) device for bleeding tests by replacing the steel wheel with a rubber wheel to perform the bleeding tests. Recently, many DOTs and research laboratories have been using the HWT device to measure the rutting performance of HMA (Boz et al. 2018). Hence, developing a laboratory bleeding test using the HWT device, which is already used by many DOTs and agencies, offers a practical advantage. In this study, the HWT device and laser texture scanner that had been developed were used to assess the bleeding susceptibility of chip seal samples.

## 6.1.1 Objectives

The major objectives of this section are as follows:

- Developing a practical chip seal bleeding test in the laboratory using the HWT device and the developed laser texture scanner.
- Comparing results by applying the developed bleeding tests on chip seal samples brought from the field (and conditioned under field conditions), as well as, on chip seal samples prepared in the laboratory (using binder and aggregates sampled from the field) and conditioned in the laboratory environment.
- Establishing a failure criterion for bleeding and evaluating the performance of the samples.

#### 6.2 MATERIALS & METHODS

Based on the research team's previous experience with chip sealing on rumble strip samples, the metal wheels were observed to crush aggregates on the surface of the chip seal specimens (Weaver et al., 2023). Hence, a pair of rubber wheels was obtained to conduct bleeding tests using the HWT. Initially, 62.5 mm thick HMA samples were compacted in the laboratory. Subsequently, the asphalt concrete samples were trimmed to fit into HWT test molds (Figure 6.1a). Then, the samples were wrapped with tape on the top surface. Asphalt emulsion, corresponding to the binder amount measured in the field, was applied to the samples. Utilizing gravity and rotational forces, the emulsion was uniformly spread over the sample surface (Figure 6.1b). Subsequently, damp aggregates were dropped onto the emulsion using an aggregate spread apparatus (Figure 6.1c), followed by compacting the samples with a 25 kg rubber wheel compactor for three cycles (each cycle consisting of one pass and one return) (Figure 6.1d). Afterward, the samples were cured at 45°C for 24 hours. The samples were then conditioned at 25°C for 30 minutes. Subsequently, any excess aggregates were removed from the surface using the sweeper employed in the sweep test (Figure 6.1e), and bleeding tests were conducted.

Additionally, field samples for both chip seal projects - Pendleton and Woodburn - (prepared using construction equipment and exposed to field conditions) were tested in the laboratory. The procedure followed for the preparation of the laboratory samples is depicted in Figure 6.1.

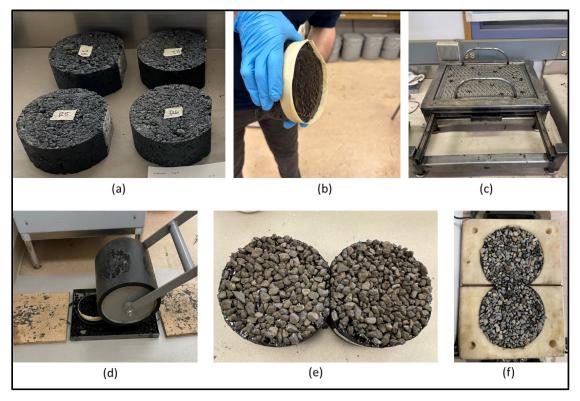


Figure 6.1: Sample preparation stages of chip seal samples for bleeding test: (a) compacted and trimmed HMA samples, (b) emulsion application, (c) aggregate spread over emulsion (d) chip seal samples compacted with rubber wheel, (e) samples after cured at 45 °C for 24 hours and excess aggregates were removed, (f) chip seal sample placed in HWT mold

After the samples were prepared, the macrotexture of chip seal samples was measured using the laser texture scanner before and after a certain number of HWT passes. Subsequently, an MPD-passes graph was plotted to determine the number of passes required to cause chip seal sample failure due to bleeding. The laser texture scanner was utilized on the wheel path of the HWT device. A total of 10 scans were taken at 5 mm intervals. MPD values were calculated as described in Section 5.2.2. Once the MPD values were obtained, outliers were identified and removed from the series following the procedure outlined in ASTM E1845 (2015).

During the trial tests, various temperatures and conditioning methods (water conditioning and air conditioning) were examined. It was determined that water conditioning in the HWT provided more stable and accurate temperature control compared to air conditioning. Subsequently, a testing temperature of 50°C was selected. The 50°C is also the temperature commonly used to evaluate the rutting performance of HMA samples in Oregon (Coleri et al. 2020a). Before initiating the HWT rolling over the samples, the specimens were conditioned at 50°C for 45 minutes to ensure the chip seal surface temperature reached 50°C. The number of HWT passes

was another parameter to be determined. Following the trial tests, the research team initially decided to use 20,000 passes, consistent with the practice for rutting tests of HMA samples in Oregon (Coleri et al. 2020a). However, it was observed that after 5,000 passes, the rubber wheel began to dislodge some aggregates from the surface of the chip seal sample, resulting in a slight increase in macrotexture (MPD). Additionally, a notable variation in MPD values was recorded at 10,000 and 20,000 passes. Considering that the chip seal does not provide any structural contribution to the pavement, it was deemed that 20,000 passes would be too harsh for the samples. Therefore, the research team decided to reduce the number of passes to 5,000.

The periods for macrotexture measurements (using a laser texture scanner) were established as follows: before HWT operation (0 passes), after 10 passes, 50 passes, 200 passes, 1,000 passes, and 5,000 passes. At each measurement interval, the sample was removed from the device, laser texture measurements were taken, the rubber wheels were cleaned and then the sample was returned to the HWT device to continue conditioning and testing. It is important to note that some time is required for the water in the HWT device to reach 50°C, and once it reaches this temperature, the device begins a 45-minute conditioning period. The temperature on the surface was maintained around 50°C. That process was repeated after each laser texture measurement. Figure 6.2 shows the steps followed in bleeding tests.

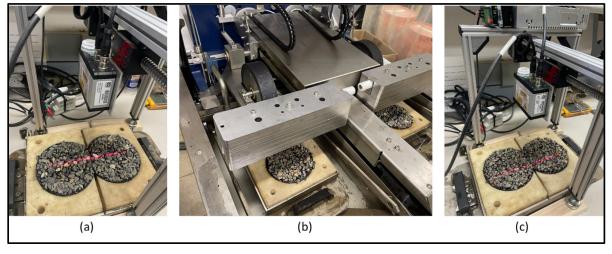


Figure 6.2: Bleeding testing of chip seal samples: (a) macrotexture measurement (MPD) with laser texture scanner before trafficking, (b) HWT test with rubber wheels, (c) macrotexture measurement after trafficking

It should be noted that the bleeding samples were prepared using the binder and aggregates sampled from the two field projects mentioned in this report (Pendleton and Woodburn). Field samples exposed to field curing conditions were also tested and compared with laboratory-prepared samples. Two replicates were tested for each project.

#### 6.3 RESULTS & DISCUSSIONS

The MPD-HWT passes plot obtained for laboratory-prepared Pendleton samples is given in Figure 6.3.

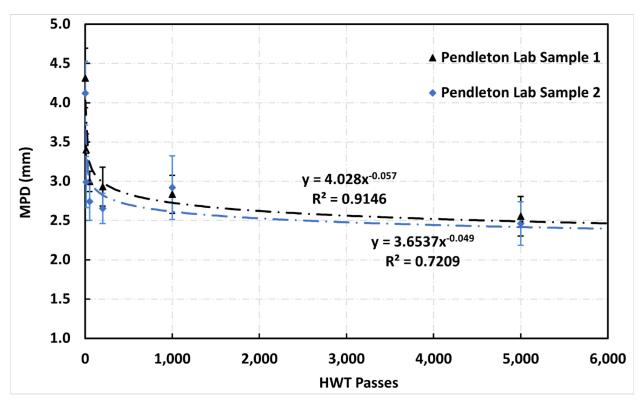


Figure 6.3: MPD-HWT Passes of laboratory-prepared Pendleton samples (Error bars are one standard deviation height)

As anticipated, the MPD values decreased with increasing HWT passes. It was observed that during the initial passes, the aggregates tended to realign, rolling through their flattest surface. Additionally, the load applied ( $156 \text{ lb} \approx 70 \text{ kg}$ ) to the HWT wheel pushed aggregates into the softened ( $50^{\circ}\text{C}$ ) binder. As embedment increased, the macrotexture value gradually decreased. The trafficking effect was more pronounced during the initial passes, as evidenced by a slowdown in the decrease of MPD at higher HWT passes. To provide a clearer evaluation of the results depicted in Figure 6.3, a plot of MPD against HWT passes with the x-axis in the logarithmic scale is also presented in Figure 6.4.

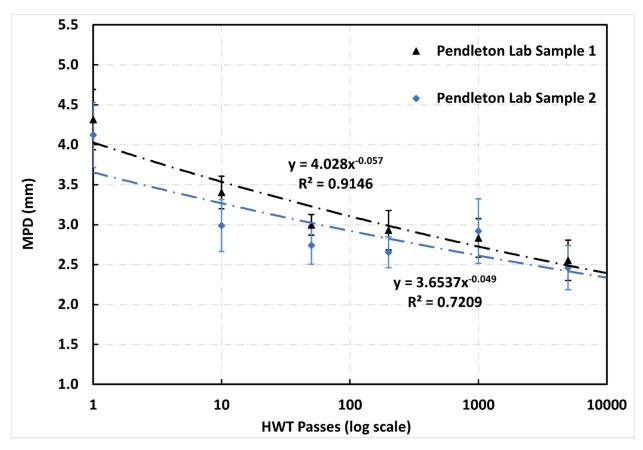


Figure 6.4: MPD-HWT Passes (log scale) of laboratory-prepared Pendleton samples (Error bars are one standard deviation height)

As shown in Figure 6.4, an almost linear relationship can be observed between the decrease in MPD and HWT passes (log scale). When a t-test is performed to compare the means of MPDs at each pass, no significant difference is obtained for all points. This indicates that the test was repeatable. The MPD-HWT passes (log scale) obtained for laboratory-prepared Woodburn samples are given in Figure 6.5.

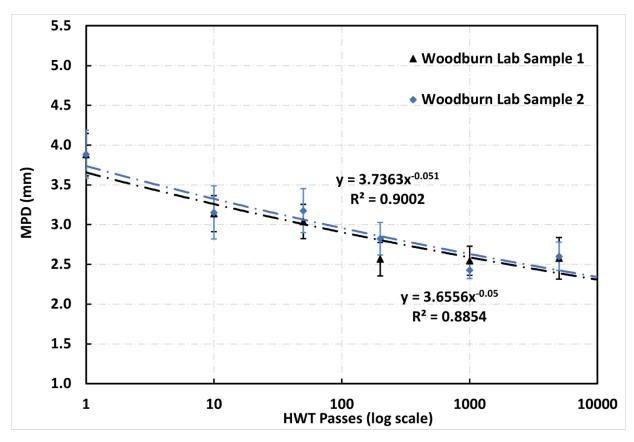


Figure 6.5: MPD-HWT Passes (log scale) of laboratory-prepared Woodburn samples (Error bars are one standard deviation height)

In general, it can be said that there is a linear decrease in MPD with HWT passes (log scale) for Woodburn-laboratory prepared samples, similar to Pendleton. According to the t-test results between the two samples, no statistically significant difference was observed at all passes. To compare the bleeding susceptibility of Pendleton with Woodburn, the MDP values of the two samples were averaged and demonstrated in Figure 6.6.

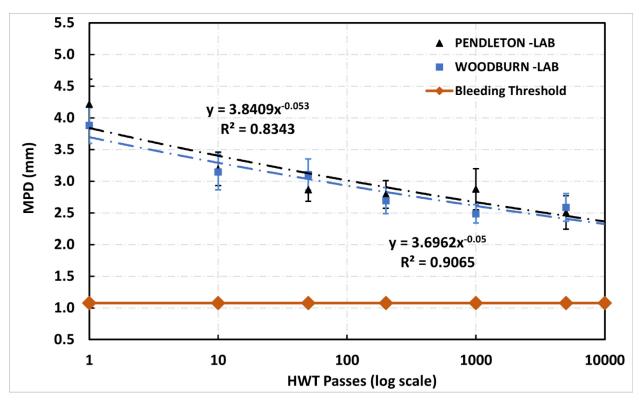


Figure 6.6: MPD-HWT Passes (log scale) of laboratory-prepared Pendleton and Woodburn samples (average values) (Error bars are one standard deviation height)

Results indicated that no statistically significant difference was observed for all passes between the laboratory-prepared samples tested for both projects. Although the sizes of the two aggregates were different, this difference was balanced with the applied EAR. Considering that the same chip seal design was applied for both projects (detailed in SPR 777 (Buss et al. 2016)), it can be concluded that the applied design yielded consistent results. Additionally, a bleeding threshold value was plotted on the graph. According to the New Zealand chip seal specification (TNZ 2005), 0.9 mm MTD is considered as failure of a chip seal section due to bleeding. This MTD value was converted to MPD using the correlation established in Figure 5.12, and 1.08 MPD value was determined as the failure criterion. Using the exponential curve fit given in Figure 6.6, the passes required to fail the sample can be calculated as  $2.49 \times 10^{10}$  passes for Pendleton and 4.85×10<sup>10</sup> passes for Woodburn. Despite the similarity of MPD data for the two, the relatively large difference can be attributed to the extrapolation to relatively high numbers. To address this, it was decided to present the results as log (HWT passes) scale, i.e., log (n), where n is the number of passes required to achieve an MPD value of 1.08. The log (HWT passes) values for the failure of the samples is shown in Figure 6.7, with error bars indicating the maximum and minimum values.

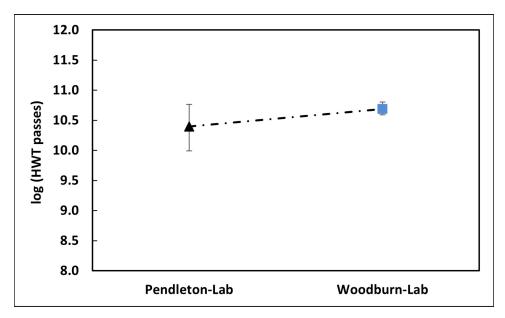


Figure 6.7: Passes required to failure for laboratory-prepared Pendleton and Woodburn samples (Error bars show maximum and minimum values)

As described in Section 3.3, bleeding test samples were also collected from the field: Compacted and trimmed AC samples were positioned on the shoulder of the chip seal construction section (Figure 3.18, Figure 3.19). The emulsion was sprayed from the distributor truck, and aggregates were spread over the samples using the aggregate spread equipment used in situ. The samples were then subjected to field conditions and later transported to the laboratory. (The sweeping process was conducted in the field for Pendleton and in the lab for Woodburn, as mentioned in Section 3.3). The bleeding test results for Pendleton were presented in Figure 6.8, and those for Woodburn were provided in Figure 6.9.

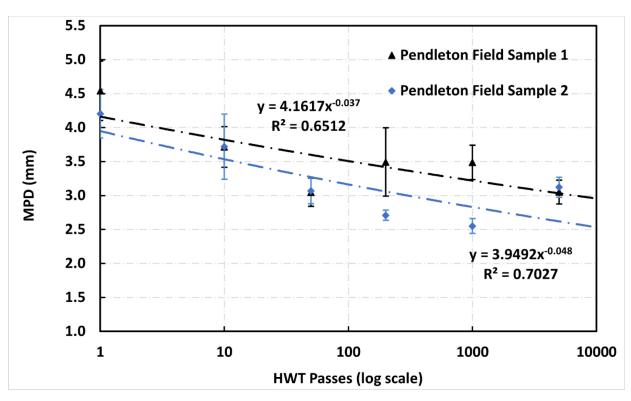


Figure 6.8: MPD-HWT Passes (log scale) of Pendleton field sample (Error bars are one standard deviation height)

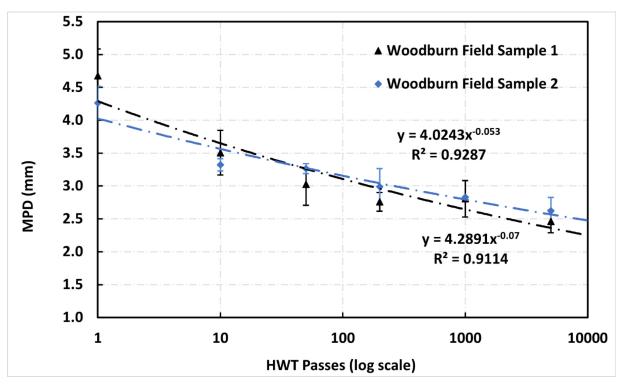


Figure 6.9: MPD-HWT Passes (log scale) of Woodburn field sample (Error bars are one standard deviation height)

When the results were analyzed, it was observed that there was a higher variability in Pendleton field samples compared to Woodburn field samples. This variation can be attributed to the fact that in Pendleton, the sweep process was performed in the field under less controlled conditions. As depicted in Figure 3.23, chip loss values were significantly high, as well as the variability, for Pendleton field samples. On the other hand, for the Woodburn field samples, there was less variability, and the difference between the averages of MPDs is statistically insignificant at all passes. However, for Pendleton field samples, the MPDs are significantly different at 100 and 500 passes. Furthermore, for the Pendleton field samples, there are some passes where MPD values slightly increased (Sample 1 – 5000 passes). These increases can be attributed to aggregates dislodged during HWT trafficking. When an aggregate is dislodged, it creates a pit-like shape in the cross-section, and during scanning, this may result in an increase in macrotexture. Given the relatively small scanned area (5 cm x 15 cm), the displacement of even a few chips can dramatically affect the MPD results. The average MPDs obtained from two replicates are given in Figure 6.10.

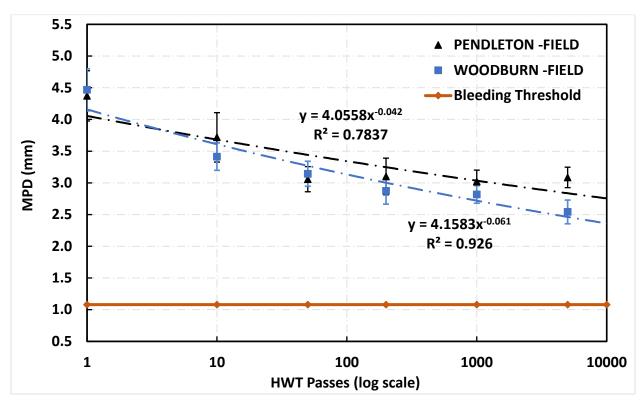


Figure 6.10: MPD-HWT Passes (log scale) of Woodburn field sample (Error bars are one standard deviation height)

When examining the results provided in Figure 6.10, it can be suggested that Woodburn field samples were more bleeding susceptible compared to Pendleton field samples. However, upon careful examination of the results, it can be said that no statistically significant difference was observed between the two samples for each pass (except for 5,000 passes). At 5,000 passes, a significant increase is observed in the second sample of Pendleton. This increase led to a general increase in the average and divergence of Pendleton results from the Woodburn results. Therefore, for the development of this test, especially to address high variability, the number of

tested samples can be increased. Another solution can be increasing the frequency of MPD scans, and disregarding the results where MPD increased. The HWT pass values corresponding to the 1.08 MPD threshold (log (HWT Passes)) are provided for both field and laboratory results of both projects in Figure 6.11.

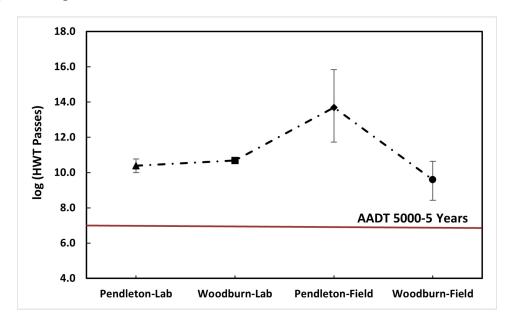


Figure 6.11: Passes required to failure (log (HWT passes)) for Pendleton and Woodburn samples (Error bars show maximum and minimum values)

The average service life for a chip seal can typically be considered as 5 years, and chip seals are usually constructed on roads with an Average Annual Daily Traffic (AADT) of 5,000 or less (Gransberg and James 2005). Based on this, the total passes for a highway with AADT of 5,000 can be calculated as shown in Equation (6-1) and Equation (6-2). This threshold value is also plotted in Figure 6.11.

Total passes in 5 years = 
$$5,000 \times 365 \times 5 = 9,125,000$$
 passes (6-1)

$$log(9, 125, 000) = 6.96$$
(6-2)

It is noted that both field and laboratory-prepared samples were observed to be resistant to bleeding according to laboratory bleeding test settings and threshold values determined in this study. As part of future work, it is crucial to calibrate and validate the threshold values established in this study using field data, where traffic, temperature, and MPD data are periodically monitored. For both projects, field samples exhibited higher variability compared to laboratory-prepared samples (see error bar lengths in Figure 6.11).

The binders and aggregates used in the two projects were different from each other (Table 3.3). Additionally, the two projects were conducted at different times and locations. Taking all of this

into consideration, understanding the reasons for the differences observed in the results can be complex. The higher variability exhibited by field samples may be due to shorter curing times. Moreover, other uncontrollable factors in the field (exposure to UV light, wind speed, etc.) could have contributed to these differences.

For Pendleton field samples, the sweep process was conducted in the field, resulting in significant chip loss (See Figure 3.23). This led to fewer aggregates on the bleeding specimens, ultimately resulting in relatively higher macrotexture (MPD). On the other hand, considering the bleeding mechanism, if there are too many aggregates on the surface after being compressed under traffic, there will be a limited volume of voids between these aggregates. With the hot weather, the softened asphalt may move upward through this narrow volume and reach the surface, causing bleeding. Conversely, if there is too little aggregate, there may be a greater volume of voids between the aggregates, making it more difficult for the binder to reach the surface. This mechanism can explain the higher MPD values obtained for Pendleton field samples. The images of samples brought from the field and prepared in the laboratory are provided in Figure 6.12.

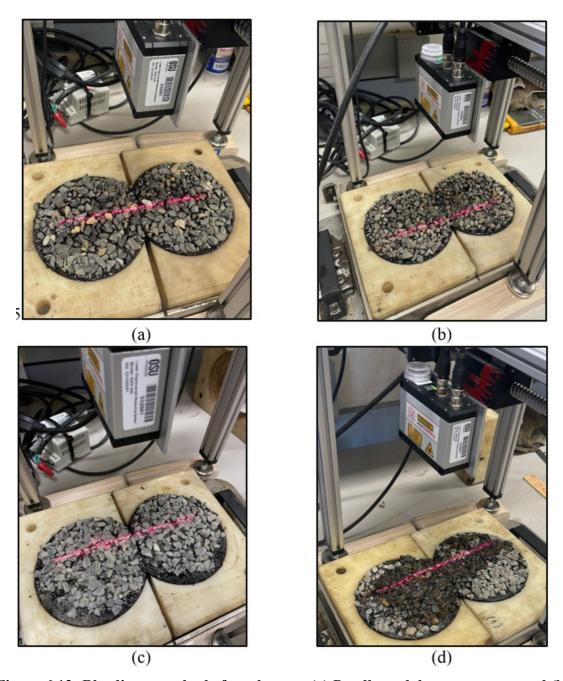


Figure 6.12: Bleeding samples before the test: (a) Pendleton laboratory-prepared (b) Woodburn laboratory-prepared (c) Pendleton field sample (d) Woodburn field sample

As depicted in Figure 6.12, fewer aggregates can be observed for field samples, with this difference being more pronounced for Pendleton samples.

#### 6.4 CONCLUSIONS

In this chapter, a laboratory bleeding test is developed using HWT and a laser texture scanner. Field and laboratory-prepared chip seal samples were analyzed using a laboratory bleeding test system. Based on the results obtained, the following conclusions can be drawn:

- 1. In all cases, the macrotexture values (MPD) decreased rapidly for the first HWT passes, and then the rate of decrease slowed down for later passes, closely aligning with field behavior.
- 2. Both laboratory-prepared and field samples met the bleeding criteria defined in this study, indicating their resistance to bleeding within the service life defined (5 years).
- 3. The difference between test results was mostly not significant between the two replicates, demonstrating the repeatability of the tests.
- 4. Field sample test results demonstrated higher variability compared to laboratory-prepared samples, attributed to the less controllable environment in situ.

As part of future work, field confirmation should be conducted, i.e., the thresholds determined in this study should be validated in the field. Additionally, a limited number of aggregates and binders were tested; therefore, in future work, more aggregate and binder combinations can be tested. A failed chip seal section (if any) could be tested at the applied AAR and EAR to further test the effectiveness of the test method developed.

# 7.0 AGGREGATE RETENTION & BLEEDING PERFORMANCE OF RAP IN CHIP SEAL

#### 7.1 INTRODUCTION

As highlighted in the literature review (Section 2.5), Recycled Asphalt Pavement (RAP) could be utilized as aggregates in chip seals for a more sustainable practice. While some field applications have been attempted, laboratory-level assessment remained limited. This section discussed laboratory experiments related to the use of RAP as aggregates (100% replacement). Chip seal samples prepared with RAP aggregates were subjected to Sweep, Vialit, and Pull-off tests, and the results have been discussed. In addition to aggregate retention tests, bleeding tests were also performed on RAP chip seal samples. It was observed that some portion of the RAP binder blends into the emulsion layer, which can help reduce the emulsion application rate while achieving similar long-term performance targets.

## 7.1.1 Objectives

The major objectives of this section are as follows:

- Assessing the aggregate retention performance of RAP when used as a 100% replacement for natural (virgin) aggregates using the test methods developed in this study (Sweep, Vialit, and pull-off tests) and comparing RAP's adhesion to that of natural aggregates.
- Evaluating the bleeding susceptibility of RAP chip seal samples using the HWT device and the laser texture scanner developed in this study and comparing the bleeding susceptibility of RAP with that of natural aggregate chip seal samples.

#### 7.2 MATERIALS & METHODS

The RAP, obtained from an asphalt plant, underwent sieving and batching processes to align with the gradations of Pendleton and Woodburn aggregates, subsequently named Pendleton-RAP and Woodburn-RAP. The specific gravity of the RAP material was measured as 2.5, while it was measured as 2.78 for Pendleton and 2.67 for Woodburn natural aggregates (Table 3.4). Following the sieving and batching, the Pendleton-RAP and Woodburn-RAP materials were utilized alongside cationic rapid set (CRS-3P) and anionic high-float rapid set (HFRS-2P) binders, which are binders used in Pendleton and Woodburn project, respectively (Table 3.3). Prior to spreading over the emulsions, the RAP aggregates were wetted with water. The samples were then cured at 45°C for 24 hours. Subsequently, the sweep test was performed at 25°C, while the Vialit test was conducted at 5°C. Pull-off tests were also conducted at both 25°C and 5°C (See Section 3.4 for details). Figure 7.1 illustrates the chip seal samples with natural aggregates (NA) and RAP.

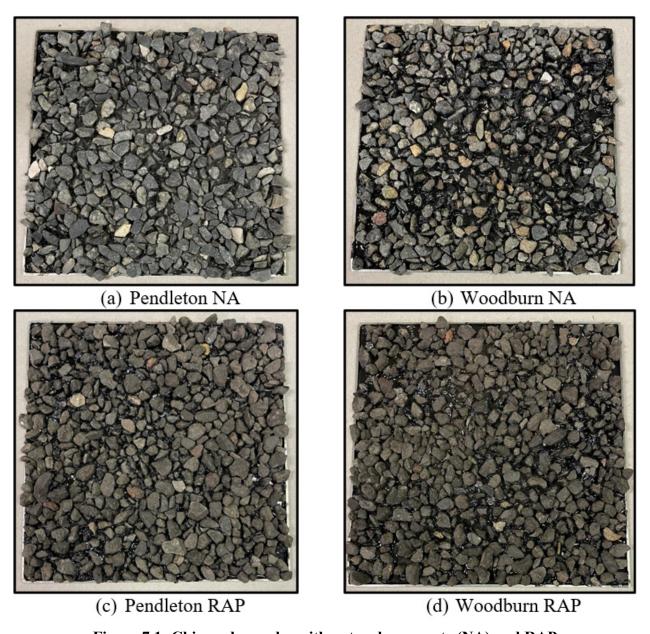


Figure 7.1: Chip seal samples with natural aggregate (NA) and RAP

For bleeding tests, the same RAP aggregates (gradations matched those of Pendleton and Woodburn) were utilized. The exact same procedure detailed in Section 6.2 was also applied to RAP chip seal samples. Figure 7.2 displays some RAP bleeding test samples alongside samples prepared using NA.

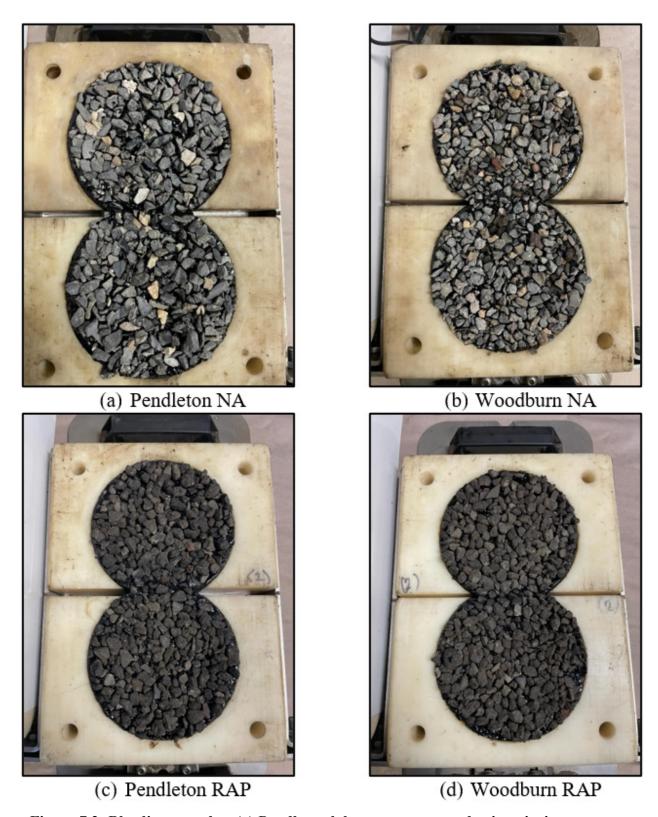


Figure 7.2: Bleeding samples: (a) Pendleton laboratory-prepared using virgin aggregates (b) Woodburn laboratory-prepared using virgin aggregates (c) Pendleton RAP (d) Woodburn RAP

#### 7.3 RESULTS & DISCUSSIONS

## 7.3.1 Adhesion Performance of RAP Chip Seal

Figure 7.3 presents the results of the Sweep and pull-off tests performed at 25°C using RAP and Natural Aggregates (NA). Overall, it can be said that both RAP and NA performed well – the chip loss values are less than 10% in the sweep test, and bond strength values are higher than 25 kPa (thresholds determined in Section 3.4.3) for all binder-aggregate combinations. According to the sweep test results (Figure 7.3a) for both Pendleton and Woodburn, RAP shows a better aggregate retention performance than NA. The improvement noted could be due to the thin asphalt film on the RAP being activated upon curing at 45°C for 24 hours, possibly increasing the binder's cohesion. According to the 25°C pull-off test results presented in Figure 7.3b, when RAP aggregates are used with cationic CRS-3P, their performance is similar to or slightly better than that of natural aggregates (NA) in both projects; however, a noticeable decrease in performance is observed with anionic HFRS-2P emulsion. Overall, it can be concluded that RAP aggregates perform better with cationic CRS-3P. As discussed previously in Section 3.4.3.3, aggregates work more compatibly with emulsions that are opposite in electrical surface charge to their own (Ignatavicius et al. 2021). The results obtained suggest that RAP aggregate has a negative surface charge, which is better matched with cationic emulsion.

When comparing the results of Pendleton RAP with those of Woodburn RAP, considering that aggregates of different gradations from the same source were used for both projects, it can be concluded that aggregate gradation has an effect on aggregate retention or aggregate-binder adhesion. The results obtained indicate that finer gradation provides better aggregate retention performance compared to coarser gradation.

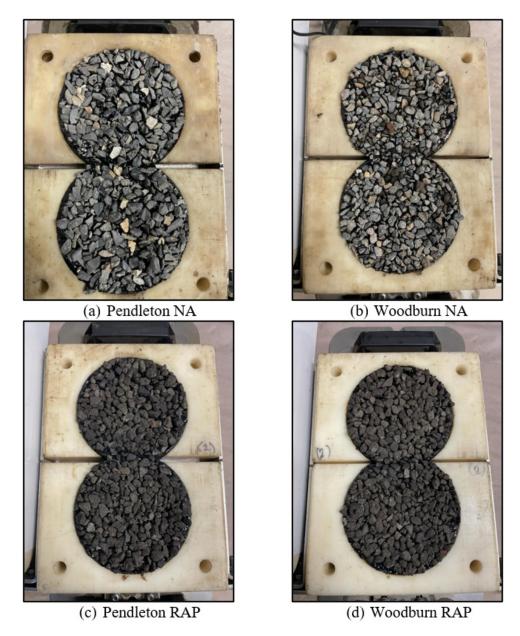
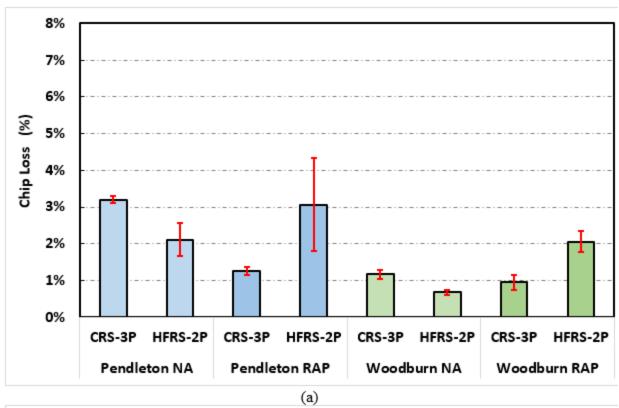


Figure 7.3: (a) Sweep test (25°C) and (b) Pull-out test (25°C) results of chip seal samples with natural aggregate (NA) and RAP (Error bars are one standard deviation height)

Figure 7.4 presents the results of Vialit and pull-off tests conducted at 5°C using NA and RAP. Upon evaluation, it can be stated that RAP aggregates exhibit slightly lower adhesion properties compared to NA aggregates. This could be attributed to the aging of the binder on the surface of RAP aggregates, which have been exposed to UV light and oxygen over time. This exposure could have led to a more brittle response in tests conducted at 5°C. However, it can be said that both binders (anionic HFRS-2P and cationic CRS-3P) exhibited sufficiently good performance with RAP aggregates (less than 8% chip loss in the Vialit test and bond strength higher than 100 kPa according to thresholds determined in Section 3.4.3). Similar to the results obtained in Figure 7.3, it can be concluded that RAP aggregates show better aggregate retention with cationic CRS-3P binder.



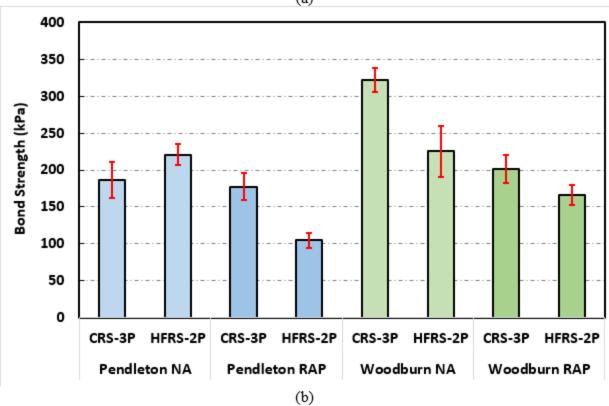


Figure 7.4: (a) Vialit test (5°C) and (b) Pull-out test (5°C) results of chip seal samples with natural aggregate (NA) and RAP (Error bars are one standard deviation height)

Overall, based on the adhesion tests conducted at 25°C, it has been concluded that RAP exhibits slightly better or equal performance compared to NA, whereas at 5°C, there was a slight reduction in aggregate retention performance, attributed to the aging of the binder film around the RAP aggregates. For both test temperatures, RAP aggregates have demonstrated better aggregate retention performance with cationic binder (CRS-3P). Thus, it is considered that the test methods developed within this study can provide crucial insights on which binder would yield better aggregate retention performance before the project commences, and chip seals designed with consideration for aggregate-binder compatibility are anticipated to be more durable. In general, the adhesion tests have concluded that RAP can show good aggregate retention performance when used at a 100% replacement rate.

## 7.3.2 Bleeding Performance of RAP Chip Seal

The bleeding test results for Pendleton RAP are provided in Figure 7.5, while the Woodburn RAP results are presented in Figure 7.6. As seen in those figures, no strong trend can be observed in MPD values and HWT passes. This situation can be attributed to RAP aggregate dislodgment during testing. Although the 50°C conditioning temperature may be considered too low to activate the aged binder film around the RAP, it may have actually activated it when the samples were exposed to 50°C for a long time. During testing, it was observed that more binder was sticking to the wheels for RAP compared to NA. Figure 7.7 shows the rubber wheel of the HWT device after the test. It should be noted here that no evidence of binder was observed on the wheel until 5000 passes for natural aggregate. For RAP, on the other hand, a visible binder film could be observed on the wheels of the HWT even after 50 passes.

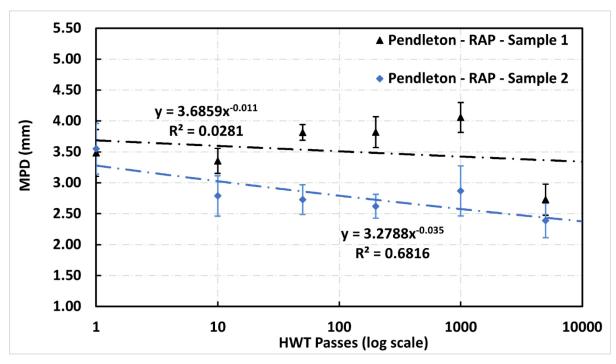


Figure 7.5: MPD-HWT Passes (log scale) of Pendleton RAP sample (Error bars are one standard deviation height)

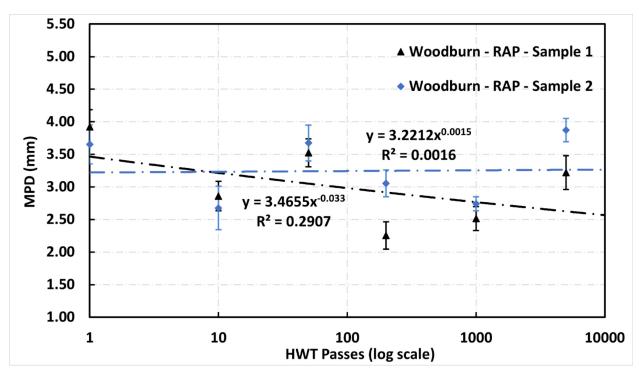


Figure 7.6: MPD-HWT Passes (log scale) of Woodburn RAP sample (Error bars are one standard deviation height)

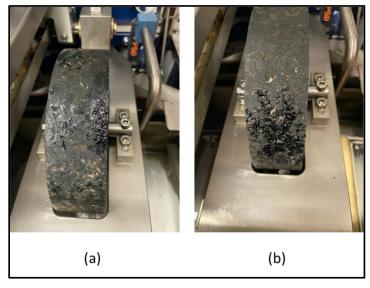


Figure 7.7: Rubber wheel of HWT device (a) Pendleton RAP after 1000 passes, (b) Woodburn RAP after 5000 passes

When considering the case shown in Figure 7.7b, a piece of aggregate became lodged between the wheel and the metal support of the device, causing the device to stop before reaching 5,000 passes. This situation might have occurred during other passes as well. The presence of binder as seen in Figure 7.7 is a clear indication of bleeding, suggesting that RAP is significantly more susceptible to bleeding compared to NA according to laboratory HWT bleeding tests. *However*,

the activation of the RAP binder and the observed bleeding show that the virgin binder application rate (the emulsions application rate) can be reduced when RAP aggregates are used for the chip seal. Consequently, using RAP in chip sealing has the potential to reduce the environmental impact of the chip sealing process, as well as make it more cost-effective. For this reason, a more comprehensive research study at the laboratory and field levels is required to revise the current chip seal design method to incorporate RAP materials and further test its effectiveness to achieve an acceptable level of in-situ performance comparable to using virgin (natural) aggregates. Field validation with pilot section construction and accelerated pavement testing are also required to determine if the aggregate pickup phenomenon observed in the HWT device also occurs with full-scale vehicles in the traffic.

#### 7.4 CONCLUSIONS

In this chapter, the RAP is utilized as a 100% replacement of NA in chip seal samples, and aggregate retention and bleeding performance were tested in the laboratory. Based on the results obtained, the following conclusions can be drawn:

- 1. RAP aggregate performed as well as NA at both 25°C and 5°C. Laboratory-level adhesion tests suggested that RAP could be utilized as a 100% replacement of NA in chip seal sections without sacrificing performance.
- 2. The RAP aggregate consistently demonstrated enhanced performance with the cationic CRS-3P binder relative to the anionic HFRS-2P binder. This situation was attributed to the negative surface charge of the RAP aggregates.
- 3. In the bleeding tests conducted, it was observed that the binder adhered to the rubber wheel of the HWT even at relatively low traffic values in chip seal samples produced with RAP aggregates. It can be said that the RAP is more susceptible to bleeding compared to NA. This finding suggests that the emulsion application rate might be reduced when RAP aggregates are used. This process would reduce the cost and environmental impact of the chip-sealing process. However, further research at the field and laboratory levels is required to prove its effectiveness. Based on the findings from the future research study, the current design process should also be revised to incorporate RAP into chip sealing.

As part of future work, field validation of the results is necessary. It is questioned if the aggregate pick-up phenomenon observed in the laboratory bleeding test can also be observed in the field. A cost analysis of RAP can be conducted to determine if using RAP can also be more cost-effective. It is known that most of the aggregate cost is transportation-related. Therefore, in some cases, using RAP may be both cheaper and more sustainable. It might also be possible to reduce the emulsion application rate by replacing NA with RAP aggregates. This study was performed with RAP sampled from one asphalt plant. Given the high variation in RAP materials, more RAP from different sources and different emulsions should be tested for more comprehensive analysis in a future study.

#### 8.0 SUMMARY AND CONCLUSIONS

The primary objective of this study is to develop test methods and technologies for QA/QC in chip seal construction in Oregon. As discussed in the literature review, two main distresses in chip seals are aggregate loss and bleeding. To address aggregate loss, modified sweep tests and pull-off tests were developed. The findings from the Vialit test were also utilized for comparison and confirmation. Samples obtained from two actual chip seal construction sites (Pendleton and Woodburn) were tested. Also, aggregates and binders sampled from these projects were used to prepare specimens in the laboratory, which were tested at varying curing times to assess their aggregate retention performance. The results obtained from the modified sweep, Vialit, and pulloff tests were analyzed and correlated to determine the most effective and applicable testing strategies. Based on these findings, threshold limits were established for the modified sweep, Vialit, and pull-off tests to distinguish between good and poor adhesion characteristics. These recommended methodologies were also employed to examine the impacts of aggregate dustiness and surface moisture on the aggregate retention performance of the chip seal samples. Additionally, natural aggregates from different regions of Oregon were tested together with the two most commonly used emulsions—one anionic and one cationic in the laboratory, and their aggregate retention performance was reported.

To address bleeding distress in chip seals, pre- and post-construction macrotexture measurements were carried out using a cost-effective laser texture scanner developed by the Oregon State University Asphalt Materials and Pavements (OSU-AMaP) research group and a commercial high-speed profiler system. Currently, ODOT utilizes the sand patch method to measure macrotexture, a technique that is prone to operator variability and necessitates traffic closures. To address these issues and enhance the practicality of macrotexture measurements, results from the sand patch test were correlated with readings from the laser texture scanner and high-speed profiler. A laboratory bleeding test was also developed using the laser texture scanner and the Hamburg Wheel Tracker (HWT) device, where rubber wheels replaced steel wheels in the HWT tests to prevent aggregate crushing. Both field samples and laboratory-prepared samples using aggregates and binders sourced from the construction site were tested. Based on the results obtained, bleeding failure thresholds were determined.

Monitoring the Emulsion Application Rate (EAR) is essential for QA and the successful application of chip seals. It is critical to ensure that the amount of emulsion applied matches the target EAR to achieve high-performance outcomes. The wireless OreTackRate system, developed in project SPR818 (Coleri et al. 2020b) for measuring tack coat application rates, was adapted to measure the in-situ EAR of chip seals in two construction projects. In addition, the tack lifter, developed by Rawls et al. (2016), was built at OSU and used to determine the amount of emulsion absorbed by the pavement.

Lastly, to promote the sustainability of future chip seal projects, Reclaimed Asphalt Pavement (RAP) was used as a replacement for natural aggregates in chip seal samples. The aggregate retention performance and bleeding susceptibility of these samples were then evaluated using the test methods developed in this study.

The importance of QA/QC processes in extending the service life of chip seals is critical. The implementation of QA/QC methods and technologies developed in this study is expected to significantly enhance the longevity, performance, and sustainability of Oregon's chip seals.

#### 8.1 MAJOR CONCLUSIONS

The following major conclusions were drawn from this study:

Adhesion properties between emulsion and aggregates

- 1. The developed modified sweep and pull-off tests, along with the Vialit test, have effectively determined the aggregate-binder adhesion properties. All three testing methods have consistently identified adhesion characteristics that vary depending on the curing time. Also, a strong correlation among these methods underscores their effectiveness in evaluating aggregate retention or aggregate-binder adhesion performance.
- 2. For practical implementation, it is recommended to perform the sweep test at 25°C and the Vialit test at 5°C (based on established high correlations) when pull-off test equipment is unavailable. When chip loss is negligible or almost zero, the pull-off test can be used to quantify adhesion levels.
- 3. The modified sweep test is particularly useful in the field for determining the optimal timing to start the power brooming process in chip seal construction. It also offers greater practicality than the ASTM D7000 standard sweep test since a modified sweep test can be conducted in the field with minimal equipment requirements.
- 4. The test methods developed in this study facilitated the assessment of adhesion properties between the aggregate and binder using specimens sampled directly from the field, exposed to field curing conditions, and with minimal or no disruption to ongoing construction activities.
- 5. For the modified sweep test (25°C), a threshold of 10% chip loss was determined to differentiate "good" from "poor" performance, aligning with a bond strength of 25 kPa for the pull-off test at the same temperature. Since binder-binder failure consistently occurs at this temperature, it serves as a reliable condition for assessing the cohesive properties of the binder. To assess the adhesion properties between the binder and the aggregate, the Vialit test (5°C) and the pull-off (5°C) test were recommended, with thresholds set at 8% and 100 kPa, respectively.
- 6. The modified sweep, Vialit, and pull-off tests effectively differentiated between samples with dusty, dry, and wet aggregate surfaces. This demonstrated the tests' sensitivity to surface conditions. Dusty surfaces resulted in lower bond strengths and higher chip loss, while wet surfaces showed better adhesion, attributed to cohesive forces between water droplets and the emulsion. This distinction highlighted the developed tests' efficacy in assessing chip seal's aggregate retention performance.
- 7. The cationic CRS-3P binder is more susceptible to dust effect compared to the anionic HFRS-2P binder. Thus, for aggregates with high dust content, HFRS-2P emulsion should

- be preferred since anionic emulsions are more resistant to the negative effects of high dust content (Ignatavicius et al. 2021).
- 8. The pull-off tests conducted on asphalt concrete (AC) discs and metal plates showed that AC disc samples typically exhibited lower bond strength compared to metal plates, due to the emulsion's absorption by the AC discs. Observations indicated that emulsions with lower viscosity were absorbed more by the AC discs. Consequently, these results support the use of metal plates for bond strength evaluations, as they offer more consistent performance and operational benefits (more practical) over AC discs. In addition, the metal plates eliminate the absorption effect and provide a clearer picture regarding the performance of aggregates, emulsions, and their interaction.
- 9. Chip seal samples prepared according to the chip seal design method developed for ODOT for commonly used aggregates and emulsions demonstrated adequate aggregate retention performance with both anionic and cationic binders (chip loss and bond strength values were within the threshold limits determined). Overall, these aggregates exhibit better aggregate retention with cationic binders.

#### In-situ EAR and effective EAR measurements

- 10. OreTackRate was found to be useful for QA/QC in chip seal construction, specifically for determining actual EAR in situ. The EAR measurements obtained from both chip seal projects closely matched the target EARs. The scale system can also be used to determine the emulsion curing time to find the best time for sweeping.
- 11. The Tack Lifter can be utilized to determine the effective EAR in situ. Results from this study indicate that 17% of the sprayed emulsion was absorbed by the AC substrate in the Pendleton project.

#### Macrotexture measurements

- 12. High correlations were observed between the Mean Profile Depth (MPD) from the laser texture scanner and high-speed profiler, and the Macrotexture Depth (MTD) from the sand patch test (R<sup>2</sup>=0.93 for the laser texture scanner and R<sup>2</sup>=0.82 for the high-speed profiler). These findings suggest that laser systems are a viable alternative to the sand patch test.
- 13. A statistically significant difference was observed when comparing the sand patch MTD data collected by the ODOT crew and the OSU AMaP research team. This variance is attributed to the operator-dependent nature of the sand patch test and the use of different sand types in the tests. However, a high correlation was observed between the two sets of measurements.
- 14. In classification analysis using derived MPD-MTD correlation equations, the laser texture scanner accurately classified all sections that failed according to the sand patch test, while the high-speed profiler accurately classified 75% of these sections. Assuming a critical macrotexture threshold of 1.5 mm for bleeding susceptibility in chip seal, the laser texture scanner achieved a classification (whether the macrotexture is below 1.5 mm or not) accuracy of 98%, compared to 95% for the high-speed profiler.

15. It was recommended that the high-speed profiler be initially used to collect data on chip seal sections. For areas with macrotexture values below 1.5 mm, further assessments should be performed using either the sand patch or laser texture scanner. This approach enables quick and comprehensive scanning of entire chip seal sections, enhancing the speed and efficiency of evaluations for bleeding susceptibility.

#### Bleeding tests

- 16. In all instances, macrotexture values (MPD) decreased rapidly during the initial passes with the Hamburg Wheel Tracker (HWT) and then slowed in subsequent passes, mirroring field behavior.
- 17. Both laboratory-prepared and field samples met the bleeding criteria set in this study, showing their resistance to bleeding within the defined service life of five years. However, future efforts should focus on calibrating and validating the established threshold values with field data that periodically monitors traffic, temperature, and MPD.
- 18. The variance in test results between the two replicates was generally insignificant, highlighting the repeatability of the tests.
- 19. Field sample test results showed higher variability than those prepared in the laboratory, a difference attributed to the less controllable conditions in situ.

The aggregate retention and bleeding resistance performance of RAP chip seal

- 20. RAP aggregates performed comparably to NA at 25°C and 5°C. Laboratory adhesion tests suggest that RAP could replace NA entirely in chip seal sections, although field trials are needed for verification.
- 21. The RAP aggregate consistently showed better performance with the cationic CRS-3P binder compared to the anionic HFRS-2P binder. This difference is considered to be due to the negative surface charge of the RAP material.
- 22. Bleeding tests revealed that RAP aggregates are more prone to bleeding compared to NA. It was observed that even at relatively low traffic values, the binder around the RAP adhered to the rubber wheel of the HWT, which was not observed for NA. This phenomenon was attributed to the activation of aged binder surrounding the RAP, leading to bleeding. This finding suggests that the emulsion application rate might be reduced when RAP aggregates are used. This process would reduce the cost and environmental impact of the chip-sealing process. However, further research at the field and laboratory levels is required to prove its effectiveness. Based on the findings from the future research study, the current design process should also be revised to incorporate RAP into chip sealing.

#### **8.2** FUTURE WORK

Below are proposed directions for future research:

- 1. In this study, aggregates from various regions of Oregon and three types of emulsion were tested. Future research could test a wider variety of aggregate types and different binders at various curing times. In addition to adhesion tests, assessments like the asphalt stripping tests and electrical conductivity analysis could be conducted to further evaluate aggregate-binder compatibility.
- 2. Due to its inherent high variability, RAP is a material that naturally exhibits significant variability. Testing RAP materials obtained from different sources with various types of binders can further evaluate the compatibility of RAP with emulsions. Also, a field application with RAP aggregates could help better evaluate its performance and can be used to validate the results obtained in the laboratory.
- 3. Incorporating RAP into chip seals may reduce the required Emulsion Application Rate (EAR), thereby decreasing both costs and environmental impacts associated with the chip-sealing process. However, to validate its effectiveness, additional research is needed at both field and laboratory levels. Depending on the outcomes of future studies, it may be advisable to update the current design process to include the use of RAP in chip sealing.
- 4. The modified sweep test developed in this study could be compared and correlated with the sweep test described in ASTM D7000. This comparison would involve testing them on the same samples to examine correlations. If a high correlation is achieved, the modified sweep test might be considered more effective due to its practicality, cost-effectiveness, and field applicability.
- 5. To monitor chip seal design performance, MPD and MTD data could be collected one and two years after chip seal construction. This data would not only measure chip seal design performance but also gather more data for MPD-MTD correlations for higher reliability.
- 6. Future research could focus on establishing a correlation between MPD and absorbed emulsion from the substrate to ascertain the extent of binder absorption by the substrate.
- 7. The bleeding limits established in this study should be validated by referencing measurements taken from an actual construction project until failure, correlating these with traffic and environmental conditions.

## 9.0 REFERENCES

- Adams, J., C. Castorena, J. H. Im, M. Ilias, and Y. Richard Kim. 2017. "Addressing raveling resistance in chip seal specifications." *Transp. Res. Rec.*, 2612: 39–46. https://doi.org/10.3141/2612-05.
- Adams, J., M. Ilias, C. Castorena, and Y. R. Kim. 2018. "Performance-Graded Specifications for Asphalt Emulsions Used in Chip Seal Preservation Treatments." *Transp. Res. Rec.*, 2672 (12): 20–31. https://doi.org/10.1177/0361198118770169.
- Adams, J. M., and Y. R. Kim. 2014. "Mean profile depth analysis of field and laboratory traffic-loaded chip seal surface treatments." *Int. J. Pavement Eng.*, 15 (7): 645–656. https://doi.org/10.1080/10298436.2013.851790.
- Ahmad, M., and R. A. Tarefder. 2020. "Mechanistic performance evaluation of chip seal." *Int. J. Pavement Res. Technol.*, 13 (3): 269–275. https://doi.org/10.1007/s42947-020-1102-0.
- Aktas, B., D. Gransberg, C. Riemer, and D. Pittenger. 2011. "Comparative analysis of macrotexture measurement tests for pavement preservation treatments." *Transp. Res. Rec.*, (2209): 34–40. https://doi.org/10.3141/2209-05.
- Aktas, B., and M. Karasahin. 2013. "Chip seal adhesion performance with modified binder in cold climates." *Transp. Res. Rec.*, (2361): 63–68. https://doi.org/10.3141/2361-08.
- Aktas, B., M. Karasahin, M. Saltan, C. Gurer, and V. E. Uz. 2013. "Effect of aggregate surface properties on chip seal retention performance." *Constr. Build. Mater.*, 44: 639–644. https://doi.org/10.1016/j.conbuildmat.2013.03.060.
- Alderson, A. 2006. Austroads Technical Report AP-T68/06, Update of the Austroads Sprayed Seal Design Method. Sydney, Australia: Austroads Incorporated Level 9.
- ASTM C778. 2021. Standard Specification for Standard Sand. American Society for Testing and Materials.
- ASTM D2995. 2014. Standard Practice for Estimating Application Rate of Bituminous Distributors and Residual Application Rate of Bituminous Distributors. American Society for Testing and Materials.
- ASTM D4541. 2022. Standard Test Method for Pull-Off Strength of Coatings Using Portable Adhesion Testers. ASTM Int. American Society for Testing and Materials.
- ASTM D6372. 2015. Standard Practice for Design, Testing, and Construction of Microsurfacing. American Society for Testing and Materials.
- ASTM D7000. 2019. Standard Test Method for Sweep Test of Emulsified Asphalt Surface Treatment Samples. American Society for Testing and Materials.

- ASTM E1845-15. 2015. Standard Practice For Calculating Pavement Macrotexture Mean Profile Depth. Astm. American Society for Testing and Materials.
- ASTM E1845. 2015. Standard Practice for Calculating Pavement Macrotexture Mean Profile Depth. American Society for Testing and Materials.
- ASTM E1911. 2019. Standard Test Method for Measuring Surface Frictional Properties Using the Dynamic Friction Tester. American Society for Testing and Materials.
- ASTM E2157. 2015. Standard Test Method for Measuring Pavement Macrotexture Properties Using the Circular Track Meter. American Society for Testing and Materials.
- ASTM E2380. 2015. Standard Test Method for Measuring Pavement Texture Drainage Using an Outflow Meter. American Society for Testing and Materials.
- ASTM E274. 2015. Standard Test Method for Skid Resistance of Paved Surfaces Using a Full-Scale Tire. American Society for Testing and Materials.
- ASTM E303. 2022. Standard Test Method for Measuring Surface Frictional Properties Using the British Pendulum Tester. American Society for Testing and Materials.
- ASTM E950. 2022. Standard Test Method for Measuring the Longitudinal Profile of Traveled Surfaces with an Accelerometer Established Inertial Profiling. American Society for Testing and Materials.
- ASTM E965. 2015. Standard Test Method for Measuring Pavement Macrotexture Depth Using a Volumetric Technique. American Society for Testing and Materials.
- Benedict, C. R. 1990. "Laboratory measurement of chip retention strength by the frosted marble modified ISSA cohesion tester." *AEMA/ISSA Conf.* Atlanta, GA.
- Boz, I., Y. Kumbargeri, M. E. Kutay, and S. W. Haider. 2018. *Establishing Percent Embedment Limits to Improve Chip Seal Performance*. Michigan Department of Transportation (MDOT).
- Boz, I., Y. S. Kumbargeri, and M. E. Kutay. 2019. "Performance-Based Percent Embedment Limits for Chip Seals." *Transp. Res. Rec.*, 2673 (1): 182–192. https://doi.org/10.1177/0361198118821370.
- BS EN 12272-3. 2003. Surface dressing -Test method Part 3: Determination of binder aggregate adhesivity by the Vialit plate shock test method.
- BS EN 13036-1. 2010. Road and Airfield Surface Characteristics-Test Methods Part 1: Measurement of Pavement Surface Macrotexture Depth using a Volumetric Patch Technique. British Standards Institution.

- Buss, A., M. Guirguis, and S. Y. Gushgari. 2021. *Implementation Phase of SPR 777 Study and Guidance for a Chip Seal Performance Specification*. Salem, Oregon: Oregon Department of Transportation.
- Buss, A., M. Guriguis, B. Claypool, D. Gransberg, and R. C. Williams. 2016. *SPR 777 Chip Seal Design and Specifications*. Salem, OR: Oregon Department of Transportation.
- Castorena, C., and M. Rawls. 2016. *In-situ Determination of Emulsion Application Rates for Tack Coats and Surface Treatments NCDOT Project 2014-03*.
- Choi, Y. 2008. *Review of Surface Texture Measurement Method for Seal Design Input.* Sydney, Australia: Austroads Incorporated Level 9.
- Coleri, E., D. Covey, A. Mahmoud, J. Batti, and N. Anisimova. 2017. *HMAC Layer Adhesion Through Tack Coat*. Salem, OR: Oregon Department of Transportation.
- Coleri, E., S. Sreedhar, and I. A. Obaid. 2020a. *Development of a Balanced Mix*. Oregon Department of Transportation.
- Coleri, E., B. Wruck, S. Sreedhar, R. Villarreal, S. Lewis, and V. Kumar. 2020b. *Implementation of ODOT Tack Coat Technologies and Procedures to Improve Long-Term Pavement Performance-SPR818*. Salem, Oregon: Oregon Department of Transportation.
- Coplantz, J. 2021. 2020 Pavement Condition Report. Salem, Oregon: Oregon Department of Transportation.
- Coplantz, J. 2023. 2022 Pavement Condition Report. Oregon Department of Transportation.
- Doty, R. 1975. "Study of the Sand Patch and Outflow Meter Methods of Pavement Surface Texture Measurement." *ASTM Int.* https://doi.org/10.1520/stp39043s.
- Duncan, G., L. Sibaja, S. Seeds, and P. David. 2020. *Using Reclaimed Asphalt Pavement in Pavement-Preservation Treatments, PUBLICATION NO. FHWA-HRT-21-007*. US Department of Transportation-Federal Highway Administration.
- Epps, J. A., B. M. Gallaway, and C. H. Hughes. 1981. *Field Manual on Design and Construction of Seal Coats*. Collage Station, Texas: Texas Transportation Institute.
- Ergin, B. 2019. "Skid Resistance Performance evaluation of Chip Seals based on Different Aggregate Type, Size and Polishing Levels, Master Thesis." Graduate School of Natural and Applied Sciences, Adana Alparslan Turkes Science and Technology University.
- Ergun, M., S. Iyinam, and A. F. Iyinam. 2005. "Prediction of road surface friction coefficient using only macro- and microtexture measurements." *J. Transp. Eng.*, 131 (4): 311–319. https://doi.org/10.1061/(ASCE)0733-947X(2005)131:4(311).
- Estakhri, C., S. Senadheera, and C. Seon Shon. 2017. "Evaluation of Seal Coat Construction Materials." *Texas A&M Transp. Inst.*, (Technical Report 0-6747-1): 1–85.

- FHWA InfoTechnology. 2022. "FHWA-Infotechnology-Pavements Inertial Profiler Pavement (IP)." https://infotechnology.fhwa.dot.gov/inertial-profiler-road-pavement/.
- Garfa, A., A. Dony, and A. Carter. 2016. "Performance evaluation and behavior of microsurfacing with recycled materials." 6th Eurasphalt Eurobitume Congr.
- Gheni, A. A., O. I. Abdelkarim, M. M. Abdulazeez, and M. A. ElGawady. 2017. "Texture and design of green chip seal using recycled crumb rubber aggregate." *J. Clean. Prod.*, 166: 1084–1101. Elsevier Ltd. https://doi.org/10.1016/j.jclepro.2017.08.127.
- Google Maps. 2024. "Google Maps." https://www.google.com/maps.
- Gransberg, D., and D. M. B. James. 2005. Chip Seal Best Practices NCHRP SYNTHESIS 342.
- Guirguis, M., and A. Buss. 2019. "Emulsion and hot asphalt chip seal evaluation and field correlation using sweep test." *Int. J. Pavement Res. Technol.*, 12 (3): 241–248. https://doi.org/10.1007/s42947-019-0030-3.
- Guirguis, M., and A. Buss. 2020. "Adopting chip sealing performance-based approaches to determine rational design quantities." *J. Test. Eval.*, 48 (2): 758–774. https://doi.org/10.1520/JTE20180296.
- Gurer, C. 2010. Determination of parameters affecting seal coat performance and development a performance model, PhD Thesis. Suleyman Demirel University Graduate School of Applied and Natural Sciences Department of Civil Engineering.
- Gurer, C., M. Karasahin, S. Cetin, and B. Aktas. 2012. "Effects of construction-related factors on chip seal performance." *Constr. Build. Mater.*, 35: 605–613. https://doi.org/10.1016/j.conbuildmat.2012.04.096.
- Haddadi, S., E. Coleri, and B. Wruck. 2017. A Network-Level Decision Making Tool For Pavement Maintenance And User Safety.
- Haider, S. W., I. Boz, Y. Kumbargeri, E. Kutay, and G. Musunuru. 2021. "Development of performance related specifications for chip seal treatments." *Int. J. Pavement Eng.*, 22 (3): 382–391. Taylor & Francis. https://doi.org/10.1080/10298436.2019.1610173.
- Hanson, F. M. 1935. "Bituminous Surface Treatment of Rural Highways." *Proceedings, New Zeal. Soc. Civ. Eng.*, 89–178.
- Howard, I. L., and G. Baumgardner. 2009. US Highway 84 Chip Seal Field Trials and Laboratory Test Results. Mississippi State.
- Howard, I. L., S. Shuler, W. S. Jordan, J. M. Hemsley, and K. McGlumphy. 2011. "Correlation of moisture loss and strength gain in chip seals." *Transp. Res. Rec.*, (2207): 49–57. https://doi.org/10.3141/2207-07.

- Ignatavicius, S., A. Kavanagh, M. J. Brennan, D. Colleran, J. Sheahan, and S. Newell. 2021. "Experimental investigation of optimum adhesion properties for anionic emulsions in road maintenance applications." *Constr. Build. Mater.*, 304 (July): 124678. Elsevier Ltd. https://doi.org/10.1016/j.conbuildmat.2021.124678.
- Im, J. H., and Y. Richard Kim. 2016. "Performance evaluation of chip seals for higher volume roads using polymer-modified emulsions: Laboratory and field study in North Carolina." *J. Test. Eval.*, 44 (1): 484–497. https://doi.org/10.1520/JTE20140544.
- Jahangirnejad, S., M. Dennis, and N. Fannin. 2019. "Using Reclaimed Asphalt Pavement (Rap) as Coarse Aggregate in Bituminous Seal Coat." *TRB Annu. Meet. TRB, Washington, DC. January 13-17, 2019*, 1.
- Johannes, P. T., E. Mahmoud, and H. Bahia. 2011. "Sensitivity of ASTM D7000 sweep test to emulsion application rate and aggregate gradation." *Transp. Res. Rec.*, (2235): 95–102. https://doi.org/10.3141/2235-11.
- Jordan, W. S. 2010. "Laboratory evaluation of surface treatments to asphaltic pavements in Mississippi." Master Thesis, Mississippi State University.
- Joslin, K., E. Lopez, D. Cheng, and G. Hicks. 2019. *Literature Review on Performance, Best Practices, and Training Needs for Chip Seals, Slurry Surfacing, and Cape Seals*. Mineta Transportation Institute.
- Kandhal, P. S., and J. B. Motter. 1991. "Criteria for Accepting Precoated Aggregates for Seal Coats and Surface Treatments." *Transp. Res. Rec.*, 1300.
- Karasahin, M., B. Aktas, A. G. Gungor, F. Orhan, and C. Gurer. 2015. "Laboratory and In Situ Investigation of Chip Seal Surface Condition Improvement." *J. Perform. Constr. Facil.*, 29 (2): 1–10. https://doi.org/10.1061/(asce)cf.1943-5509.0000470.
- Kearby, J. P. 1953. "Tests and Theories on Penetration Surfaces." *Highw. Res. Board Proc.*
- Kim, R. Y., and J. Lee. 2008. *Quantifying the Benefits of Improved Rolling of Chip Seals*. Raleigh, North Carolina: North Carolina Department of Transportation.
- Kim, Y. R., J. Adams, C. Castorena, M. Ilias, J. H. Im, H. Bahia, P. Chaturabong, A. Hanz, and P. T. Johannes. 2017. *Performance-Related Specifications for Emulsified Asphaltic Binders Used in Preservation Surface Treatments. Performance-Related Specif. Emuls. Asph. Bind. Used Preserv. Surf. Treat.*
- Kim, Y., P. Tien, T. Minh, and D. Park. 2023. "Case Studies in Construction Materials Evaluation of chip seal mixture design methods using modified Hamburg wheel tracking test and sweep test." *Case Stud. Constr. Mater.*, 18 (February). Elsevier Ltd.
- Kumbargeri, Y. S., M. E. Kutay, and I. Boz. 2018. "Effect of percent embedment on chip seal performance using fe modeling." *Adv. Mater. Pavement Perform. Predict. Proc. Int. AM3P Conf. 2018*, (April): 583–586. https://doi.org/10.1201/9780429457791-141.

- Kutay, M. E., and U. Ozdemir. 2016. *An Acceptance Test for Chip Seal Projects Based on Image Analysis*. US Department of Transportation-Research and Innovative Technology Administration (RITA).
- Kutay, M. E., U. Ozdemir, D. Hibner, Y. Kumbargeri, and M. Lanotte. 2016. "Development of an Acceptance Test for Chip Seal Projects (No. SPR-1649). Michigan State University." (3546): 95.
- Lee, J., and R. Y. Kim. 2014. "Evaluation of polymer-modified chip seals at low temperatures." *Int. J. Pavement Eng.*
- Lee, J., and Y. R. Kim. 2010a. "Evaluation of performance and cost-effectiveness of polymer-modified chip seals." *Transp. Res. Rec.*, (2150): 79–86. https://doi.org/10.3141/2150-10.
- Lee, J., and Y. R. Kim. 2010b. "Optimizing Rolling Patterns for Chip Seals Using Laboratory Aggregate Loss Performance Tests on Field Fabricated Samples." *J. Perform. Constr. Facil.*, 24 (3): 249–257. https://doi.org/10.1061/(asce)cf.1943-5509.0000096.
- Lee, J., Y. R. Kim, and E. O. McGraw. 2006. "Performance evaluation of bituminous surface treatment using third-scale model mobile loading simulator." *Transp. Res. Rec.*, (1958): 59–70. https://doi.org/10.3141/1958-07.
- Lee, J., J. Lee, Y. R. Kim, and S. Mun. 2012. "A comparison study of friction measurements for chip seal." *J. Test. Eval.*, 40 (4): 603–611. https://doi.org/10.1520/JTE103863.
- Lee, J. S., and Y. R. Kim. 2008. "Understanding the effects of aggregate and emulsion application rates on performance of asphalt surface treatments." *Transp. Res. Rec.*, (2044): 71–78. https://doi.org/10.3141/2044-08.
- Lee, S. 2003. "Long-Term Performance Assessment of Asphalt Concrete Pavements Using the Third Scale Model Mobile Loading Simulator and Fiber Reinforced Asphalt Concrete, PhD Thesis." North Carolina State University.
- Louw, K., D. Rossman, and D. Cupido. 2004. "The Vialit Adhesion Test: Is It An Appropriate Test To Predict Low Temperature Binder/Aggregate Failure?" 8th Conf. Asph. Pavements South. Africa, 7.
- Mahoney, J. P., M. Slater, C. Keifenheim, J. Uhlmeyer, T. Moomaw, and K. Willoughby. 2014. "WSDOT Chip Seals Optimal Timing, Design and Construction Considerations." *Rep. No. WA-RD 837.1*, (December).
- Malladi, H., and C. Castorena. 2019. "Field measurements of emulsion application rates and pavement emulsion absorption in tack coats and chip seals." *Constr. Build. Mater.*, 218: 701–711. Elsevier Ltd. https://doi.org/10.1016/j.conbuildmat.2019.05.105.
- Map of US. 2023. "Map of US." https://www.mapofus.org/oregon/.

- Mataei, B., H. Zakeri, M. Zahedi, and F. M. Nejad. 2016. "Pavement Friction and Skid Resistance Measurement Methods: A Literature Review." *Open J. Civ. Eng.*, 06 (04): 537–565. https://doi.org/10.4236/ojce.2016.64046.
- McLeod, M. W. 1969. "A General Method of Design for Seal Coats and Surface Treatments." *Proc. Assoc. Asph. Paving Technol.*
- Miller, B., R. T. Terrel, and J. E. Wilson. 1991. *Polymer modified chip seal test: Oregon Route* 22.
- Miller, T. D., Z. A. Arega, and H. U. Bahia. 2010. "Correlating rheological and bond properties of emulsions to aggregate retention of chip seals." *Transp. Res. Rec.*, (2179): 66–74. https://doi.org/10.3141/2179-08.
- Mohammad, L. N., M. A.Elseifi, A. Bae, and N. Patel. 2012. *Optimization of Tack Coat for HMA Placement (NCHRP Report 712)*. *NCHRP Rep. 712*. Washington, D.C.: Transportation research Board, National Academy of Sciences.
- Muench, S. T., and T. Moomaw. 2008. *De-Bonding Cracking De-Bonding of Hot Mix Asphalt Pavements in Washington State: An Initial Investigation. WSDOT Res. Rep.* Washington.: Washington State Department of Transportation WSDOT.
- National Road Board (NRB). 1968. *Manual of sealing and paving practice prepared for Road Research Unit*. Wellington, New Zealand: National Roads Board.
- ODOT. 2023. "U.S. 730 and OR 11 Chip Seal locations and schedule." https://content.govdelivery.com/attachments/ORDOT/2023/06/02/file\_attachments/25158 12/M21039\_project map-schedule-revised.png.
- Oregon Department of Transportation (ODOT). 2021. *Oregon Standard Specifications for Construction*. Salem, Oregon: Oregon Department of Transportation.
- Oregon Department of Transportation (ODOT). 2022. *Laboratory Manual of Test Procedures*. Salem, Oregon: Oregon Department of Transportation.
- Ozdemir, U., M. E. Kutay, D. Hibner, M. Lanotte, and Y. S. Kumbargeri. 2018. "Quantification of Aggregate Embedment in Chip Seals Using Image Processing." *J. Transp. Eng. Part B Pavements*, 144 (4): 04018047. https://doi.org/10.1061/jpeodx.0000068.
- Pasquini, E., A. Bonati, F. Giuliani, and F. Canestrari. 2014. "Advanced Characterization of Clear Chip Seals." *J. Test. Eval.*, 45 (5): 1213–1227. https://doi.org/10.1520/JTE20130119. ISSN 0090-3973.
- Patrick, S. 2016. Selection and Design of Initial Treatments for Sprayed Seal Surfacings. Sydney, Australia: Austroads Ltd.

- Pidwerbesky, B., J. Waters, D. Gransberg, and R. Stemprok. 2006. "Road Surface Texture Measurement Using Digital Image Processing and Information Theory." *L. Transp. New Zeal. Res. Rep.* 290, (June): 65–79.
- Pierce, L. M., and N. Kebede. 2015. *Chip Seal Performance Measures—Best Practices. Urbana*. The State of Washington Department of Transportation.
- Plati, C., M. Pomoni, and T. Stergiou. 2017. "Development of a mean profile depth to mean texture depth shift factor for asphalt pavements." *Transp. Res. Rec.*, 2641 (1): 156–163. https://doi.org/10.3141/2641-18.
- Praticò, F. G., and R. Vaiana. 2015. "A study on the relationship between mean texture depth and mean profile depth of asphalt pavements." *Constr. Build. Mater.*, 101: 72–79. https://doi.org/10.1016/j.conbuildmat.2015.10.021.
- Praticò, F. G., R. Vaiana, and T. Iuele. 2015. "Macrotexture modeling and experimental validation for pavement surface treatments." *Constr. Build. Mater.*, 95: 658–666. https://doi.org/10.1016/j.conbuildmat.2015.07.061.
- Queensland Department of Transport and Main Roads. 2022. *Materials Testing Manual. Transp. Main Roads*. Queensland, Australia: The State of QueenslandDepartment of Transport and Main Roads.
- Rahman, M. N., M. T. A. Sarkar, M. A. Elseifi, C. Mayeux, and S. B. Cooper. 2020. "Effects of emulsion types, application rates, and crumb rubber on the laboratory performance of chip seal." *Constr. Build. Mater.*, 260: 119787. Elsevier Ltd. https://doi.org/10.1016/j.conbuildmat.2020.119787.
- Rawls, M., and C. Castorena. 2019. "In situ measurements of emulsion application rates." *Int. J. Pavement Eng.*, 20 (7): 811–819. https://doi.org/10.1080/10298436.2017.1347438.
- Rawls, M., J. H. Im, and C. Castorena. 2016. "Tack lifter for in situ measurement of effective emulsion application rates." *Transp. Res. Rec.*, 2550: 80–88. https://doi.org/10.3141/2550-11.
- Robbins, M., R. Green, A. Buss, A. Durrani, I. Pintp, and K. Madson. 2021. *Design of Microsurfacing and Chip Seal Mixes with RAP for Local Roadway Application*. Ohio Research Institute for Transportation and the Environment.
- Roque, R., D. Anderson, and M. Thompson. 1991. "Effect of material, design, and construction variables on seal-coat performance." *Transp. Res. Rec.*, (August): 108–115.
- Saghafi, M., N. Tabatabaee, and S. Nazarian. 2019. "Performance Evaluation of Slurry Seals Containing Reclaimed Asphalt Pavement." *Transp. Res. Rec.*, 2673 (1): 358–368. https://doi.org/10.1177/0361198118821908.
- Schonfeld, R. 1970. "Photo-Interpretation of Skid Resistance." *Highw Res Rec*, (311): 11–25.

- Senadheera, S., T. R. Wm., S. H. M., Y. Baris, and D. Subrata. 2006. A Testing and Evaluation Protocol to Assess Seal Coat binder-Aggregate Compatibility. Texas Dep. Transp.
- Shuler, S. 2011. "When to broom or remove traffic control safely on fresh emulsified asphalt chip seals." *Transp. Res. Rec.*, (2235): 82–87. https://doi.org/10.3141/2235-09.
- Shuler, S., A. Epps-Martin, A. Lord, and D. Hoyt. 2011. *Manual for Emulsion-Based Chip Seals for Pavement Preservation. Man. Emuls. Chip Seals Pavement Preserv.*
- Southern African Bitumen Association (SABITA). 2020. Technical Guideline: The Use of Modified Bituminous Binders in Road Construction. Cape Town, South Africa: Southern African Bitumen Association.
- Surface Systems & Instruments Inc. 2023. "SSI INERTIAL PROFILING SYSTEMS Technical Specifications." https://www.smoothroad.com/wp-content/uploads/2023/02/SSI-High-Speed-Profiling-System-Technical-Specifications 2023.pdf.
- Tarefder, R. A., and M. Ahmad. 2018. "Cost-effectiveness analysis of chip seal with and without millings." *Int. J. Pavement Eng.*, 19 (10): 893–900. Taylor & Francis. https://doi.org/10.1080/10298436.2016.1219599.
- Texas Department of Transportation (TxDOT). 2010. Seal Coat and Surface Treatment Manual. Texas Department of Transportation.
- The Road and Traffic Authority (RTA). 2012. *Test method T238 Initial adhesion of cover aggregates and binders*. New South Wales, Australia: The Road and Traffic Authority.
- Transit New Zealand (TNZ). 2005. *Chipsealing in New Zealand*. Wellington, New Zealand: Transit New Zealand.
- Transit New Zealand (TNZ T/3). 1981. Standard Test Method for Measurement of Texture by the Sand Circle Method. Transit New Zealand.
- Updyke, B. E., and D. Ruh. 2016. "Abundance of RAP Spurs New Uses in Preservation Treatments." *Pavement Preserv. J.*, 9 (4).
- Uz, V. E., and I. Gokalp. 2017. "Comparative laboratory evaluation of macro texture depth of surface coatings with standard volumetric test methods." *Constr. Build. Mater.*, 139: 267–276. https://doi.org/10.1016/j.conbuildmat.2017.02.059.
- Walter S. Jordan III, and Isaac L. Howard. 2011. "Applicability of Modified Vialit Adhesion Test for Seal Treatment Specifications." *J. Civ. Eng. Archit.*, 5 (3): 215–223. https://doi.org/10.17265/1934-7359/2011.03.002.
- Wang, A., S. Shen, X. Li, and B. Song. 2019. "Micro-surfacing mixtures with reclaimed asphalt pavement: Mix design and performance evaluation." *Constr. Build. Mater.*, 201: 303–313. Elsevier Ltd. https://doi.org/10.1016/j.conbuildmat.2018.12.164.

- Wasiuddin, N. M., A. Marshall, N. E. Saltibus, A. Saber, C. Abadie, and L. N. Mohammad. 2013. "Use of Sweep Test for Emulsion and Hot Asphalt Chip Seals: Laboratory and Field Evaluation." *J. Test. Eval.*, 41 (2). Journal of Testing and Evaluation. https://doi.org/10.1520/JTE20120051.
- Weaver, J., E. Coleri, and V. Chitnis. 2023. *Centerline Rumble Strip Effects on Pavement Performance*. Oregon Department of Transportation.
- Zheng, N., J. Bi, S. Dong, J. Lei, Y. He, Z. Cui, and L. G. Chen. 2022. "Testing and evaluation for long-term skid resistance of asphalt pavement composite seal using texture characteristics." *Constr. Build. Mater.*, 356 (September): 129241. Elsevier Ltd. https://doi.org/10.1016/j.conbuildmat.2022.129241.
- Zhou, F., H. Li, P. Chen, and T. Scullion. 2014. *Laboratory Evaluation of Asphalt Binder Rutting, Fracture, and Adhesion Tests*. College Station, Texas: Texas A&M Transportation Institute.
- Van Zyl, G., and A. Van der Gryp. 2015. "Correlation between Mean Profile Depth Estimated Macro Texture Depth." *Conf. Asph. pavements South. Africa (CAPSA'15)*", *Sun City, South Africa.*, 6p.

APPENDIX A: ONE-YEA	AR POST-CONSTRUCT MEASUREMENTS	ION MACROTEXTURE

Table A.1: One-year post-construction (22 July 2024) sand patch (MTD) and laser texture scanner (MPD) measurements of sections along US-730 and OR-11 (STD is the standard deviation).

	Section No	Dire ction	PM	Sand Patch			Laser Texture Scanner				
Highway				WP		BWP		WP		BWP	
				MT D (mm	STD (mm	MT D (mm	STD (mm	MPD (mm	STD (mm	MPD (mm	STD (mm
US-730	1	SB	203	1.82	0.05	2.17	0.09	1.70	0.27	2.42	0.31
	2	SB	202	1.80	0.12	1.99	0.09	2.14	0.30	2.30	0.30
	3	SB	201	1.66	0.05	2.40	0.09	2.04	0.22	2.75	0.16
	4	SB	200	1.62	0.03	1.99	0.06	1.82	0.16	2.27	0.06
	5	SB	199	1.55	0.06	2.01	0.11	1.90	0.28	2.42	0.22
	6	SB	197	1.53	0.08	2.01	0.11	1.67	0.25	2.31	0.19
	7	SB	195	1.52	0.10	1.93	0.15	1.48	0.25	2.54	0.28
	8	SB	190	1.55	0.21	2.22	0.16	2.07	0.18	2.39	0.28
	9	SB	188	1.58	0.07	1.94	0.07	N/A	N/A	N/A	N/A
	10	SB	180	1.29	0.08	2.43	0.18	N/A	N/A	N/A	N/A
	11	SB	178	1.06	0.05	1.27	0.20	N/A	N/A	N/A	N/A
	12	SB	171	2.00	0.14	2.03	0.13	N/A	N/A	N/A	N/A
OR-11	1	SB	26	1.42	0.12	1.44	0.09	2.15	0.14	2.27	0.24
	2	SB	24	1.06	0.09	1.30	0.05	1.41	0.16	2.04	0.24
	3	SB	22	1.15	0.05	1.15	0.07	1.55	0.08	1.48	0.13
	4	SB	3	0.95	0.07	1.71	0.05	1.19	0.14	1.93	0.23
	5	NB	1	1.32	0.08	1.85	0.17	1.99	0.20	2.30	0.32